REPORT DOCUMENTATION PAGE

Form Approved OMB NO. 0704-0188

1. REPORT DATE (DD-MM-YYYY)	2. REPORT TYPE	3. DATES COVERED (From - To)
07-11-2016	Final Report	1-Oct-2014 - 30-Sep-2016

4. TITLE AND SUBTITLE
Final Report: Bioelectrocatalyzed Nitrogen Fixation under Standard Conditions

5a. CONTRACT NUMBER

5b. GRANT NUMBER
W911NF-14-C-0162

5c. PROGRAM ELEMENT NUMBER
665502

6. AUTHORS
John Watkins

5d. PROJECT NUMBER

5e. TASK NUMBER

5f. WORK UNIT NUMBER

7. PERFORMING ORGANIZATION NAMES AND ADDRESSES
Fulcrum Bioscience
615 Arapeen Dr.

Salt Lake City, UT 84108 -1239

8. PERFORMING ORGANIZATION REPORT NUMBER

9. SPONSORING/MONITORING AGENCY NAME(S) AND ADDRESS (ES)
U.S. Army Research Office
P.O. Box 12211
Research Triangle Park, NC 27709-2211

10. SPONSOR/MONITOR'S ACRONYM(S)
ARO

11. SPONSOR/MONITOR'S REPORT NUMBER(S)
66150-CH-ST2.1

12. DISTRIBUTION AVAILIBILITY STATEMENT
Approved for Public Release; Distribution Unlimited

13. SUPPLEMENTARY NOTES
The views, opinions and/or findings contained in this report are those of the author(s) and should not contrued as an official Department of the Army position, policy or decision, unless so designated by other documentation.

14. ABSTRACT
Report developed under topic A13A-T007, contract W911NF-14-C0162. This final report describes the development of a bioelectrocatalyzed nitrogen fixation process using algae biofilm electrodes. The Phase II effort included: Algae biofilm testing of lifetime and robustness, isolation and investigation of nitrogenase, nitrite/nitrate reductase enzymes, electrochemical stimulation of algae, electrolyte concentration and cation identity, process scale-up, ammonia separation, in-situ ammonia generation, studies on the nitrogen fixation method in algae including modelling and cost modelling of the process. The process achieved 16 uM ammonia at 8% coulombic

15. SUBJECT TERMS
algae, nitrogen, fixation, standard, conditions, ammonia, bioelectrocatalysis

16. SECURITY CLASSIFICATION OF:			17. LIMITATION OF ABSTRACT	15. NUMBER OF PAGES	19a. NAME OF RESPONSIBLE PERSON
a. REPORT	b. ABSTRACT	c. THIS PAGE			John Watkins
UU	UU	UU	UU		19b. TELEPHONE NUMBER: 801-792-0652

Report Title

Final Report: Bioelectrocatalyzed Nitrogen Fixation under Standard Conditions

ABSTRACT

Report developed under topic A13A-T007, contract W911NF-14-C0162. This final report describes the development of a bioelectrocatalyzed nitrogen fixation process using algae biofilm electrodes. The Phase II effort included: Algae biofilm testing of lifetime and robustness, isolation and investigation of nitrogenase, nitrite/nitrate reductase enzymes, electrochemical stimulation of algae, electrolyte concentration and cation identity, process scale-up, ammonia separation, in-situ ammonia generation, studies on the nitrogen fixation method in algae including modelling and cost modelling of the process. The process achieved 16 uM ammonia at 8% coulombic efficiency in a 400 mL volume. Ammonia separation without additional chemicals reached >90% efficiency. The process was scaled from 20 cm2 to 200 cm2. Results suggest that the process is viable for a small-scale industrial process, tons/day, with further improvements. Potential applications include distributed commodity chemical manufacturing for fuel, propellants and fertilizer.

Enter List of papers submitted or published that acknowledge ARO support from the start of the project to the date of this printing. List the papers, including journal references, in the following categories:

(a) Papers published in peer-reviewed journals (N/A for none)

Received Paper

TOTAL:

Number of Papers published in peer-reviewed journals:

(b) Papers published in non-peer-reviewed journals (N/A for none)

Received Paper

TOTAL:

Number of Papers published in non peer-reviewed journals:

(c) Presentations

J. D. Lyon and J. Leddy, “Exploration of Ammonia Production in Blue Green Algae By Bioelectrocatalytic Methods,” 25 May 2015 Electrochemical Society Meeting, Chicago, IL, oral presentation, Published Abstract http://ma.ecsdl.org/content/MA2015-01/45/2299.abstract

Number of Presentations: 1.00

Non Peer-Reviewed Conference Proceeding publications (other than abstracts):

Received Paper

TOTAL:

Number of Non Peer-Reviewed Conference Proceeding publications (other than abstracts):

Peer-Reviewed Conference Proceeding publications (other than abstracts):

Received Paper

TOTAL:

Number of Peer-Reviewed Conference Proceeding publications (other than abstracts):

(d) Manuscripts

Received Paper

TOTAL:

Number of Manuscripts:

Books

Received Book

TOTAL:

Received	Book Chapter

TOTAL:

Patents Submitted

Ammonia Production Using Bioelectrocatalytic Devices, 20140011252A1

Patents Awarded

Awards

Graduate Students

NAME	PERCENT_SUPPORTED	Discipline
Jacob Lyon	0.80	
Matthew Lovander	0.40	
Kristi Knoche	0.12	
FTE Equivalent:	**1.32**	
Total Number:	**3**	

Names of Post Doctorates

NAME	PERCENT_SUPPORTED
Kristi Knoche	0.50
Michelle Rasmussen	0.75
Kamrul Hasan	1.00
FTE Equivalent:	**2.25**
Total Number:	**3**

Names of Faculty Supported

NAME	PERCENT_SUPPORTED	National Academy Member
Shelley Minteer	0.00	
Johna Leddy	0.20	
FTE Equivalent:	**0.20**	
Total Number:	**2**	

Names of Under Graduate students supported

NAME	PERCENT_SUPPORTED
FTE Equivalent:	
Total Number:	

Student Metrics

This section only applies to graduating undergraduates supported by this agreement in this reporting period

The number of undergraduates funded by this agreement who graduated during this period:	0.00
The number of undergraduates funded by this agreement who graduated during this period with a degree in science, mathematics, engineering, or technology fields:.....	0.00
The number of undergraduates funded by your agreement who graduated during this period and will continue to pursue a graduate or Ph.D. degree in science, mathematics, engineering, or technology fields:.....	0.00
Number of graduating undergraduates who achieved a 3.5 GPA to 4.0 (4.0 max scale):.....	0.00
Number of graduating undergraduates funded by a DoD funded Center of Excellence grant for Education, Research and Engineering:.....	0.00
The number of undergraduates funded by your agreement who graduated during this period and intend to work for the Department of Defense	0.00
The number of undergraduates funded by your agreement who graduated during this period and will receive scholarships or fellowships for further studies in science, mathematics, engineering or technology fields:	0.00

Names of Personnel receiving masters degrees

NAME
Total Number:

Names of personnel receiving PHDs

NAME	
Kristi Knoche	
Total Number:	**1**

Names of other research staff

NAME	PERCENT_SUPPORTED
Ashley Salcedo	1.00
Tim Parent	1.00
Sherry Kirkland	0.50
John Davison	0.20
FTE Equivalent:	**2.70**
Total Number:	**4**

Sub Contractors (DD882)

1 a. University of Utah

1 b. 75 South 2000 East

Salt Lake City UT 841128930

Sub Contractor Numbers (c):
Patent Clause Number (d-1):
Patent Date (d-2):
Work Description (e):
Sub Contract Award Date (f-1):
Sub Contract Est Completion Date(f-2):

---

1 a. University of Utah

1 b. 1471 East Federal Way

Salt Lake City UT 841021821

Sub Contractor Numbers (c):
Patent Clause Number (d-1):
Patent Date (d-2):
Work Description (e):
Sub Contract Award Date (f-1):
Sub Contract Est Completion Date(f-2):

---

1 a. The university of iowa

1 b.

00000

Sub Contractor Numbers (c):
Patent Clause Number (d-1):
Patent Date (d-2):
Work Description (e):
Sub Contract Award Date (f-1):
Sub Contract Est Completion Date(f-2):

Inventions (DD882)

Scientific Progress

See Attachment

Technology Transfer

Contact was made with United Suppliers, a large agronomy company based in Iowa to discuss potential commercialization through their SUSTAIN program.

Contract Number: W911NF-14-C-0162
Proposal Number: A2-5774

Contractor: Fulcrum BioScience
615 Arapeen Dr. Ste 310
Salt Lake City, UT 84108-1254

Project Title: Bioelectrocatalyzed Nitrogen Fixation under Standard Conditions

Contract Period: September 30, 2014- September 30, 2016

Total Contract Amount: $999,499.84

Amount Paid by DFAS to Date: $956,227.73

Amount Expended/Invoiced to Date: $999,538.66

Number of Employees Working on Project: 3

Number of New Employees Placed on Contract this Month: 0
24th Progress Technical Report (Final) – September 2016

No Classified Data

Table of Contents

Identification and Significance of the Problem Studied

The objective of the Phase II effort was the development of a bench-top nitrogen fixation process that operates at standard conditions of temperature and pressure with an efficiency higher than the Haber-Bosch process, 10-15%. The key component of the process is the cathode with a biofilm of *Anabaena Variabilis* cyanobacteria. The only inputs to the process were nitrogen, water and electricity. The Fulcrum process achieved a coulombic efficiency >50% of the Haber-Bosch process. The Fulcrum process takes advantage of the enzymatic pathways developed through plant evolution by using a biofilm-modified cathode that electrocatalyzes the synthesis of ammonia from nitrogen and water as the hydrogen source. Plants and photosynthetic organisms depend on fixed nitrogen for growth and development. The most easily used form is ammonium ion. Ammonium is an essential element of amino acids. When the availability of free ammonium in the local environment is low, organisms rely on their own ability to produce ammonium. Many organisms use atmospheric nitrogen, N_2, that is very abundant by also very stable. Despite the fact that nitrogen makes up 80% of Earth's atmosphere, it is not usable by plants due to its chemical stability. Nitrogen must be reduced to more reactive, but stable species of nitrogen such as ammonia, nitrate and nitrite. Biological nitrogen fixation is the evolutionary response of many organisms to obtain nitrogen from the environment and produces an estimated 1.8×10^{14} tons of ammonia annually worldwide.[1] In plants, there are at least 2 pathways for ammonia production; the nitrogenase enzyme that fixes atmospheric nitrogen to ammonia and the nitrate/nitrite reductase enzymes that catalyze fixed nitrogen, e.g. nitrate/nitrite to ammonia. These enzymes are contained within the cell cytosol and depend on a sufficient supply of substrate. The nitrogen fixing reaction centers and associated co-factors are shown in Figure 1. *In vivo*, these enzymes depend on other biochemical paths for recycling of redox pathways, generation of substrates, and low potential electron carrier recycling. Together, the enzyme and dependent chemical processes are the reaction centers within the cell. All of these reaction centers involve electrons which suggest that they can be incorporated into an electrochemical synthetic process. The reaction centers illustrated in Fig. 1A represent the most probable and important pathways and chemicals in the electrochemically induced synthesis of ammonia from immobilized cyanobacteria. The reaction centers are nitrogenase, hydrogenase, nitrate/nitrite reductase and photosystem I/II.

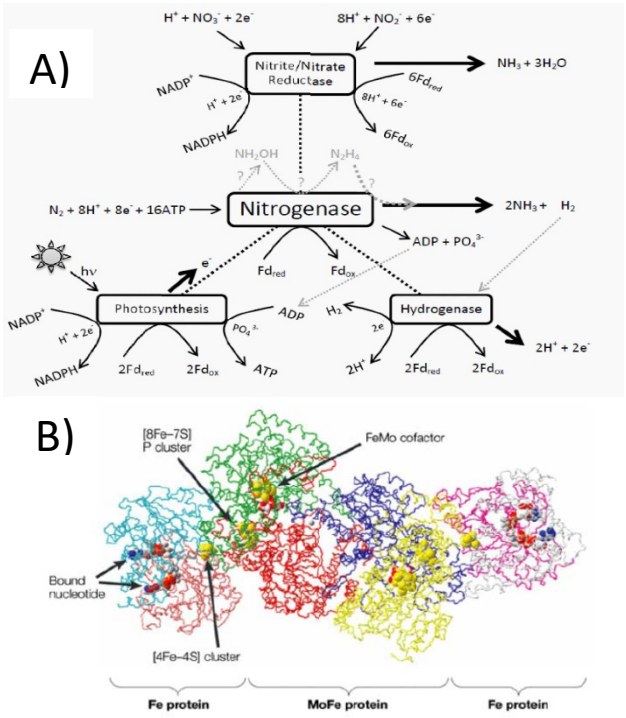

Figure 1.Structure and reaction pathway for the nitrogenase enzyme. A) Illustration of the interrelated reaction centers in Anabaena variabilis. Nitrogenase is one target enzyme for its ability to generate NH3 from N2. Peripheral reaction centers have shared mediators, co-factors, reactants, and products. B) Protein structure of the nitrogenase enzyme showing the Fe protein, FeMo protein, and Fe protein.

uses two redox centers consisting of metalloproteins, Fe and FeMo proteins. Figure 1B shows a crystal structure of the nitrogenase enzyme and reaction chemistry. The substrate for nitrogenase is N_2 and the product is NH_3. The protein structure shows the 3 distinct proteins, and the binding of ATP, the Fe-S based P cluster and FeMo cofactor intercalated into the protein residues. The basic reaction steps are shown and include ATP to ADP hydrolysis, electron transfer, complex formation and complex dissociation. The overall nitrogenase reaction is:

$$N_2 + 8H^+ + 8e^- + 16ATP \leftrightarrow 2NH_3 + H_2 + 16ADP + 16Pi$$

The proposed Fulcrum process uses electrocatalyzed biological nitrogen fixation to synthesize ammonia from nitrogen. The process is essentially an electrochemical synthesis process widely used in industrial processes, where electrons and reactants are combined at an electrode to form a product, e.g. nylon, sodium hypochorite, sodium hydroxide, etc. The innovation is using a cathode structure modified with a biofilm of *Anabaena Variabilis* cyanobacteria cultured for increased nitrogen fixation capacity via the internal nitrogenases in the cyanobacteria. To date, there are no industrial processes using a biologically modified electrode for synthetic purposes. The individual technical objectives, tasks and results toward achieving this objective are discussed below.

Technical Objectives and Results of Phase 2 Effort
Algae Biofilm Lifetime, Robustness, and Electrochemical Flux.

The SA-1 cyanobacteria bio-films in Phase I were formed by first allowing a free-standing biofilm to adhere to a porous carbon electrode. The biofilm was then electrostimulated via cyclic voltammetry to promote electrical connection and then used to electrocatalyze nitrogen fixation in a separate electrolyte solution. The viability of the biofilm was not studied, nor was the long-term stability. Biofilms have shown lifetimes of greater than 5 years for carbohydrate oxidation studies, but have not been studied for nitrogen fixation [8]. For a large-scale process to be successful, the biofilm must have long lifetimes without the need to continually start new cultures. The biofilm must also be stable following electrochemical perturbation.

As part of this effort, differential pulse amperometry, DPA, was performed on a culture more than 6 months old and exhibiting inconsistent nitrogen fixation. Cyclic voltammetry was first performed from -0.4 to 1 V to confirm and quantify the voltammetric response of peaks that are indicative of the bioelectrocatalysis. Figure 2 shows the third voltammograms for two biofilm electrodes in 0.1 M Na_2SO_4 at 20 mV/s over a window of -0.4 to 1 V vs Ag/AgCl with a stainless-steel mesh counter electrode.

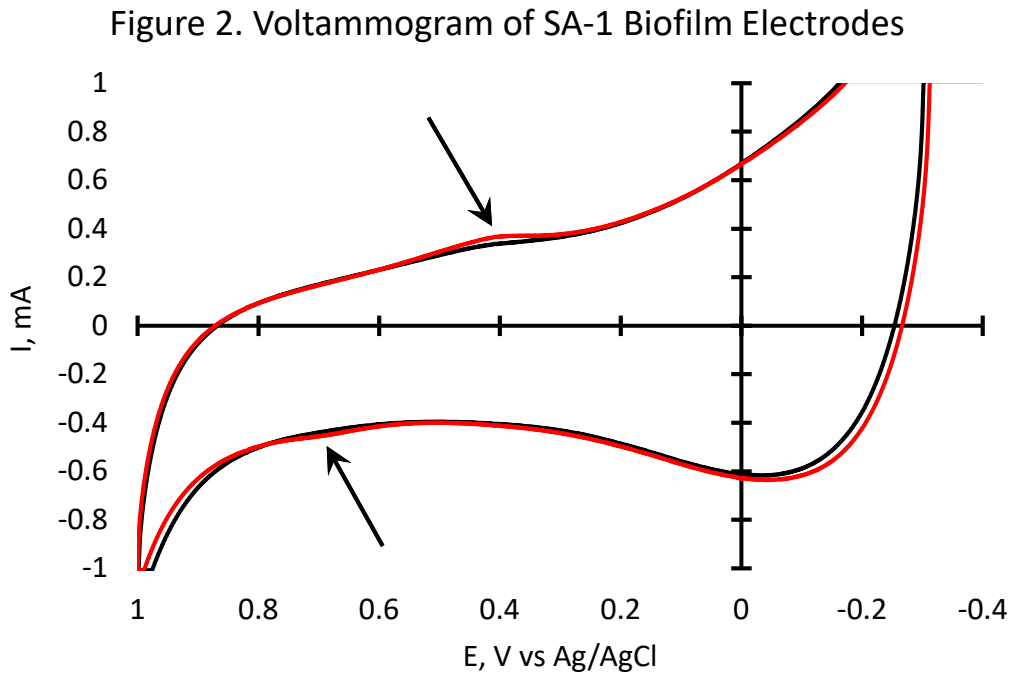

Figure 2. The third voltammograms for 2 SA-1 biofilm electrodes, more than 6 months old, in 0.1 M Na_2SO_4 at 20 mV/s over a window of -0.4 to 1 V vs Ag/AgCl with a stainless steel mesh counter electrode. The voltammetric peaks have shifted toward more positive potentials.

The voltammetric peak position has shifted toward more positive potentials, ~0.55 V, compared to earlier voltammograms. This suggests that biofilm maturity results in more positive voltammetry. Of note is the near identical response for both biofilms in regards to capacitance. The voltammetric peak height is smaller than previously, especially for the oxidation peak.

Differential pulse amperometry was carried out on both biofilm electrodes in identical experimental conditions with 0.5 s duration steps from 0 to 0.1 to 0.8 V. A 25 uM ammonia standard solution was used to confirm the Berthelot assay. Figure 3 shows the ammonia concentration at 10 min. intervals. Despite the smaller voltammetric peak height, the ammonia generated is consistent between the 2 biofilm electrodes. The error bars signify the experimental uncertainty. These ammonia concentrations at 0.5 s DPA step durations is consistent with earlier results of ~40 ug/mL, and show greater uniformity between electrodes.

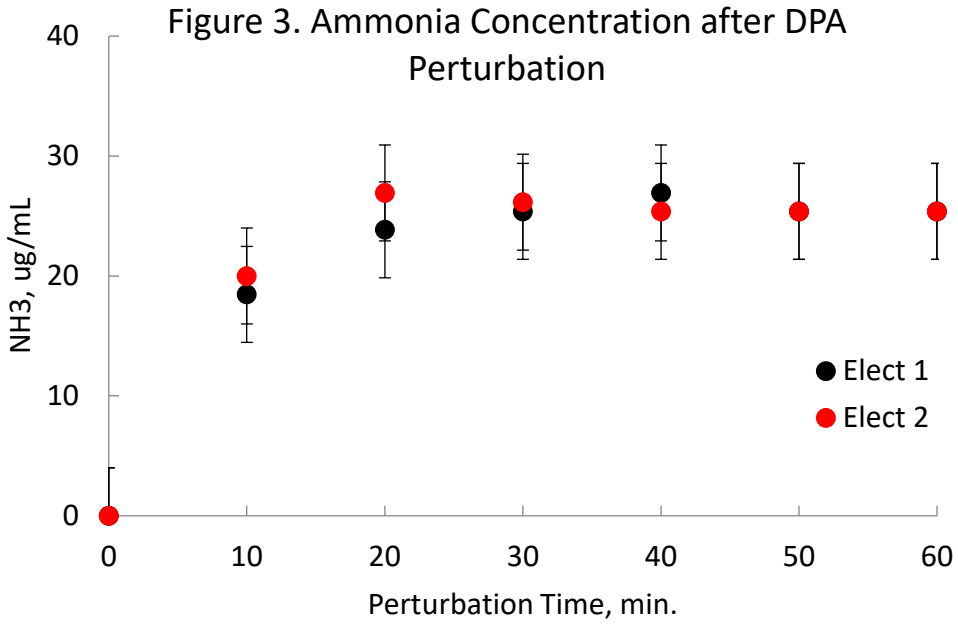

Figure 3. The ammonia concentration measured at 10 min. intervals for both electrodes in Figure 2. The electrodes were perturbed via DPA with 0.5 s duration steps from 0 to 0.1 to 0.8 V. The ammonia concentration is consistent with previous results of ~40 ug/mL, and show greater uniformity between electrodes

Phase I SA-1 biofilm electrodes had dimensions of approximately 1x1x4 cm. A culture with 2 larger ~1x4x6 cm porous vitreous carbon electrodes grew for 6 months. The biofilm was electrostimulated by applying +/- 0.6 V for 48 hrs in alternating 8 hr segments. Cyclic voltammetry was performed at 50 mV/s in 0.1 Na_2SO_4 over a window of 0 to 1 V vs Ag/AgCl with a stainless steel counter electrode. Figure 4 shows the initial voltammograms for each electrode. The voltammetric peak heights are an order of magnitude larger than for the smaller electrodes. The peaks are in approximately the same position as for the smaller electrodes.

The biofilm electrodes were perturbed via cyclic voltammetry to bioelectrocatalyze nitrogen fixation. Intervals of 10 cycles were used with samples collected between intervals. The samples were analyzed with Berthelot assay. The ammonia concentration achieved is shown in Figure 5. The concentration is lower than that previously achieved with the smaller electrode. This is probably due to cyclic voltammetry being used rather than DPA.

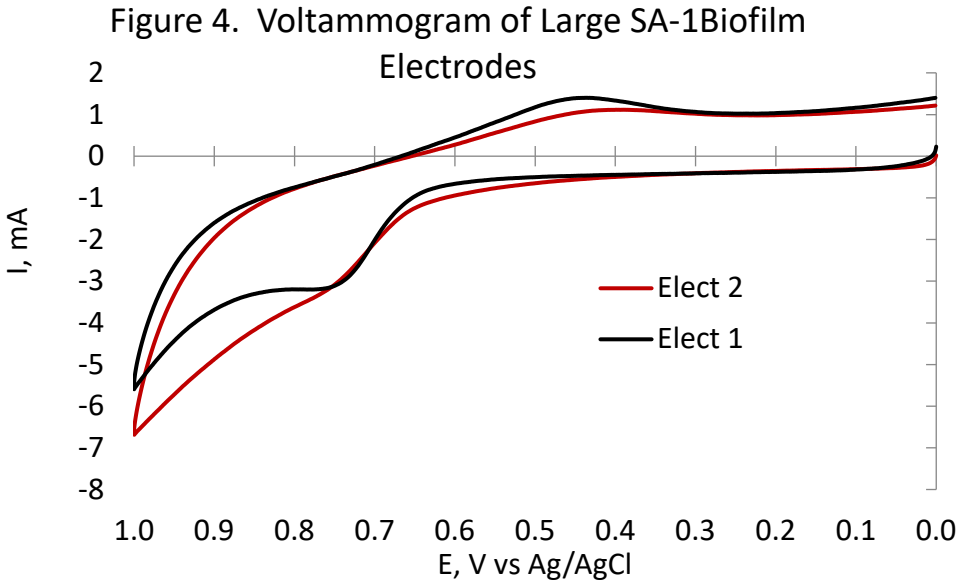

Figure 5. Cyclic voltammograms for 2 larger biofilm electrodes; 1x4x6 cm. The voltammetry was performed in0.1 Na_2SO_4 over a window of 0 to 1 V vs Ag/AgCl with a stainless steel counter electrode.

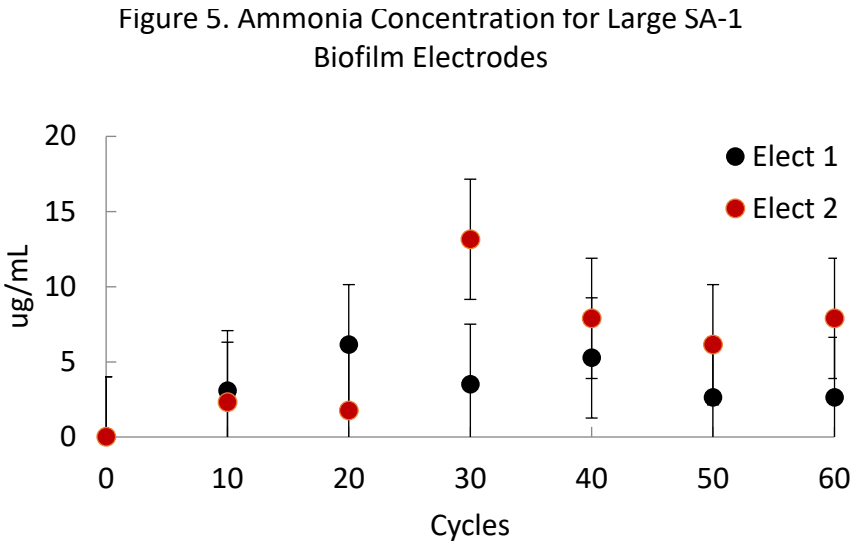

Figure 4. Ammonia concentration measured in intervals of 10 CVs for the larger biofilm electrodes. The ammonia concentration is lower than for the smaller electrodes and may be due to using CV and larger electrolyte volume

It was observed that some biofilm electrodes exhibit poor biofilm coverage or poor adhesion, i.e. the algae slough off the electrode when removed from solution. It was also observed that some electrodes had very little algae on them. These electrodes were replaced with new porous vitreous carbon electrodes. The growth cultures with fresh media were stirred at a slower rate, 60 rpm vs 100 rpm, and biofilm adhesion was electrostimulated for 48 hours by applying ± 650 mV in 4 hour intervals in a square wave. The resulting biofilms were more consistent and exhibit higher ammonia concentrations and greater consistency. Figure 6, shows comparisons of

the 3 biofilm electrodes before and after new biofilms were formed. Each electrode was subjected to square-wave voltammetry, 1 to -0.4 V vs Ag/AgCl, with 10 sec holds and a stainless steel mesh counter electrode. Samples were collected every 75 cycles. Each new biofilm shows significantly higher ammonia production rates.

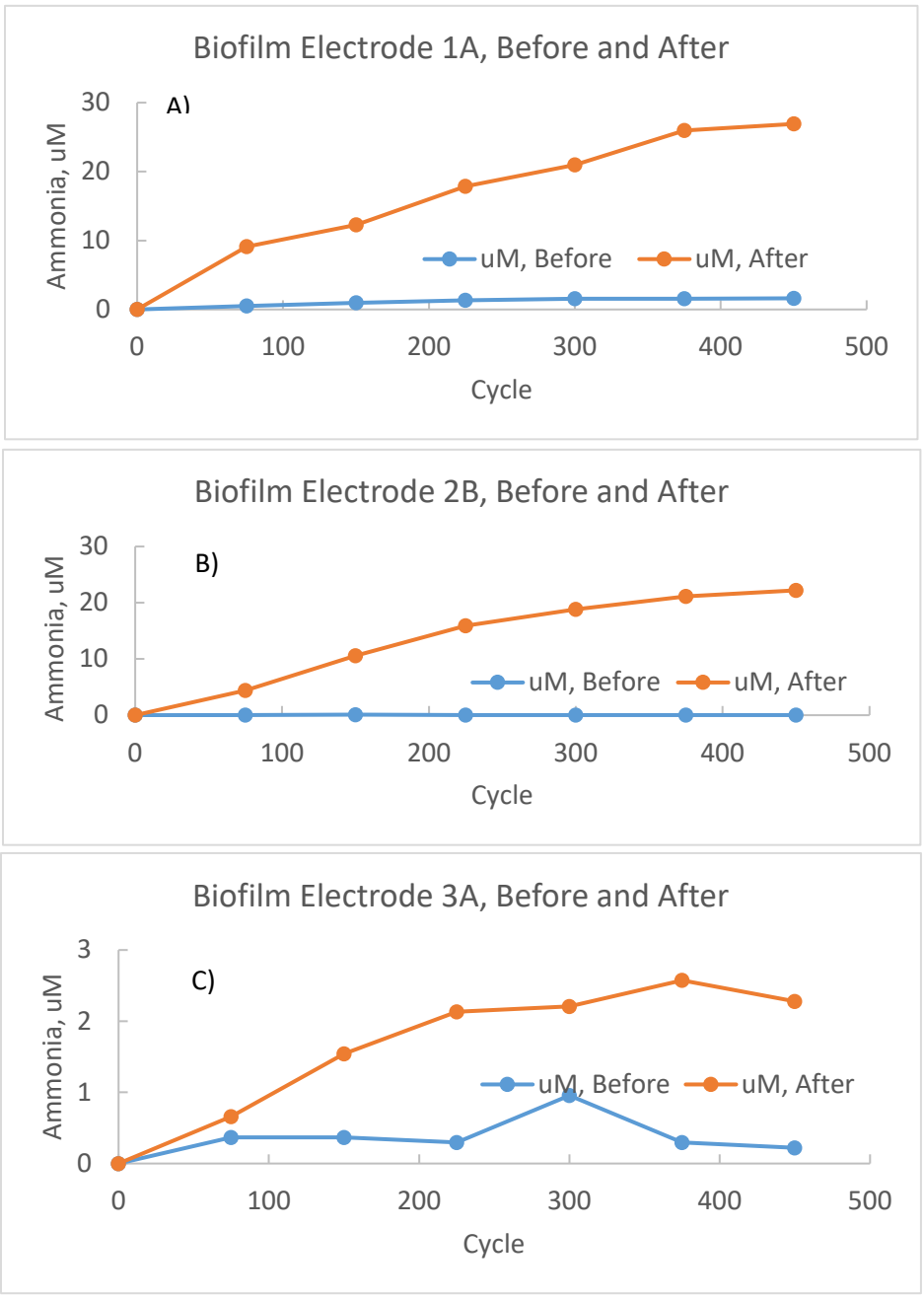

Figure 6. Measured ammonia concentrations for 3 biofilm electrodes, before and after new biofilms were formed and electrostimulated. The new biofilms were formed with a less vigorous agitation and observed to have higher surface coverage and better adhesion.

The improved performance of previously poor performing electrodes, strongly indicates that biofilm integrity is key to bioelectrocatalytic nitrogen fixation. The ammonia concentration

levels achieved are comparable to the highest achieved. It is observed that cultures with long algae filaments perform better than cultures with short algae colonies. Gently agitation, ~60 rpm, appears to promote the desired growth.

A mature carbon foam biofilm electrode has been tested regularly to determine the effect of continuous testing and rest periods on ammonia production. The biofilm electrode was tested with chronoamperometry, 450 cycles total, by applying 1 to -6 V vs Ag/AgCl in 200 mL of 0.05 M Na_2SO_4 with 10 sec holds. Figure 7 shows the ammonia concentration achieved at the end of each test. This test has been ongoing for more than 1000 hrs and achieves an average ammonia concentration of 5 ± 3 uM.

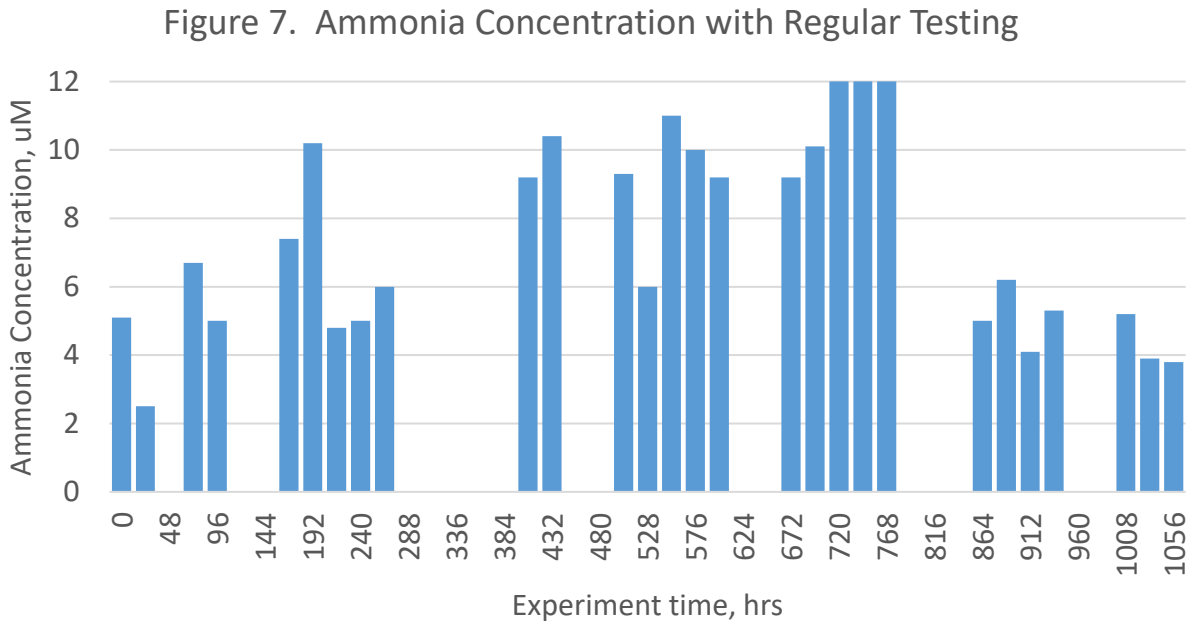

Figure 7. Highest ammonia concentration achieved through regular testing of the same biofilm electrode.

Culturing Bacteria with Enhanced Nitrogen-Fixing Capability.

Atmospheric oxygen is a known inhibitor of ammonia production. However, ideally, we would like to be able to produce ammonia directly from the nitrogen in air and air contains considerable oxygen. The amine enzyme responsible for ammonia production in the cyanobacteria is nitrogenase. Nitrogenases do not function in the presence of oxygen. There are many proposed mechanisms for this, including oxygen inhibition of the enzyme, oxygen producing reactive oxygen and nitrogen species that degrade protein activity, oxygen presence activating protease function, etc. The goal of this project is to produce ammonia in the presence of oxygen (air environment).

Mechanism of electrosynthesis of ammonia

A Toray paper electrode was placed in a solution of ~60 mg of harvested SA-1 *A. variabilis* resuspended in 0.1 M Na_2SO_4, and cyclic voltammetry (CV) was performed with a three-electrode setup (Pt counter electrode, saturated calomel reference electrode, SCE) at 10 mV/s from 0.8 to -0.8 V vs SCE. As CVs were repeatedly taken over time, reductive and oxidative peaks grew in.

For *A. variabilis* grown in BG-11 media (with nitrate), a redox couple with $E_{1/2}$ 0.42 V vs SCE is observed, as shown in Figure 8. For *A. variabilis* grown in BG-11_0 media (without nitrate), a redox couple with $E_{1/2}$ 0.30 V is observed, as shown in Figure 9. No redox peaks with an $E_{1/2}$ in the potential region expected for flavins (-0.4 to -0.6 V vs SCE) were ever observed.

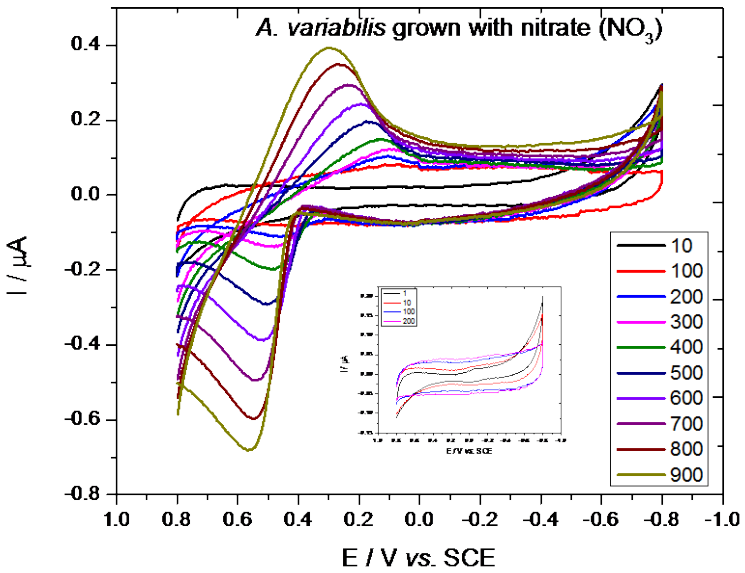

Figure 8. Overlay of 10 mV/s CVs taken over time for a Toray paper electrode in a solution of SA-1 A. variabilis grown in BG-11 and resuspended in 0.1 M Na_2SO_4. Inset is for a control experiment where all conditions are the same except there is no A. variabilis present. Legend indicates cycle number.

Electrochemically stimulated ammonia production by the whole cells was probed using a fluorescence ammonia assay to compare whole SA-1 *A. variabilis* and wild type *A. variabilis*. Some wild type *A. variabilis* was treated with L-Methionine sulfoximine (MSX), which inhibits glutamine synthetase – the same enzyme that is inhibited in the SA-1 mutant so that it outputs the ammonia it produces. Figure 10 shows an overlay of cyclic voltammograms for SA-1 *A. variabilis* grown in BG-11_0 (no nitrate, nitrogenase derepressed), SA-1 *A. variabilis* grown in BG-11 (with nitrate, nitrogenase repressed), wild type *A. variabilis* grown in BG-11 (with nitrate, nitrogenase repressed), and wild type *A. variabilis* grown in BG-11 (with nitrate, nitrogenase repressed) and inhibited by MSX. Fluorescence intensity from the ammonia assay are listed at the top of Figure 10. SA-1 *A. variabilis* grown in BG-11_0 (no nitrate, nitrogenase derepressed) had the highest ammonia concentration, followed by SA-1 *A. variabilis* grow n in BG-11 (with nitrate, nitrogenase repressed). Wild type *A. variabilis* grown in BG-11 (with nitrate, nitrogenase repressed) had lower values, with the MSX inhibited wild type having a slightly higher ammonia concentration than the uninhibited wild type.

Non-electrochemically stimulated nitrogenase activity was investigated using an acetylene assay to compare whole SA-1 *A. variabilis* and wild type *A. variabilis*. Harvested cells were

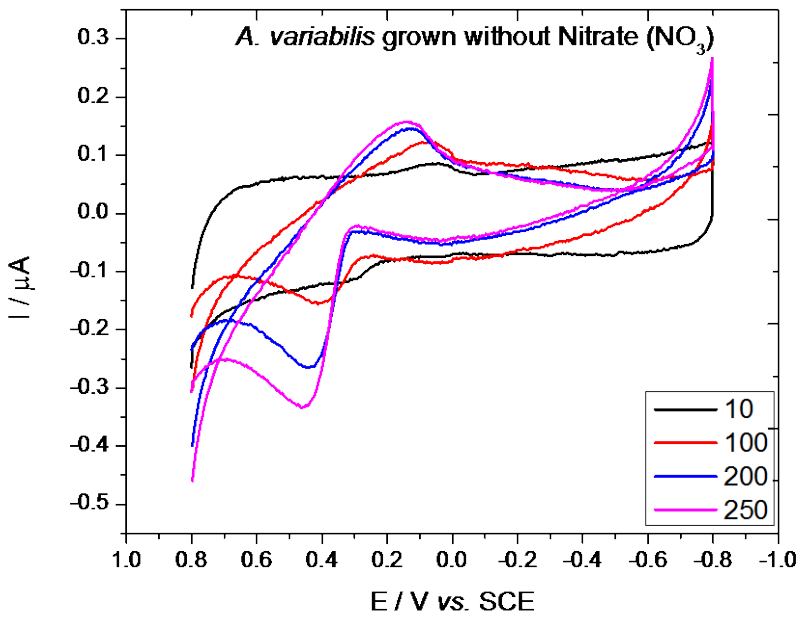

Figure 9. Overlay of 10 mV/s CVs taken over time for a Toray paper electrode in a solution of SA-1 A. variabilis grown in BG-11$_0$ and resuspended in 0.1 M Na_2SO_4. Legend indicates cycle number.

incubated with 10 % v/v acetylene on a shaker under light for 30 minutes to reduce acetylene to ethylene, then the headspace was analyzed by GC-FID. Figure 11a is a chromatogram for SA-1 *A. variabilis* grown in BG-11 media (with nitrate), where only a peak for acetylene is observed at 6.8 minutes indicating no nitrogenase activity. The presence of nitrate in the media represses nitrogenase. Nitrogenase is derepressed when there is no nitrate present in the growth media so that the cyanobacteria can produce ammonia from nitrogen. Figure 11b is a chromatogram for SA-1 *A. variabilis* grown in BG-11$_0$ media (without nitrate); here, a peak for ethylene is observed at 5.9 minutes along with an acetylene peak at 6.8 minutes. Figure 11c is a chromatogram for wild type *A. variabilis* grown in BG-11$_0$ media (without nitrate); a peak for ethylene is observed at 5.9 minutes along with an acetylene peak at 6.8 minutes. When peak areas are adjusted by the relative amount of cells present in each sample, the wild type nitrogenase appears to be three times more active than the SA-1 variant. This is inconsistent with removal of the glutamine synthetase enzyme in the mutant.

Samples of whole wild type *A. variabilis* grown in BG-11 were sonicated for different periods of time to disrupt vegetative cells to make any heterocysts (containing nitrogenase) more electrochemically accessible. Samples were sonicated at 30% amplitude for either 30 seconds or 5 minutes. Electrodes were then prepared as described above and tested in the same electrochemical conditions

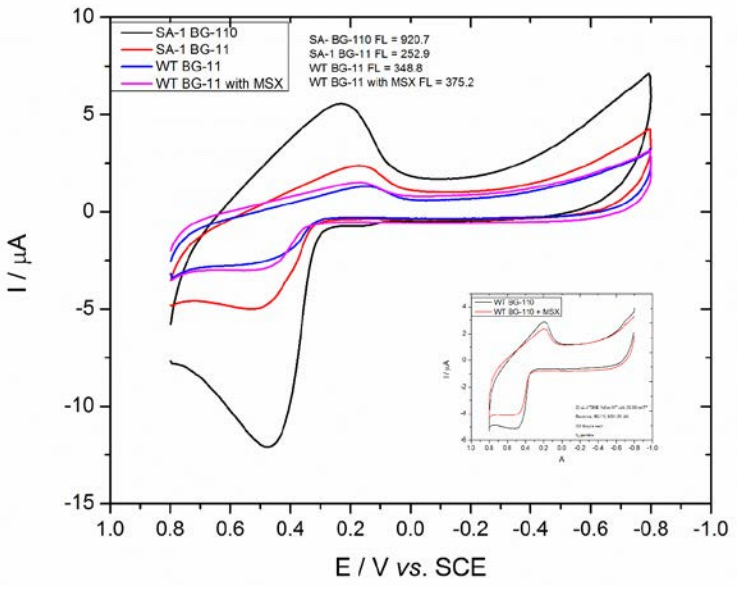

Figure 10. Overlay of 10 mV/s cyclic voltammograms for SA-1 A. variabilis grown in BG-11$_0$ (black line), SA-1 A. variabilis grown in BG-11 (red line), wild type A. variabilis grown in BG-11 (blue line), and wild type A. variabilis grown in BG-11 and inhibited by MSX (pink line). Inset is a magnification of wild type A. variabilis grown in BG-11, and wild type A. variabilis grown in BG-11 and inhibited by MSX, also shown in Figure 9.

described above. Figure 12 shows an overlay of cyclic voltammograms of these electrodes. Current is higher for the sonicated cells. Given that wild type *A. variabilis* grown in BG-11 should not be outputting its produced ammonia, it seems unlikely that this current increase is due to a higher ammonia concentration even if higher ammonia production has been stimulated by the electrode. However, if the vegetative cells have been disrupted, perhaps there is a higher probability of heterocysts being on the electrode surface, even given the relatively few number of heterocysts that will be present in nitrogenase repressed (by the presence of nitrate in the media) cyanobacteria.

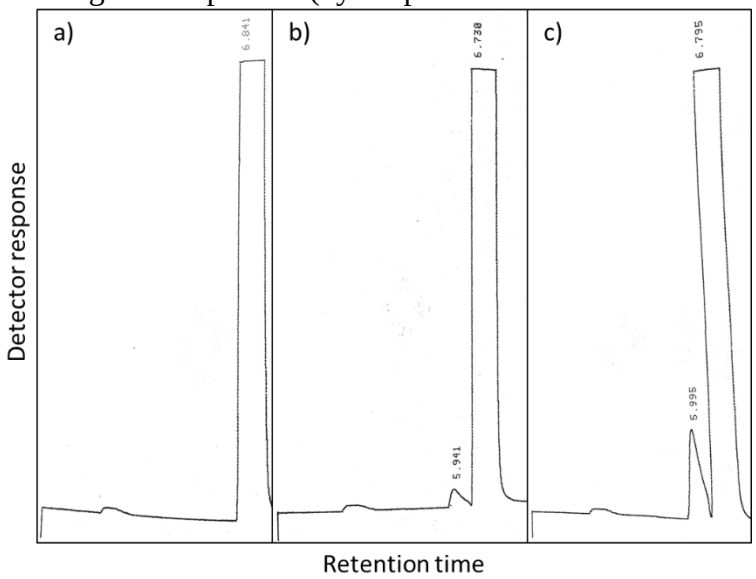

Figure 11. GC-FID chromatograms of headspace (injection volume 200 µL) from a) SA-1 A. variabilis grown in BG-11 media (with nitrate), b) SA-1 A. variabilis grown in BG-11$_0$ media (without nitrate), and c) wild type A. variabilis grown in BG-11$_0$ media (without nitrate). In each chromatogram, the peak at retention time 5.9 minutes is due to ethylene, and the peak at retention time 6.9 minutes is due to acetylene.

There are no inhibitors which inhibit only one of the enzymes of interest. Therefore, nitrite reductase (NiR) was isolated from BG-11 grown SA-1 *A. variabilis* in order to investigate a single enzyme outside of the whole cyanobacteria as a means of probing the mechanism. Cold acetone was used to extract the membrane bound enzyme. Ion chromatography (quaternary ammonium Q-sepharose) with a salt gradient and size exclusion centrifuge filters were then used to separate the enzyme. Fractions were collected and analyzed by SDS PAGE (sodium dodecyl sulfate polyacrylamide gel electrophoresis) and a Griess reagent colorimetric activity assay. From the optimized isolation protocol, the activity measured for the purified NiR was 600 mU/mg protein. One unit of enzyme activity corresponds to the amount of enzyme that catalyzed the reduction of 1 µmol of nitrite per minute.

First, direct electron transfer with adsorbed NiR was studied electrochemically. Nitrite reductase was adsorbed on an edge plane pyrolytic graphite electrode by drop casting, then suspended in a 0.2 M phosphate/citrate buffer solution, pH 7.6, and immediately analyzed by cyclic voltammetry from 0 to -0.9 V vs SCE. The counter electrode was a platinum mesh flag. Figure 13a is a 10 mV/s scan in buffer only. $E_{1/2}$ is observed around -0.6 V vs SCE. Figure 13b is an overlay of 50 mV/s scans with buffer only (solid black line) and 500 µM sodium nitrite in buffer

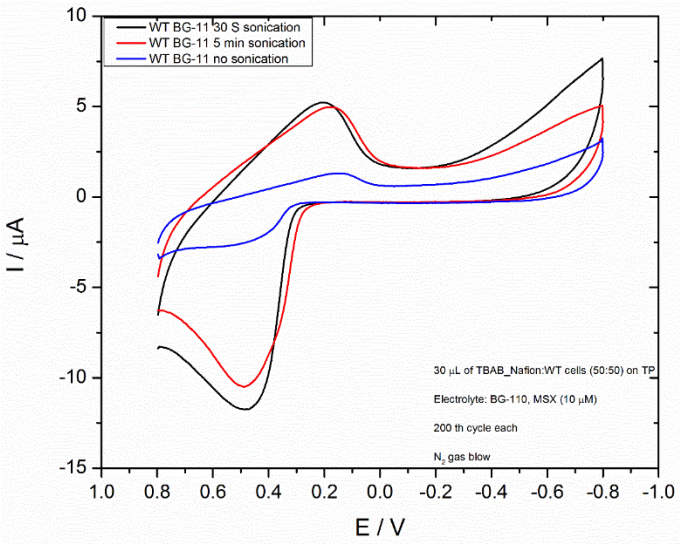

Figure 12. Overlay of 10 mV/s cyclic voltammograms for nonsonicated wild type A. variabilis grown in BG-11 (blue line) and wild type A. variabilis grown in BG-11 sonicated for 30 seconds (black line) and 5 minutes (blue line).

(dashed black line). The solutions were sparged with N_2 gas before analysis and a N_2 blanket was maintained during voltammetry. Results were consistent with data reported by Moura et al.[1] An increase in current was observed in the presence of nitrite. However, the nitrite reductase appeared to quickly desorb from the electrode before more than one concentration of nitrite could be tested.

Next, several mediators for NiR electrochemistry were investigated including methyl viologen, Neutral Red, and ferredoxin. FAD (Flavin adenine dinucleotide) adsorbed on a Toray paper electrode with polymer immobilized enzyme was found to work the best, however at least some portion of the FAD desorbs into solution over time. A method to immobilize the FAD with carbon nanotubes was not successful. Therefore, electrodes with adsorbed FAD were characterized for utilization with NiR. Toray carbon paper electrodes were modified by first drop casting FAD on the electrode and drying in air, then drop casting a mixture poly(vinylamine), cross-linker ethylene glycol diglycidyl ether (EGDGE), and enzyme, and drying in air. Cyclic voltammetry (CV) was performed in a 0.2 M MOPS buffer, pH 7.0, at 10 mV/s from 0 to -0.8 V vs SCE. All solutions were sparged with N_2 gas and an N_2 blanket was maintained during analysis. A redox couple for

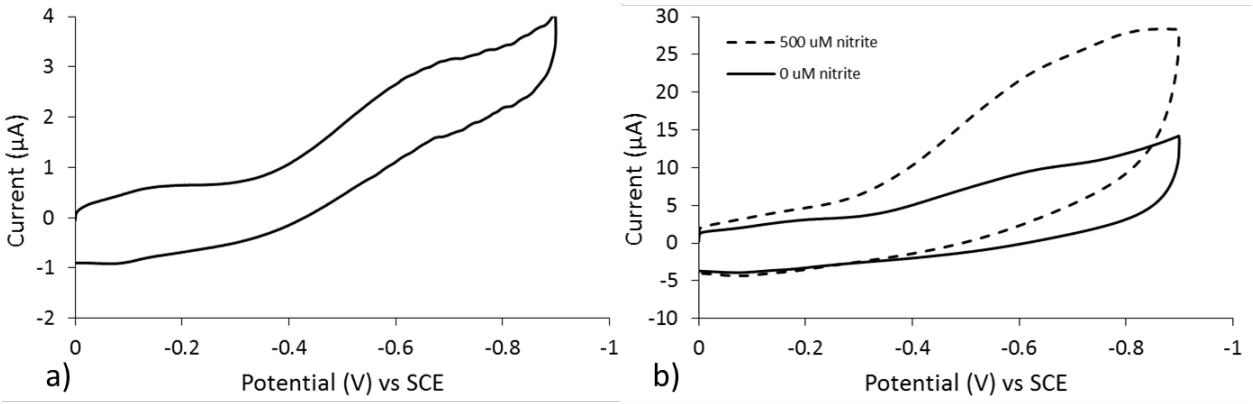

Figure 13. a) 10 mV/s cyclic voltammogram of nitrite reductase adsorbed on edge plane pyrolytic graphite in 0.2 M phosphate/citrate buffer solution, pH 7.6. b) Overlay of 50 mV/s cyclic voltammograms of nitrite reductase adsorbed on edge plane pyrolytic graphite in 0.2 M phosphate/citrate buffer solution, pH 7.6. No nitrite is present for the solid black line. Dashed black line is in presence of 500 µM sodium nitrite.

FAD is observed with an $E_{1/2}$ around -0.45 V vs SCE. In buffer, only, initially the FAD redox currents decrease over time as some FAD desorbs and diffuses into solution. Figure 14 shows CVs taken over the period of one hour. After one to two hours, the current stabilizes, indicating that desorption has stopped, and the FAD that remains adsorbed on the electrode surface is fixed.

Figure 15 shows plots of peak reductive current versus scan rate and peak reductive current versus the square root of the scan rate. There appears to be linearity for scan rates 5-200 mV/s for

peak reductive current versus scan rate, indicating a surface bound process is occurring. With stabilized mediator current, the addition of substrate can be explored.

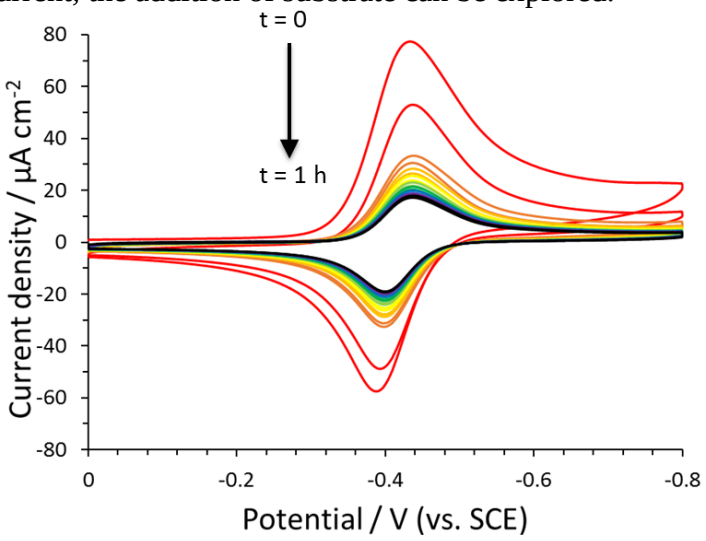

Figure 14. 10 mV/s overlays of CVs for FAD and NiR on Toray paper, taken over the period of one hour.

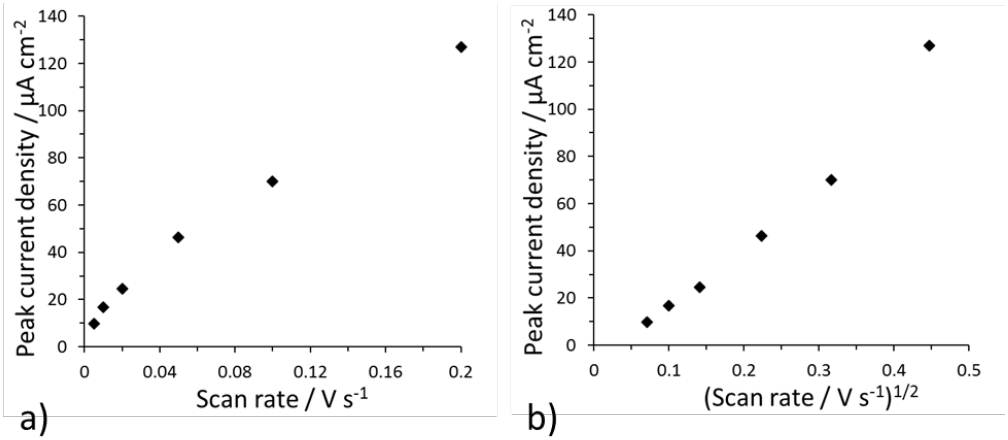

Figure 15. a) Plot of peak reductive current versus scan rate. b) Plot of peak reductive current versus the square root of the scan rate.

After waiting 2 hours until the FAD current stabilized, injections of nitrite were made to the buffer with various electrodes suspended in it. Figure 16 shows peak current densities versus nitrite concentration for FAD only, FAD with denatured NiR, and FAD with active NiR. There is a clear difference between the active NiR and the controls, where the currents are at least three times larger at all concentrations. Evaluation of the active NiR current versus concentration plot by a Michaelis Menten model gives a K_M of 64 mM.

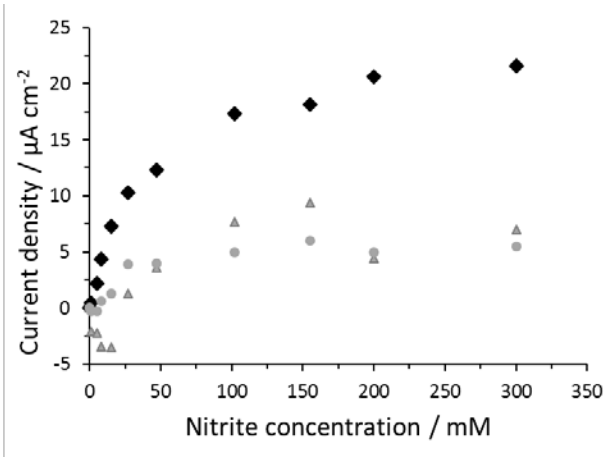

Figure *16*. Peak currents from 10 mV/s cyclic voltammograms for Toray paper electrodes modified with FAD, nitrite reductase, and polyvinylamine (black diamonds); FAD and polyvinylamine only (grey triangles); and FAD, denatured nitrite reductase, and polyvinylamine (grey circles) in different concentrations of nitrite in buffer.

The same method of FAD mediation was then used with whole SA-1 A. variabilis grown in BG-11 media (with nitrate). Both nitrite and nitrate were investigated as substrates, under the assumption that FAD can mediate both NiR and NaR. Electrodes were prepared in the same way as with NiR, except the polymer mixture contained whole cyanobacteria that had been harvested from the media and resuspended in buffer. Control electrodes were prepared with FAD only. CV was performed in a 0.2 M MOPS buffer, pH 7.0, at 10 mV/s from 0 to -0.8 V vs SCE. All solutions were sparged with N_2 gas and an N_2 blanket was maintained during analysis. Injections of sodium nitrite prepared in buffer were made for total cell concentrations of 1 – 300 mM nitrite or nitrate. Figure 17 shows peak current densities versus nitrite concentration for FAD only, FAD with isolated NiR, and FAD with whole SA-1 *A. variabilis*. All current densities have been normalized to allow for different amounts of FAD on the electrode surface by dividing to make the currents at 0 mM nitrite equal for all electrodes. Behavior for the whole cyanobacteria is similar to behavior for isolated NiR, with slightly higher currents. Evaluation of the whole SA-1 A. variabilis current

versus concentration plot by a Michaelis Menten model yields a **K_M of 27 mM**. Evaluation of the isolated NiR current versus concentration plot gave a **K_M of 64 mM**. Figure 18 shows peak current

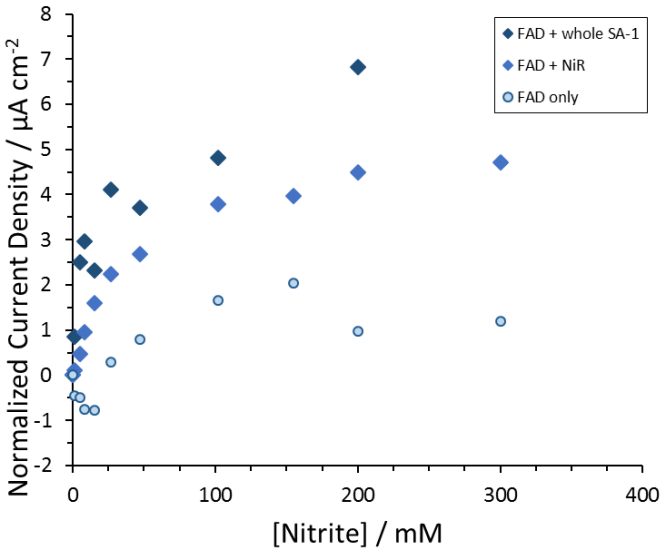

Figure 17. Peak currents from 10 mV/s cyclic voltammograms for Toray paper electrodes modified with FAD, whole SA-1 *A. variabilis*, and polyvinylamine (dark blue diamonds); FAD, nitrite reductase isolated from SA-1 *A. variabilis*, and polyvinylamine (medium blue diamonds); and FAD and polyvinylamine only (light blue circles) in different concentrations of nitrite in buffer.

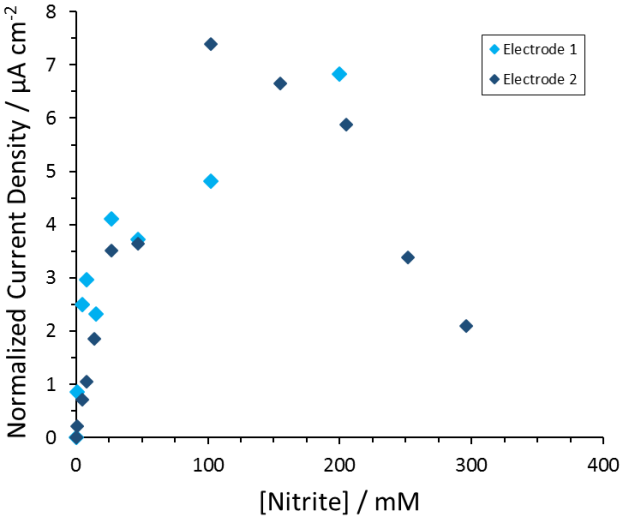

Figure 18. Peak currents from 10 mV/s cyclic voltammograms for two Toray paper electrodes modified with FAD, whole SA-1 A. variabilis, and polyvinylamine in different concentrations of nitrite in buffer.

densities versus nitrite concentration for two different electrodes of FAD with whole SA-1 *A. variabilis*. The second electrode was evaluated for higher concentrations of nitrite. After 200 mM, the currents begin to decrease rapidly. It was unclear whether this was due to inhibition of nitrite reductase by high concentrations of nitrite, or because FAD was desorbing from the electrode surface.

Figure 19 shows peak current densities versus nitrate concentration for FAD only and FAD with whole SA-1 *A. variabilis*. Both electrodes also showed a trend of decreasing current after 100 mM. Thus, current densities for FAD with whole SA-1 *A. variabilis* were corrected by subtracting current densities from the FAD only electrode, as if the FAD only electrode provides information about FAD desorbing over time. When the correction is made, the plot does more closely resemble typical Michaelis Menten type behavior.

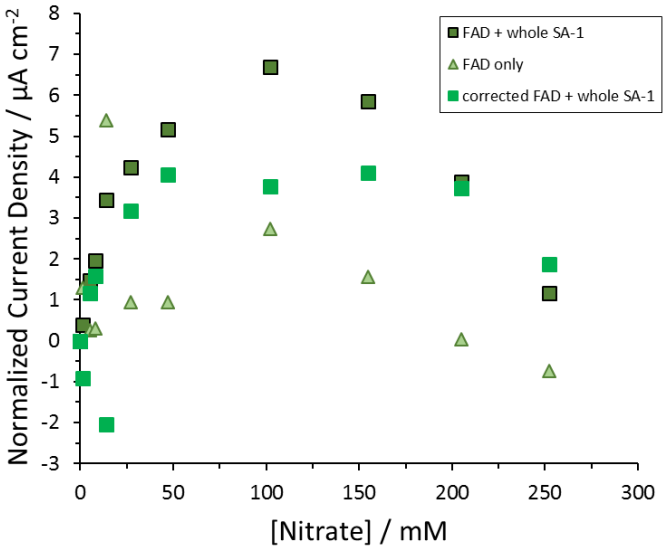

Figure *19*. Peak currents from 10 mV/s cyclic voltammograms for Toray paper electrodes modified with FAD, whole SA-1 A. variabilis, and polyvinylamine (dark green squares); FAD and polyvinylamine only (light green triangles); and FAD, whole SA-1 A. variabilis, and polyvinylamine modified by the FAD only concentrations (medium green squares) in different concentrations of nitrate in buffer.

Figure 20 compares current density versus nitrate or nitrite concentration for uncorrected and corrected whole SA-1 *A. variabilis*. Whether or not the currents are corrected by the FAD only electrode, larger current densities are observed when the substrate is nitrate rather than nitrite. This is an indication that in the whole cyanobacteria on the electrode, NaR is reducing nitrate to nitrite, and then NiR is further reducing nitrite, both reactions mediated by FAD.

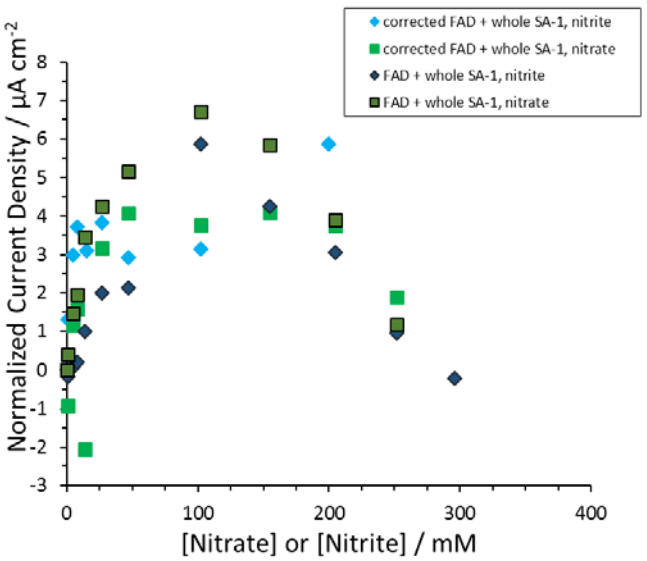

Figure *20*. Peak currents from 10 mV/s cyclic voltammograms for Toray paper electrodes modified with FAD, whole SA-1 A. variabilis, and polyvinylamine (dark colors) and FAD, whole SA-1 A. variabilis, and polyvinylamine modified by the FAD only concentrations (light colors) in different concentrations of nitrite (blue diamonds) or nitrate (green squares) in buffer.

To compare the electrochemically stimulated activity of mediated and nonmediated NiR with nonelectrochemically stimulated NiR in the whole cyanobacteria, continuous CV cycles were performed at 10 mV/s from 0.8 to -0.8 V vs SCE for one hour in 50 mM nitrite and 0.2 M MOPS, pH 7.0, for a Toray paper electrode modified with only poly(vinylamine) and SA-1 *A. variabilis* grown in BG-11 media and an electrode modified with FAD, poly(vinylamine), and SA-1 *A. variabilis* grown in BG-11. An electrode modified with only poly(vinylamine) and SA-1 *A. variabilis* grown in BG-11 was incubated in 50 mM nitrite and 0.2 M MOPS, pH 7.0, for the same amount of time as the electrochemically stimulated electrodes. Nitrite concentration was then measured for spent electrolyte for each system. 3 mM more nitrite was consumed by the electrochemically stimulated, FAD mediated cyanobacteria than the electrochemically stimulated, nonmediated cyanobacteria. 0.5 mM more nitrite was consumed by the electrochemically stimulated, nonmediated cyanobacteria than the nonelectrochemically stimulated, nonmediated cyanobacteria.

To further elucidate the origin of the redox peaks observed at $E_{1/2}$ = 0.3 V vs SCE, SA-1 A. variabilis grown in BG-11_0 was immobilized on an indium tin oxide (ITO) electrode following the previously described poly(vinylamine) protocol. CV was performed in a 0.2 M MOPS buffer, pH 7.0, at 2 mV/s from 0.8 to -0.8 V vs SCE. All solutions were sparged with N_2 gas and an N_2 blanket was maintained during analysis. Immediately following the first sweep, distinct redox peaks were observed with an $E_{1/2}$ near 0 V vs SCE. Similar results have been obtained by the University of Iowa. However, in this case, the signal was stabile over 100 cycles. Figure 21 shows an overlay of multiple sweeps for an ITO electrode modified with live cyanobacteria and an ITO electrode modified with dead cyanobacteria (the cyanobacteria was suspended in buffer and left

for two weeks until it had lost all green color). CV of the dead cyanobacteria does not have the same redox peaks.

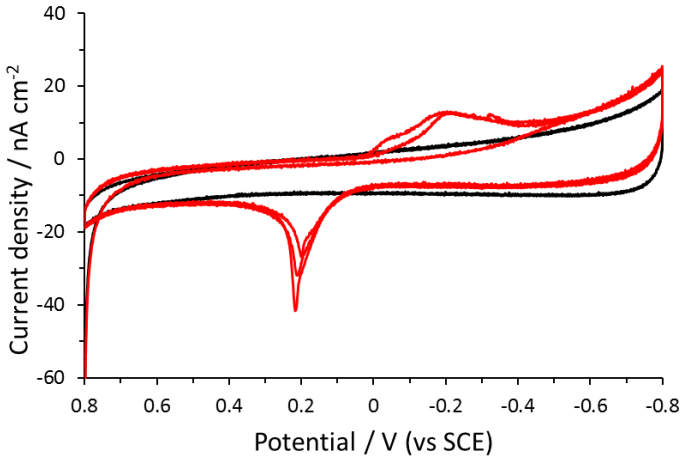

Figure *21*. Overlay of 2 mV/s cyclic voltammograms for dead SA-1 A. variabilis grown in BG-11$_0$ (black line), and live SA-1 A. variabilis grown in BG-11$_0$ (red line) immobilized with poly(vinylamine) on ITO.

The potential and the fact that the signal is more clearly observed on ITO indicates that the redox peaks commonly observed for *A. variabilis* may be due to the presence of cytochromes in the heterocyst membrane. Signal from membrane cytochromes has previously been observed on ITO for *Geobacter sulfurreducens* by Liu, et al. (ChemPhysChem 2011, 12, 2235 - 2241) at very similar $E_{1/2}$s. And membranes isolated from heterocysts and vegetative cells of the closely related species *Anabaena* 7120 (*Nostacles*) have been investigated for content of various cytochromes by Houchins and Hind (Plant Physiol. 1984. 76(2):456-60) via reduced-minus-oxidized difference spectra. The level of cytochrome aa(3) in heterocyst membranes was between 4 to 100 times higher than that in vegetative cells of *Anabaena* 7120 or other species of cyanobacteria. The sharpness of the oxidative peak may indicate that some iron from the cytochrome is depositing on the ITO surface, denaturing the cytochrome.

If the observed redox signal is from a cytochrome, this may explain the fact that the redox peaks are observed at potentials that do not match with the known potentials for nitrate/nitrite reductase (-0.6 V vs SCE) and nitrogenase (-0.54 V vs SCE).

Conclusions

Flavin adenine dinucleotide, FAD, mediates nitrite and nitrate reduction by SA-1 *A. variabilis* grown in BG-11 media at -0.45 V vs SCE, suggesting that the nitrate and nitrite reductase reactions occur near this potential. Electrochemical stimulation increases the amount of nitrite consumed by the cyanobacteria, especially when mediated by FAD. The potential for N_2 reduction to ammonia by nitrogenase is known to be around -0.54 V vs SCE. Redox peaks observed with an $E_{1/2}$ around 0.3 V vs SCE have been correlated with ammonia production by electrochemically stimulated SA-1 *A. variabilis*. These peaks increase when cyanobacteria are sonicated such that the vegetative cells are lysed, but the heterocysts remain intact. Comparison of the peaks to literature investigations of cytochromes suggests that the observed peaks may be due to cytochromes in the heterocyst membrane. These cytochromes may be facilitating electron transfer from nitrogenase producing ammonia from N_2. This is supported by the fact that University of Iowa saw much higher (almost five times higher) ammonia production when cycling CV for heterocyst only electrodes versus vegetative cell only electrodes.

Alternative bacteria strains, non-heterocyst

Nitrogenase isolated from the bacteria *Azotobacter vinelandii* (which does not have a thickened cell membrane typical of heterocysts) was investigated for ammonia production. Several mediators were explored, and an anaerobic bag was used to keep the isolated nitrogenase in an oxygen free environment. It has been shown to mediate reduction of H^+ (See Figure 22), azide, and nitrite in an Argon environment to produce ammonia (Energy Environ. Sci., 2016, 9, 2550--2554). Cobaltocene was found to work best with an E^0 of -1.15 V vs SCE. This is a potential that can only be observed in an anaerobic environment. The presence of oxygen causes electrolysis of the electrolyte to happen at more positive potentials, obscuring signal that might have been observed from the cobaltocene. Further fundamental studies need to be done to understand electrochemical communication with nitrogenase before it can be applied to whole *A. vinelandii* or other non-heterocyst cyanobacteria. However, several challenges can be predicted for whole cells. First, if there are no membrane moieties to facilitate extracellular electron transfer, mediating nitrogenase will be challenging given the low potential required. Additionally, inhibiting glutamate synthetase will mean that the A. vinelandii will require a source of inorganic nitrogen other than ammonia to grow. But, providing a source (such as nitrate or nitrite) will repress nitrogenase expression, defeating the purpose.

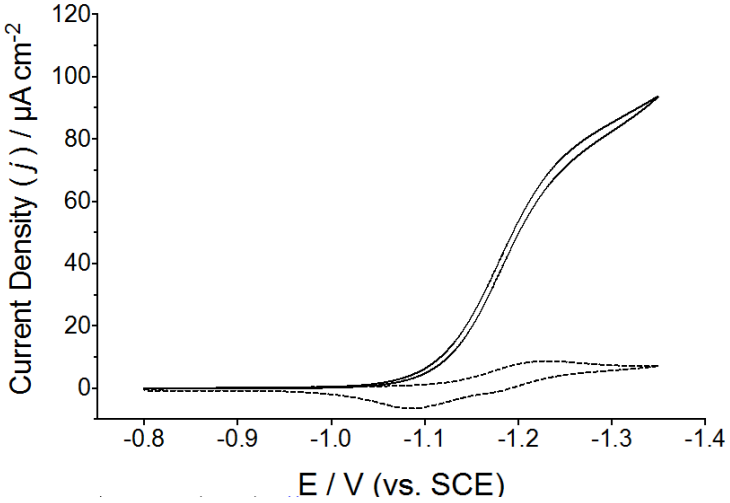

Figure 22. Overlay of 2 mV/s CVs of control bovine serum albumin (dotted line) and nitrogenase (solid line) mediated by cobaltocene.

Nitrogen Fixation Process Parameter Optimization.

The effort in Phase I portion of this project demonstrated that bioelectrocatalyzed nitrogen fixation is possible at an algae biofilm electrode. However, the amount of the ammonia generated was in the micromolar concentration range, which is not of practical use. Also, the time required to generate this amount of the ammonia was on the orders of hours. A significant portion of the Phase II effort was devoted to increasing the rate and amount of ammonia generated. A main thrust was focusing on several process parameters and how they affect the nitrogen fixation rate.

Electrostimulation waveform. Cyclic voltammetry and differential pulse amperometry (DPA) were used in the Phase I to stimulate the algae to increase the nitrogen fixation rate. While these methods have shown to be effective they can be time consuming and may be unnecessarily

complex for an industrial-scale synthesis process. Many industrial processes apply a simple DC voltage sufficient to drive the reaction at the desired current density. However, the algae biofilm requires both the oxidative and reductive reactions to fix nitrogen. This means an AC voltage waveform is required. This could be a sine wave, triangle wave or potential step. The ideal amplitude, frequency and duty cycle of the applied waveform will be determined for specific process conditions, e.g. electrolyte concentration which produces the most ammonia

The bioelectrocatalysis of nitrogen fixation with algae biofilms requires both the oxidation and reduction reactions. This was previously achieved using cyclic voltammetry and differential pulse amperometry (DPA). Amperometry is simpler electronically and is more likely to be used in a commercial process than a high-fidelity triangular waveform. The Phase I project demonstrated DPA's ability to stimulate nitrogen fixation via perturbation of SA-1 biofilms. It was a project goal to determine the optimum waveform for nitrogen fixation; what waveform stimulates the highest nitrogen fixation rate at the lowest power cost.

Differential pulse amperometry (DPA) was selected because both oxidation and reduction reactions are required for nitrogen fixation. Replicate experiments, at least 4, using a 3-electrode cell and square wave perturbation were finished in 0.1M Na_2SO_4. A Ag/AgCl reference electrode and stainless steel counter electrode were used. The Berthelot ammonia assay was used to measure ammonia generated, which included a 10 uM ammonium chloride standard solution to confirm the assay. Samples of the electrolyte solution, 5 mL, were collected and filtered through a 0.22 µm polypropylene syringe filter before analysis. Table 1 presents the final ammonia concentration for each square wave hold time. The general trend on longer hold time resulting higher ammonia concentration is followed.

Table 1. Ammonia Concentration, uM, for Various Square Wave Hold Times

Time	0.2 s	0.5 s	1 s	2 s	5 s	10 s
Culture 1, new	2 ± 1	0.3 ± 0.2	3 ± 3	8 ± 13	1.0 ± 0.7	11 ± 11
Culture 2	3 ± 2	3 ± 2	2 ± 2	2 ± 1	3 ± 2.0	4 ± 1
Culture 3, old	2 ± 1	1 ± 1	3 ± 2	2 ± 2	6 ± 6	20 ± 10

How the voltage window affects ammonia generation with carbon felt counter electrodes in 2 and 3-electrode configurations in Na_2SO_4 electrolyte solution was also examined. Figure 23 shows the measured ammonia concentration as a function of voltammetric cycle for 6 biofilm electrodes grown in each culture over 2 potential windows. A 2 -electrode configuration with carbon felt counter electrodes were used. The carbon felt counter electrodes were Alfa Aesar, 3.18mm, # 43199. Algae biofilm electrodes from each culture were tested by measuring the ammonia production when subjected to square-wave voltammetry, -0.6 to 0.8 and 1 V with 10 sec holds. Samples were collected every 75 cycles and analyzed for ammonia via Berthelot assay. Each point is the average concentration for 3 replicates and the error bars represent 1 standard deviation. No significant change in ammonia generation is observed when the voltage window is increased.

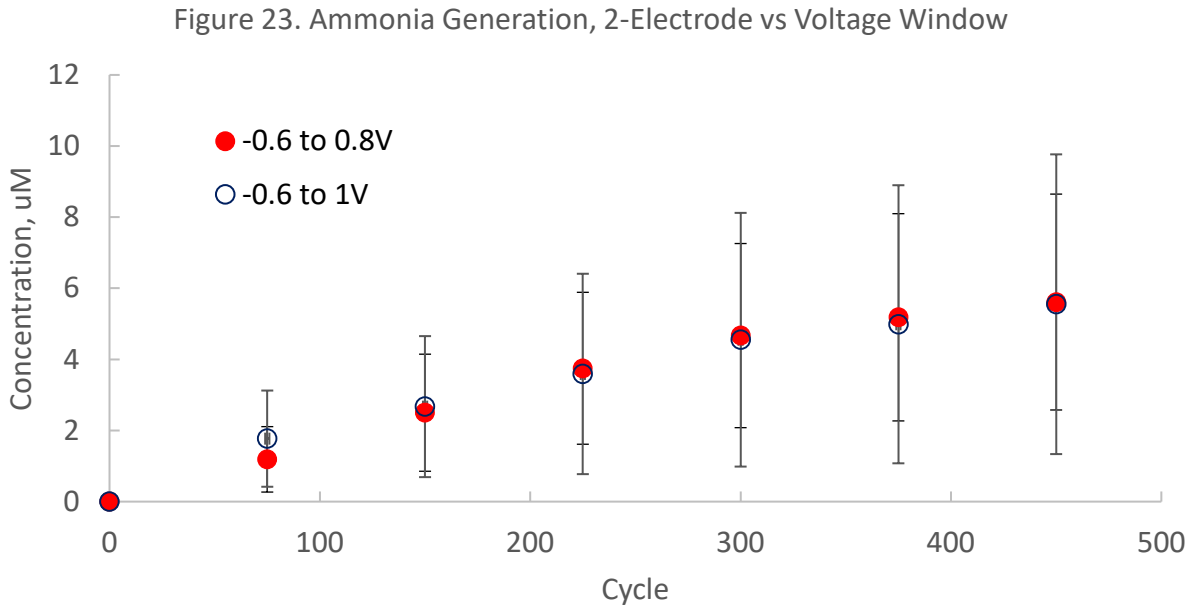

Figure 23. Measured ammonia concentrations for algae biofilm electrodes in a 2-electrode cell using carbon felt counter electrodes and 0.1 M Na_2SO_4 electrolyte. The biofilms were electrostimulated with square-wave voltammetry, -0.6 to 0.8 and 1 V, 10 sec steps, 50% duty cycle. Samples were collected every 75 cycles and analyzed with Berthelot assay. No significant difference is observed when the voltage window is increased.

For comparison, the same experiment was performed, in triplicate, with a Ag/AgCl reference electrode, Figure 24. Two voltage windows were used, -0.6 to 0.8 and 1 V vs Ag/AgCl. Samples were collected every 75 cycles and analyzed for ammonia via Berthelot assay. The error bars represent 1 standard deviation. Again, the 3-electrode configuration generates more ammonia with smaller standard deviation. This result is consistent with previous experiments and suggests that to achieve maximum ammonia production a reference electrode is necessary. While many industrial electrosynthesis processes, e.g. chloro-alkali, use 2-electrode configurations, the algae biofilms contain more complex electrochemical pathways that may require more precise voltages.

Of interest is that the smaller voltage window generated more ammonia than the larger window. This may be explained by the work performed at the University of Iowa which show increased ammonia generation at potentials that correspond to certain enzymatic pathways.

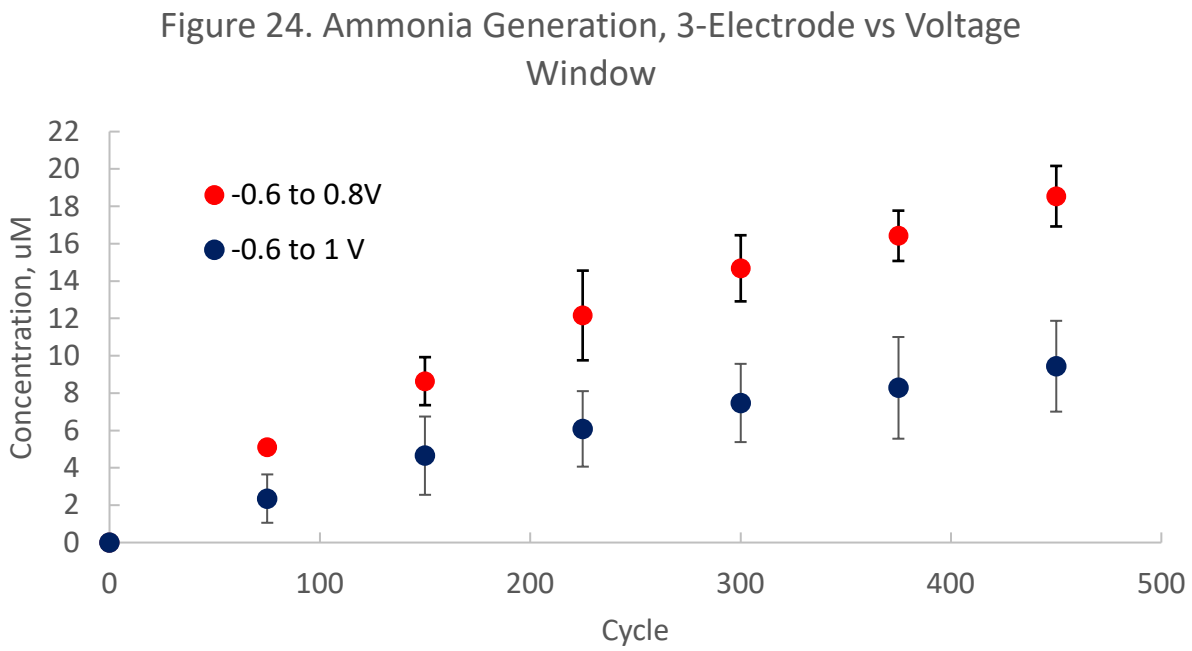

Figure 24. Measured ammonia concentrations for 6 biofilm electrodes in 3 cultures using carbon felt counter electrodes in 0.1 M Na_2SO_4. The biofilms were electrostimulated with square-wave voltammetry, 1 to -0.6 V, 10 sec steps, 50% duty cycle. Samples were collected every 75 cycles and analyzed with Berthelot assay. Ammonia production is essentially identical to that produced with a smaller potential window.

Following these results, attempts to make ammonia in BG-11° growth media were revisited. A Ag/AgCl reference electrode and carbon felt counter electrode were used. The voltage window -0.6 to 0.8 V was used. Chronoamperometry with 10 sec holds and 50% duty cycle was used. Samples were collected every 75 cycles and analyzed for ammonia via Berthelot assay. The results in triplicate are presented in Figure 25. The error bars represent 1 standard deviation.

The ammonia produced was relatively consistent, although more variable than when Na_2SO_4 electrolyte was used; 10 uM is readily achieved. This is the first successful production of ammonia in growth media. We attribute this to better algae biofilms and moving the voltage window negative 200 mV from -0.4 to 1 to -0.6 to 0.8 V vs Ag/AgCl. Experiments are underway to examine the voltage window of -0.6 to 1 V vs Ag/AgCl in Bg-11° growth media.

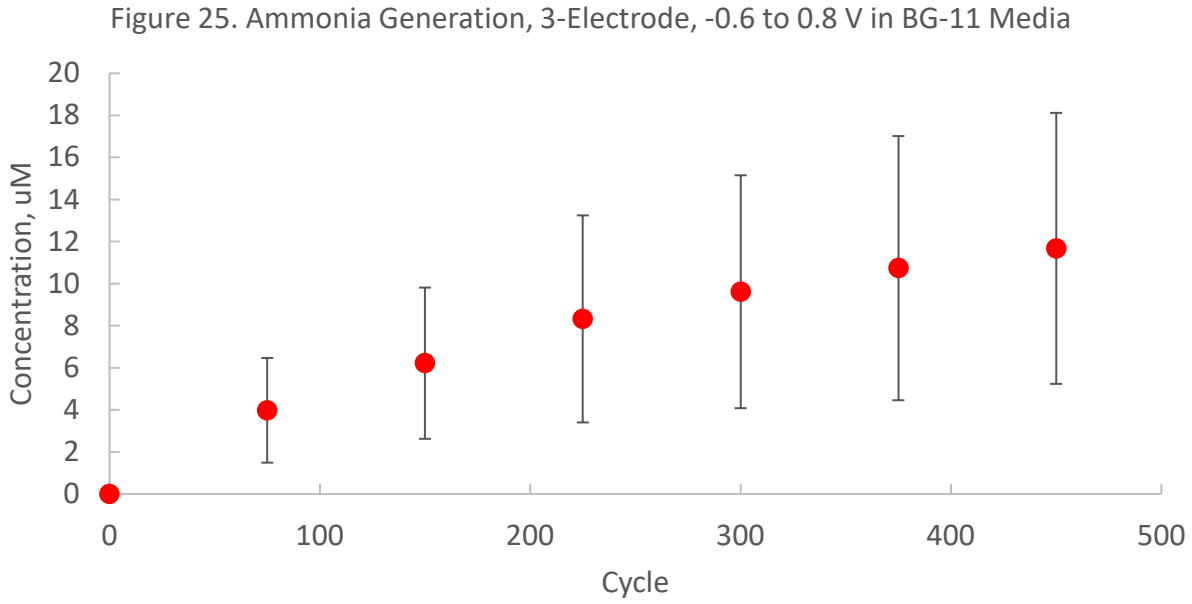

Figure 25. Measured ammonia concentrations for 6 biofilm electrodes in triplicate, carbon felt counter and Ag/AgCl reference electrodes in BG-11 growth media. The biofilms were electrostimulated with square-wave voltammetry, -0.6 to 0.8 V vs Ag/AgCl, 10 sec steps, 50% duty cycle. Samples were collected every 75 cycles and analyzed with Berthelot assay. Ammonia production is relatively consistent and a concentration 10 uM is regularly achieved. This is the first time ammonia was reliably generated in growth media.

Electrode Size

Electrosynthetic production rate is usually proportional to electrode surface area. However, the algae utilize enzymatic pathways which are unique to this system. The ammonia generation rate as a function of electrode size in BG-11° growth media with a 0.05M added electrolyte was measured.

We successfully generated ammonia in 400 mL of 0.1M Na_2SO_4 electrolyte solution at 16 µM concentration, 8% coulombic efficiency. However, more voltammetric perturbation was required, >1100 cycles: square-wave voltammetry, -0.6 to 1 V with 10 sec holds. It is hypothesized and reasonable that the limitation on making more ammonia is the size of the electrode. To test this, 6 biofilm electrodes, 20 cm^2 geometric area, were tested in 80, 120, 240 and 400 mL solutions of BG-11° media with 0.05M Na_2SO_4 electrolyte. Each biofilm electrode was subjected to 375 cycles, 1.0 to -0.6 V vs Ag/AgCl, with samples collected every 75 cycles. The ammonia concentrations were converted micromoles generated. Figure 26 shows the results and error, 1 standard deviation for the 6 biofilm electrodes.

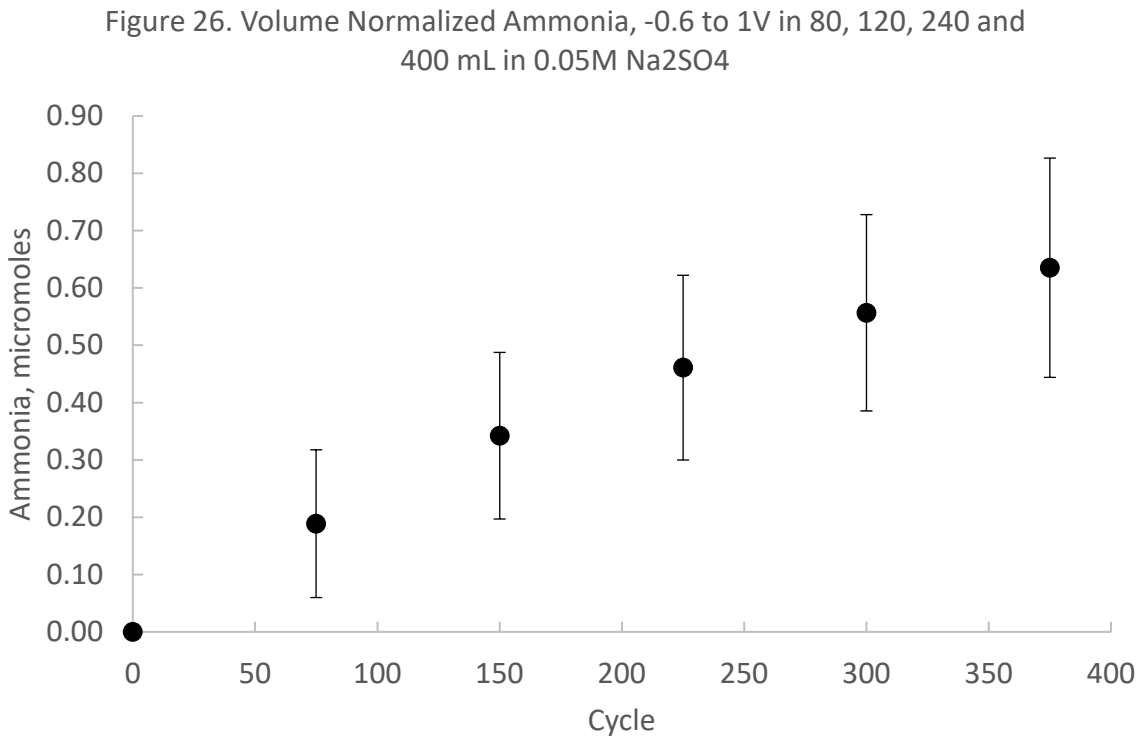

Figure 26. Measured ammonia concentration for 6 biofilm electrodes, carbon felt counter and Ag/AgCl reference electrode in 80, 120, 240 and 400mL of 0.05 M Na_2SO_4 electrolyte. The biofilms were electrostimulated with square-wave voltammetry, -0.6 to 1 V vs Ag/AgCl, 10 sec steps, 50% duty cycle. Samples were collected every 75 cycles and analyzed with Berthelot assay.

As expected, the ammonia generated was consistent with electrode area, **0.013 µmoles/cm^2/hr**, with the concentration decreasing with larger solution volume. Two larger carbon felt working electrodes, 40 cm^2, were grown in SA-1 culture for 3 weeks and electrostimulated for biofilm growth for 48 hours. These 2 larger carbon felt biofilm electrodes were tested in triplicate in 120 mL of BG-11° media with 0.05M Na_2SO_4 electrolyte. The same voltammetric perturbation conditions were used and samples analyzed by Berthelot assay.

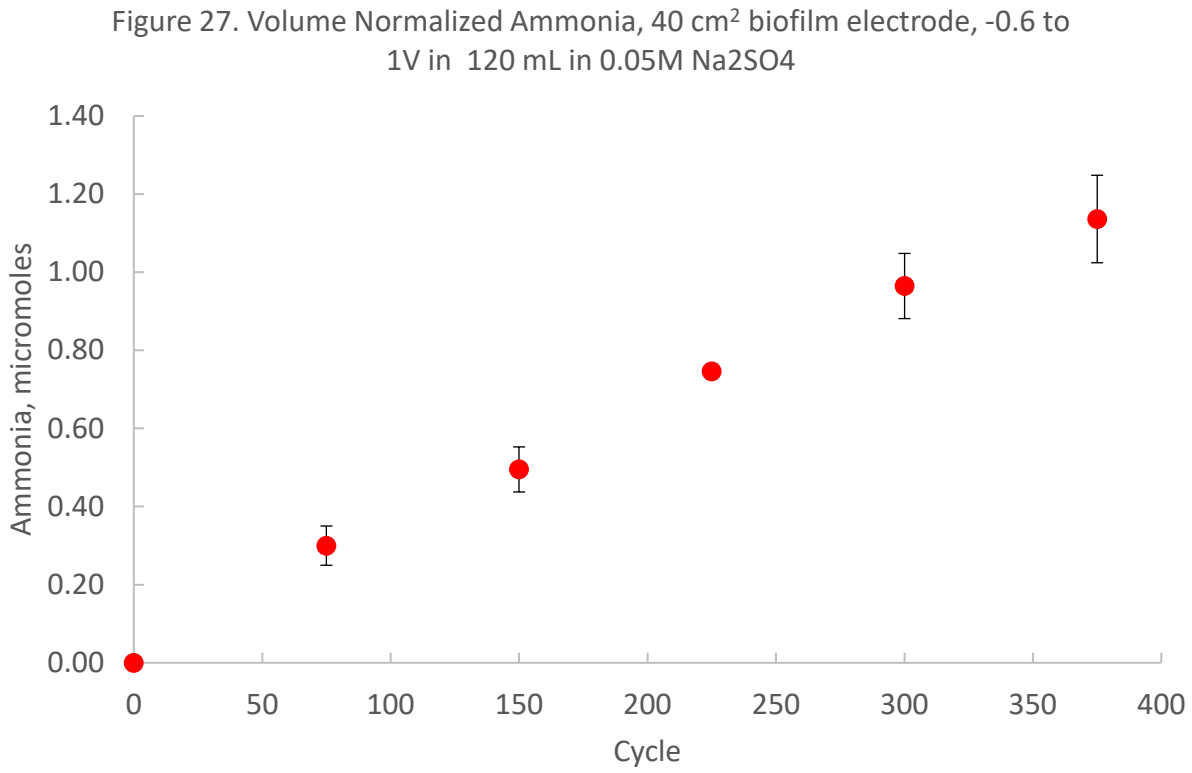

Figure 27. Measured triplicate ammonia concentration for 2 larger biofilm electrodes, 40 cm^2, carbon felt counter and Ag/AgCl reference electrode in 120 mL of 0.05 M Na_2SO_4 electrolyte. The biofilms were electrostimulated with square-wave voltammetry, -0.6 to 1 V vs Ag/AgCl, 10 sec steps, 50% duty cycle. Samples were collected every 75 cycles and analyzed with Berthelot assay.

The amount of ammonia generated is proportional to the area of the biofilms. The larger carbon felt biofilms generated **0.011 µmoles/cm^2/hr**, which is comparable to the earlier carbon foam electrodes, suggesting that carbon felt is comparable to vitreous carbon foam.

Cost Model

Assuming a production rate of 0.5 µmole ammonia per cm^2 per hour and a goal of 1 ton of ammonia per day, it would require ~450,000 m^2 of active electrode area. By increasing the production rate to 25 µmoles ammonia per cm^2 per hour, the required area is on ~9,000 m^2, approximately 2 football fields and within the realm of actual industrial processes such as chloro-alkali. The potential revenue for a 10 ton/day plant is $2.5MM/year with after electricity cost **profit of $500,000/year**. A wholesale electricity cost of $25/MWhr, 15% coulombic efficiency and a market sale price of $700/ton is assumed. From that total revenue, payroll for 3 full time equivalent employees, $41k/year/employee, and 100% G&A, leaves $250k/year for facilities, repayment and net profit. Our current ammonia generation rate of **0.013 µmoles/cm^2/hr** will need to be significantly increased for a commercially viable process.

Electrolyte Cation Identity

It was hypothesized that sodium ions are necessary for the bioelectrocatalytic fixation of nitrogen. The presence of sodium ions has been shown to enhance the activity of the whole cell algae. We suspected that the low concentration of sodium ions in the growth media inhibited nitrogen fixation. To test this hypothesis, and experiment was performed in 0.1 M K_2SO_4, which will maintain the ionic strength of the electrolyte, but remove the sodium. The biofilm electrode 3A and 3B were used, after the new biofilms were grown. Figure 28 shows the ammonia measured for both electrodes using Na_2SO_4 and K_2SO_4 as electrolyte.

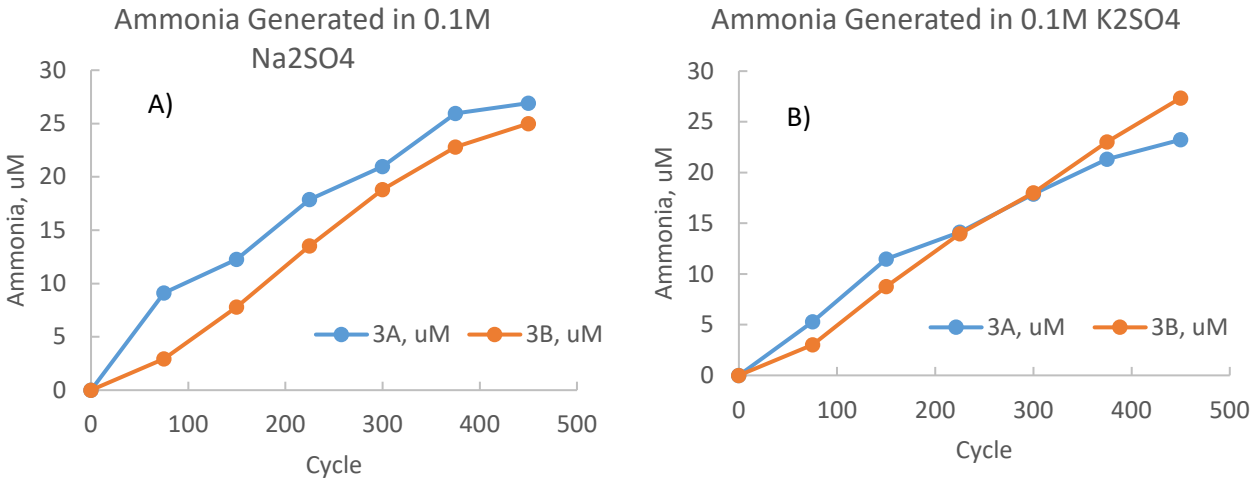

Figure 28. A) Ammonia production for 2 biofilm electrodes in 0.1M Na_2SO_4 and B) 0.1M K_2SO_4. The square-wave voltammetric perturbation was 1 to -0.4 V vs Ag/AgCl, with 10 sec. holds and 50% duty cycle. The similar results suggest that sodium is not the required for bioelectrocatalytic nitrogen fixation and electrolyte concentration/conductivity is more important.

The ammonia generated is remarkably consistent, irrespective of the electrolyte cation. It is hypothesized that it is the electrolyte concentration and conductivity that affects the ammonia bioelectrocatalysis.

Counter Electrode Material

One of the goals of the Phase II project is to develop the algae-based nitrogen fixation process from a laboratory to a commercial process. One aspect of this is the use of non-noble metals for the counter electrodes. Previous electrochemistry used Pt mesh counter electrodes. While chemically inert, Pt is too expensive for a commercial process. The SA-1 algae biofilms were grown on P100 vitreous carbon electrodes for 3 weeks. Electrical connection was stimulated by applying a 0.6V bias to the electrodes for 36 hours. A stainless steel mesh counter electrode (DexMet 5SS 316L 7-077) was made and compared to Pt and Ni. Cyclic voltammetry was performed on 2 SA-1 biofilm electrodes in 0.1M Na_2SO_4 solution at 20 mV/s from 1 to -.4 V vs Ag/AgCl. Figure 29 shows the third voltammogram for both biofilm electrodes with different counter electrodes.

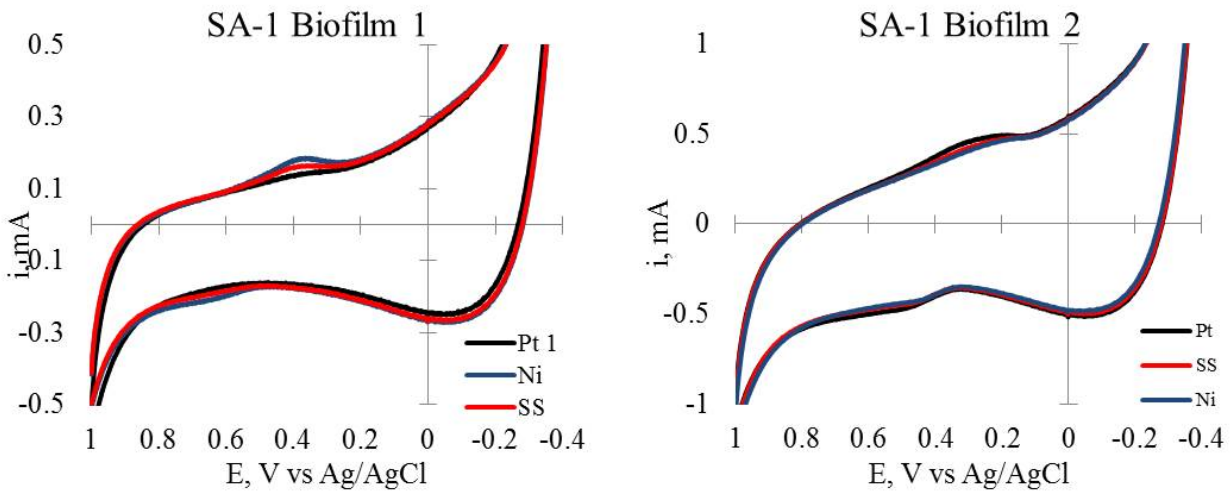

Figure 29. Cyclic voltammograms, 20 mV/s, of 2 biofilm electrodes with different counter electrodes. The electrodes were both grown in the same incubator. The height of the reductive and oxidative peak decrease with continuing cycling. There is no significant difference in peak position between the counter electrode materials. Electrode 2 exhibits a peak shift toward negative potentials.

The voltammetric response are similar between the different counter electrodes. There are differences in voltammetric peak height but peak position is nearly identical and importantly, there are no new peaks that would indicate metal corrosion under these conditions. The oxidative and reductive peaks are at 0.375 and 0.650 V vs Ag/AgCl, respectively. This is more negative than 10 days after media refreshing when the oxidative and reductive peaks are at 0.300 and 0.610 V vs Ag/AgCl, respectively and closer to the aged biofilm response.

During DPA experiments to generate ammonia, the stainless-steel electrodes slowly discolor and corrode over time. The potential window and electrolyte concentrations suggest that non-precious metal counter electrodes will all corrode and it is uneconomical for a large scale industrial process to use platinum or the like. A low-cost alternative is carbon felt.

Carbon felt counter electrodes were cut to shape and waxed to prevent solution wicking, Alfa Aesar, 3.18mm, # 43199. Algae biofilm electrodes from each culture were tested by comparing the ammonia production with stainless steel and carbon felt counter electrodes. Each biofilm electrode was subjected to square-wave voltammetry, 1 to -0.4 V vs Ag/AgCl, with 10 sec holds, Ag/AgCl reference electrode and either carbon felt or stainless steel mesh counter electrode. Samples were collected every 75 cycles and analyzed for ammonia via Berthelot assay.

The results for the 6 biofilm electrodes are tabulated in Table 2. The ammonia generation is remarkably consistent. The one significant difference is with biofilm electrode 3B, which repeatedly exhibited no ammonia production with a stainless steel counter electrode, however produced 10 uM ammonia when a carbon felt counter electrode was substituted. This enhancement is currently unexplained. Carbon felt is being used on all subsequent biofilm electrochemistry.

Table 2. Biofilm Ammonia Production with Different Counter Electrodes						
	1A	1B	2A	2B	3A	3B
Cycle	Stainless Steel Counter Electrode					
75	2.0	0.1	10.0	3.6	2.5	0.0
150	4.4	2.4	13.9	5.9	3.5	0.0
225	7.5	1.6	19.1	12.4	6.0	0.0
300	7.8	3.2	18.4	17.7	7.4	0.0
375	9.3	2.7	20.9	19.9	8.8	0.0
450	11.1	3.5	26.0	24.3	10.2	0.0
Cycle	Carbon Felt Counter Electrode					
75	3.5	2.7	4.3	1.7	4.5	6.1
150	6.0	4.3	11.4	4.7	10.3	4.2
225	8.7	6.0	12.9	8.5	10.4	7.1
300	8.9	6.6	16.8	12.9	12.4	7.3
375	10.4	7.8	18.8	16.2	14.3	8.6
450	11.7	8.8	21.2	21.9	15.3	10.7

Results showed that carbon felt counter electrodes can be used in lieu of metal mesh counter electrodes with little to no degradation in ammonia generation. Replicate experiments were conducted in 2 and 3-electrode configurations to improve statistical confidence. Algae biofilm electrodes from each culture were tested by measuring the ammonia production when subjected to square-wave voltammetry, 1 to -0.4 V vs Ag/AgCl, with 10 sec holds, Ag/AgCl reference electrode and carbon felt counter electrodes. Samples were collected every 75 cycles and analyzed for ammonia via Berthelot assay. When in 2-electrode configuration, the same 1 to -0.4 V potential window was used. Figure 30 shows the measured ammonia concentration as a function of voltammetric cycle for 3 different cultures and 2 biofilm electrodes grown in each culture. Each graph is the average concentration for 3 replicates and the error bars represent 1 standard deviation. The graphs show that an ammonia concentration of ~10 uM can be reliably obtained by most electrodes with the proper algae biofilms.

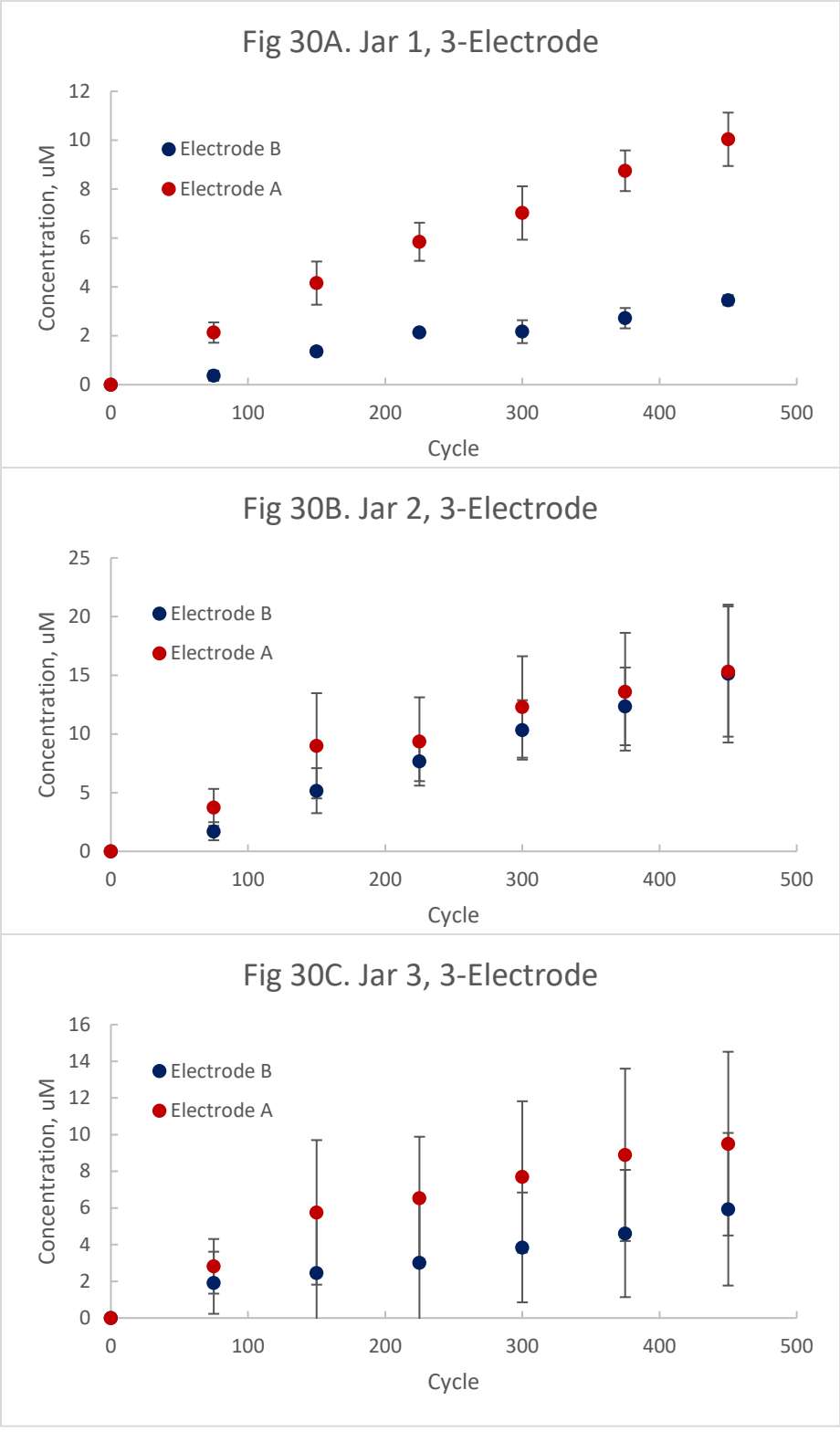

Figure 30. Measured ammonia concentrations for 6 biofilm electrodes from 3 algae cultures using carbon felt counter electrodes and Ag/AgCl reference electrode. The biofilms were electrostimulated with square-wave voltammetry, 1 to -0.4 V vs Ag/AgCl, 10 sec steps, 50% duty cycle. Samples were collected every 75 cycles and analyzed with Berthelot assay.

Further replicates were performed on the 2-electrode cell configuration. Each biofilm electrode was subjected to square-wave voltammetry, 1 to -0.4 V vs carbon felt counter electrode with 10 s holds. Samples were collected every 75 cycles and analyzed for ammonia via Berthelot assay. Figure 31 shows the ammonia concentration versus cycle for the same 6 biofilm electrodes grown in 3 cultures. The error bars represent 1 standard deviation.

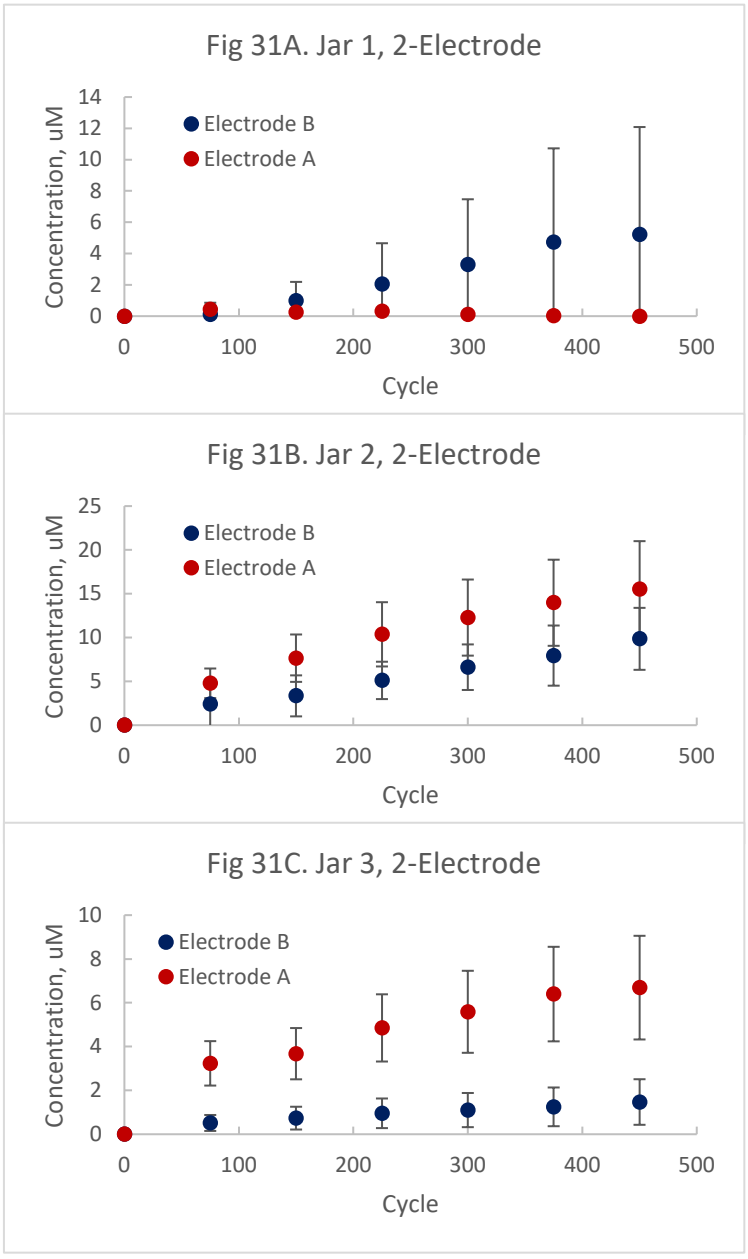

Figure 31. Measured ammonia concentrations for 6 biofilm electrodes in 3 cultures, 2A, 2B and 2C, using carbon felt counter electrodes and Ag/AgCl reference electrode. The biofilms were electrostimulated with square-wave voltammetry, 1 to -0.4 V vs Ag/AgCl, 10 sec steps, 50% duty cycle. Samples were collected every 75 cycles and analyzed with Berthelot assay. Ammonia production was generally lower, but still measurable.

Ammonia generation was lower and less consistent than in 3-electrode configuration. Some biofilm electrodes perform comparably when used with a reference electrodes, while others do not make measurable ammonia amounts.

Fabrication, testing and evaluation of bioelectrocatalyzed nitrogen-fixation test stand.

Because the Fulcrum process utilizes a cathode with a biofilm grown on it, the process parameters will be uniquely complex compared to a typical electrosynthesis process. Larger algae growth cultures were fabricated along with test cells which contained biofilm electrodes for in-situ testing of ammonia generation. Several factors were investigated including:

Electrolyte Concentration. The algae are grown in a low electrolyte media. In an electrosynthetic process, a lower conductivity increases costs through ohmic losses. Therefore it is necessary to determine the lowest practical electrolyte concentration that enables ammonia generation while also maintaining algae viability.

Ammonia extraction. The ammonia generated by the SA-1 cyanobacteria is solubilized as ammonium ion at pH below 9.25. While this may be acceptable for some applications, e.g. fertilizer, pure ammonia is required for many applications. The extraction of ammonia from an ammonium solution can be easily achieved by increasing the pH through the addition of base. However, the addition of chemical base adds another feedstock, increases costs and complexity. One possible solution is an electrolytic separation cell that voltammetrically splits water into protons and hydroxide. The locally increased pH at the cathode should drive the deprotonation of ammonium to ammonia. The current density will be matched to the nitrogen fixation rate to minimize lowering the pH of the overall cell media.

Electrode materials, design and interconnects. The Phase I effort used a variety of electrode materials but focused on high-surface area carbon electrodes, e.g. porous vitreous carbon. A large platinum anode was used, but this is impractical from a cost standpoint. The feasibility of using algae biofilm electrodes in a 2-electrode cell as both working and counter will be investigated. The electrode geometry and separation distance will need to be optimized; too far and ohmic resistance is high, too close and solution flow is inhibited. Another consideration is connecting the electrodes to external power. The connections must be robust and corrosion resistant. Initial experiments used simple copper connections and resulted in corrosion and copper salt deposits.

Applied current and therefore voltage or overpotential. Any commercial electrosynthesis process attempts to maximize production rate, roughly equivalent to current density, while minimizing overpotential. However, a high current density can result in too high of an overpotential. This condition can lead to parasitic side reactions that lower efficiency or dielectric breakdown of reactants or products. Neither of which is acceptable for commercial process.

Electrolyte Concentration

The bioelectrocatalyzed synthesis of ammonia in BG-11° media was performed media without the trace metal ions to highlight the voltammetry of the biofilm. The series of experiments using SA-1 biofilm electrodes and chronoamperometric square wave voltammetry with varying step times produced essentially no ammonia compared to the same experiments in performed in 0.1 M Na_2SO_4.

The voltammetric peak position was measured for the 6 biofilm electrodes, 2x3 cultures, as function of increasing electrolyte strength. While some electrodes exhibited nearly ideal voltammetry, others exhibited significantly different voltammetry. Figure 32 shows a comparison of the 3rd voltammogram, 20 mV/s of electrode 3B in BG-11 and Na_2SO_4. Electrode 2A is shown for comparison of a nearly ideal response.

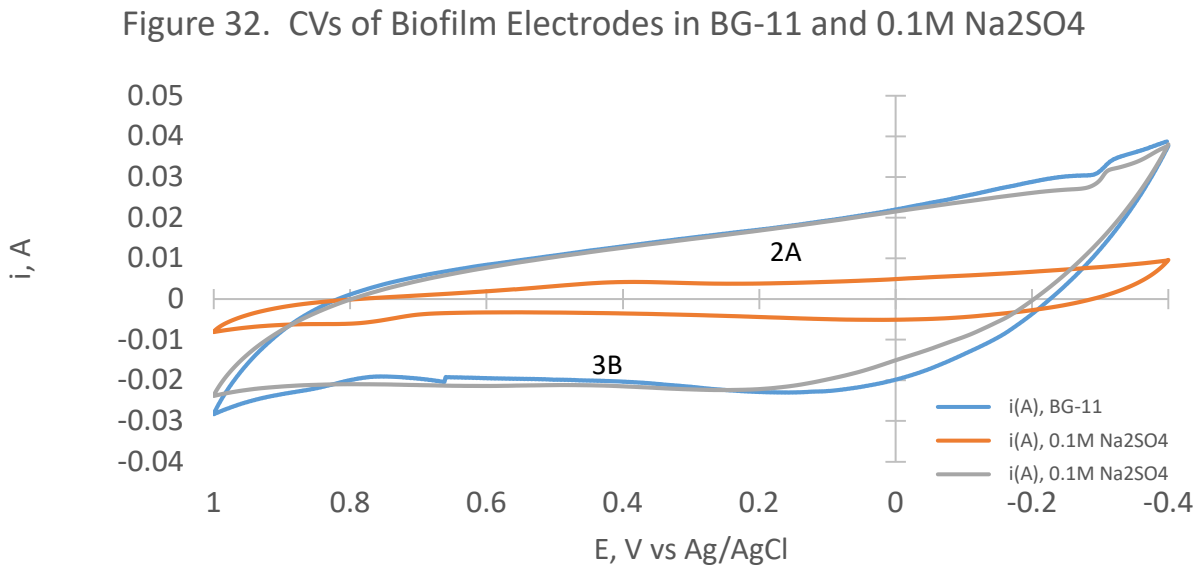

Figure 32. Cyclic voltammograms at 20 mV/s for biofilm electrodes 2A in 0.1 M Na_2SO_4 and 3B in 0.1 M Na_2SO_4 and BG-11 media.

Of note is the oxidation peak for electrode 3B is more positive and the reductive peak is significantly more negative than for electrode 2A, regardless of electrolyte. The capacitive response is also significantly larger than electrode 2A regardless of electrolyte strength. Compared to previously reported result on electrode 2A, this result suggests that the voltammetry of electrodes is characteristic of each individual biofilm and not overly reliant on the electrolyte, as both electrodes generate ammonia when electrochemically stimulated.

The position of the reduction and oxidation peaks as function of the electrolyte concentration is shown in Figure 33. The results are comparable to those reported in the Phase I effort, in that the peaks move together by ~300 mV. The absolute position of the peaks can vary significantly from electrode to electrode.

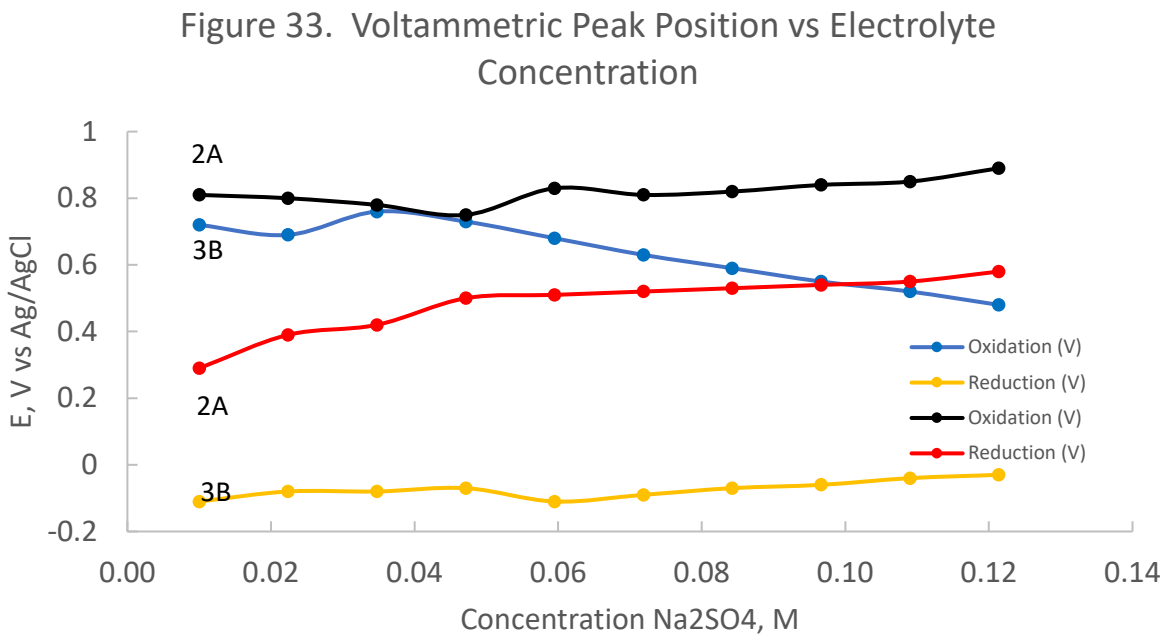

Figure 33. Voltammetric peak position as a function of electrolyte concentration for 2 different biofilm electrodes. The difference in the voltammetric response appears characteristic of each individual electrode. Both electrodes produce ammonia when perturbed via chronoamperometry.

To further explore the relationship of electrolyte concentration and ammonia generation, a series of experiments was performed where the electrolyte concentration is increased and decreased while applying square-wave chronoamperometry at 10 sec holds. The electrolyte concentration was increased from 0.01 to 0.12 M and decreased from 0.12 and 0.025 M Na_2SO_4 by serial addition or dilution. Cyclic voltammetry was performed at each concentration and samples were collected for Berthelot assay analysis. The experiment was repeated for all biofilm electrodes and several different responses were observed. Figure 34, 35 and 36 show the ammonia generated for each biofilm electrode in the 3 different algae cultures.

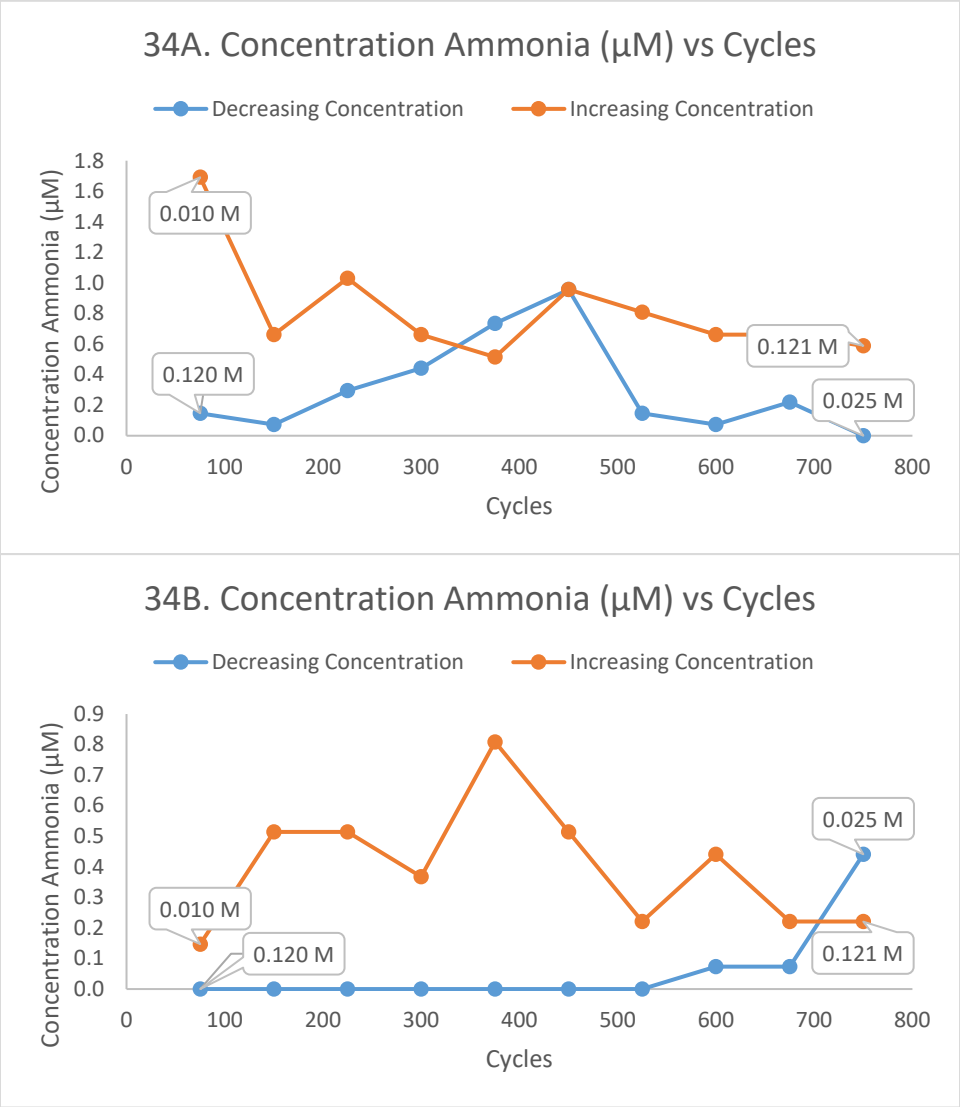

Figure 34. Ammonia generation as a function of electrolyte concentration and voltage perturbation cycle for biofilm electrode A and B grown in culture 1.

For culture 1, electrode A shows little response to the direction of concentration change or total concentration. However, unlike the previous results, there was also no response to the electrochemical cycling. Electrode B exhibited inconsistent ammonia generation with increasing electrolyte concentration. When decreasing the electrolyte concentration, no trend nor ammonia was observed, which is consistent with previous results.

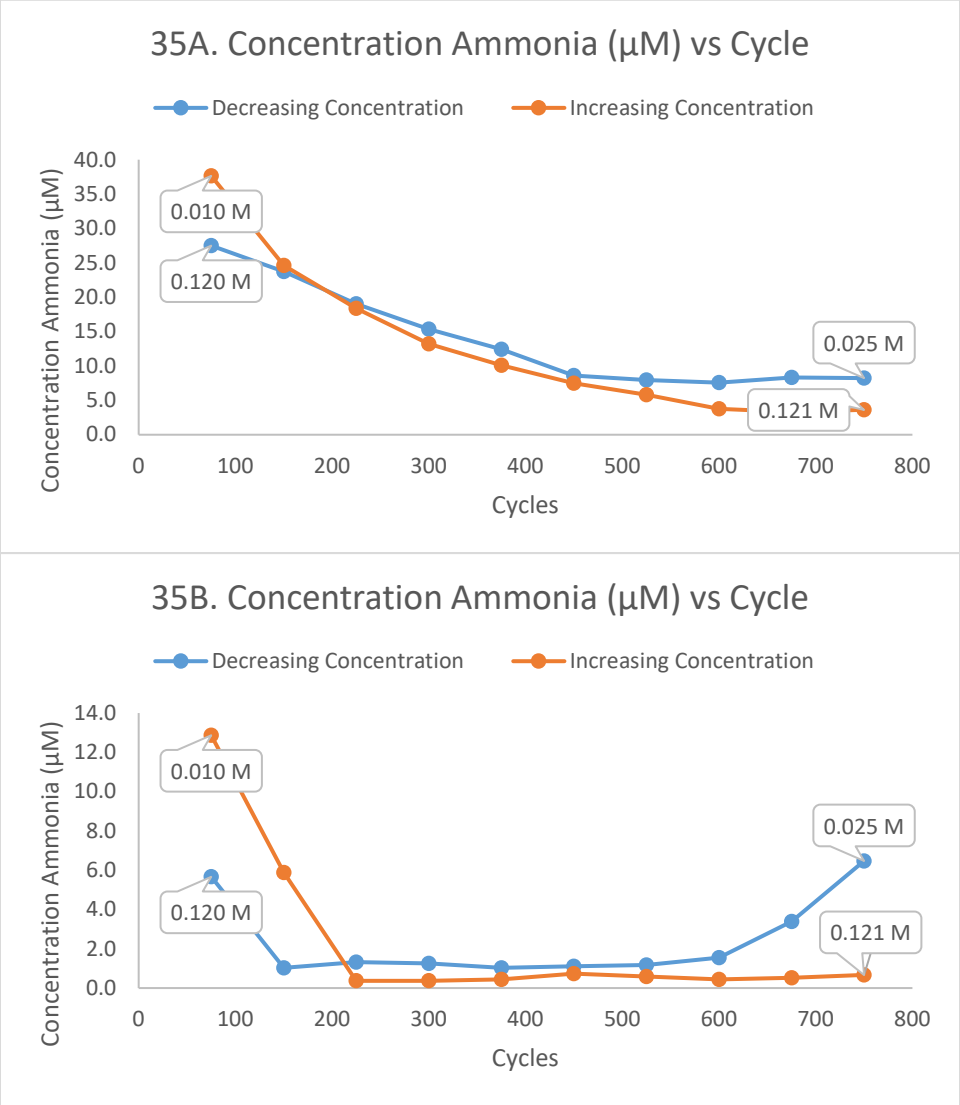

Figure 35. Ammonia generation as a function of electrolyte concentration and voltage perturbation cycle for biofilm electrode A and B grown in culture 2.

Biofilm electrode 2A showed no trend for either electrolyte concentration or voltammetric cycle, consistent with previous. However, it exhibited some of the highest ammonia concentrations achieved to date, >25 uM, which decreased as electrode was cycled. Blanks and controls ruled out contamination of the electrolyte or growth media. Electrode 2B generated exhibited the same trend of not responding to electrolyte concentration or cycling and also decreasing in measured ammonia with cycling, except a small increase with increasing cycling.

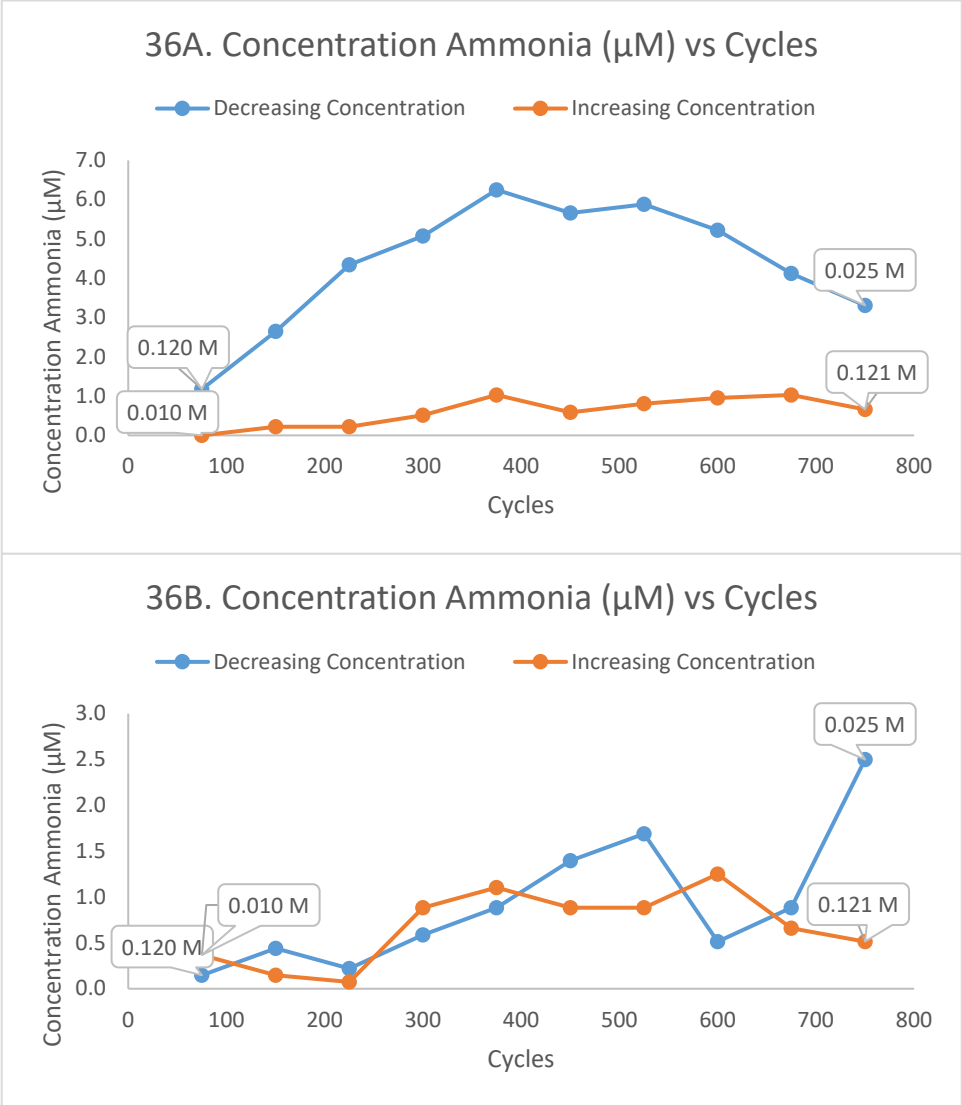

Figure 36. Ammonia generation as a function of electrolyte concentration and voltage perturbation cycle for biofilm electrode A and B grown in culture 3.

Biofilm electrode 3A exhibited higher ammonia generation as the electrolyte concentration decreases with more cycling, reaching a maximum at ~400 cycles and 70 mM electrolyte. Previously, this biofilm showed increased ammonia as the electrolyte concentration increased. Increasing the electrolyte during this replicate slowly increased ammonia production while cycling. Electrode 3B exhibited roughly similar behavior with increasing ammonia production with decreasing and increasing electrolyte concentration. However, the ammonia production was more variable and the voltammetric cycling had the greatest influence on ammonia production. The response of electrode 3B is consistent with the previously reported response of the biofilm.

These results are highly variable, however, generally the ammonia generation increased with increasing electrolyte concentration and voltammetric perturbation. Decreasing the electrolyte concentration, while voltammetrically cycling resulted in little ammonia generation. **Further supporting the hypothesis that both electrolyte and voltammetric perturbation is needed for ammonia generation.**

In-Situ Ammonia Generation

Ammonia generation was performed in 80 mL of BG-11 growth media with DPA a 3-electrode cell and a voltage window of -0.6 to 0.8 V vs Ag/AgCl, 10 sec holds. The data set is presented in Figure 37. A final average ammonia concentration of 12 ± 6 uM after 450 cycles was achieved.

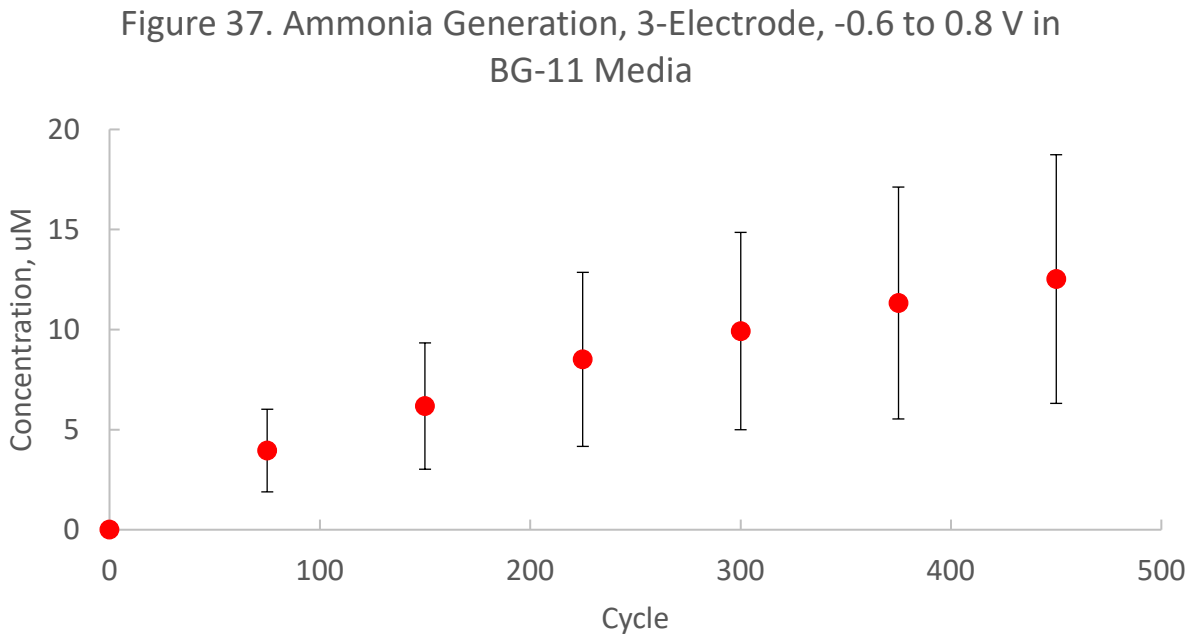

Figure 37. Measured ammonia concentrations for 6 biofilm electrodes, 4 replicates, carbon felt counter and Ag/AgCl reference electrodes in BG-11 growth media. The biofilms were electrostimulated with square-wave voltammetry, -0.6 to 0.8 V vs Ag/AgCl, 10 sec steps, 50% duty cycle. Samples were collected every 75 cycles and analyzed with Berthelot assay. Ammonia production is relatively consistent and a concentration 10 uM is regularly achieved.

Following this result, experiments were performed in-situ, in the growth culture flasks, ~500 mL. Carbon felt counter electrodes were suspended in solution and reference electrode was inserted through a port. The algae biofilm electrodes subjected to square-wave voltammetry, -0.6 to 0.8 V with 10 sec holds. Due to the larger volume, samples were collected every 150 cycles and analyzed for ammonia via Berthelot assay. Even though an estimated 3uM ammonia should have been generated, multiple runs did not result in detected ammonia.

It was suspected that the large volume was diluting the ammonia to below the detection limit of the assay. The solution volume was reduced to 250 mL and the number of cycles between samples increased to 225. All other parameters were the same. Figure 38 shows ammonia concentration generated in a neat growth media solution.

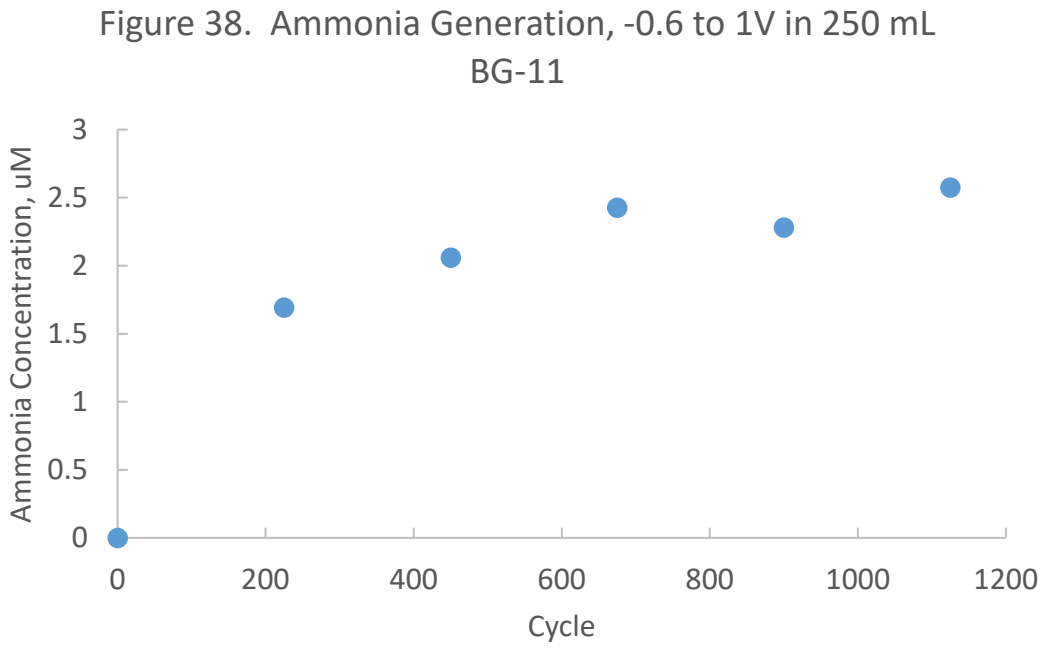

Figure 38. Measured ammonia concentrations for a biofilm electrode using a carbon felt counter electrodes in 250 mL BG-11° growth media. The biofilms were electrostimulated with square-wave voltammetry, -0.6 to 1 V, 10 sec steps, 50% duty cycle. Samples were collected every 225 cycles and analyzed with Berthelot assay.

These results suggest that scaling up to a large volume and performing in situ are 2 more parameters essential to ammonia generation. While ammonia was generated when the volume was reduced to 250 mL, only one successful run was achieved. Therefore, effort was directed at performing ammonia generation in larger volumes, 400 mL vs 80 mL, of BG-11° growth media with a minimal amount of added electrolyte. It was hypothesized that ammonia generation is possible in larger volumes if electrolyte is added to solution. An experiment was performed in 400 mL of 0.1M Na_2SO_4 electrolyte solution. The algae biofilm electrode was subjected to square-wave voltammetry, -0.6 to 1 V with 10 sec. holds. Due to the larger volume, samples were collected every 225 cycles and analyzed for ammonia via Berthelot assay. A final concentration of **16 µM at 8% coulombic efficiency** was achieved.

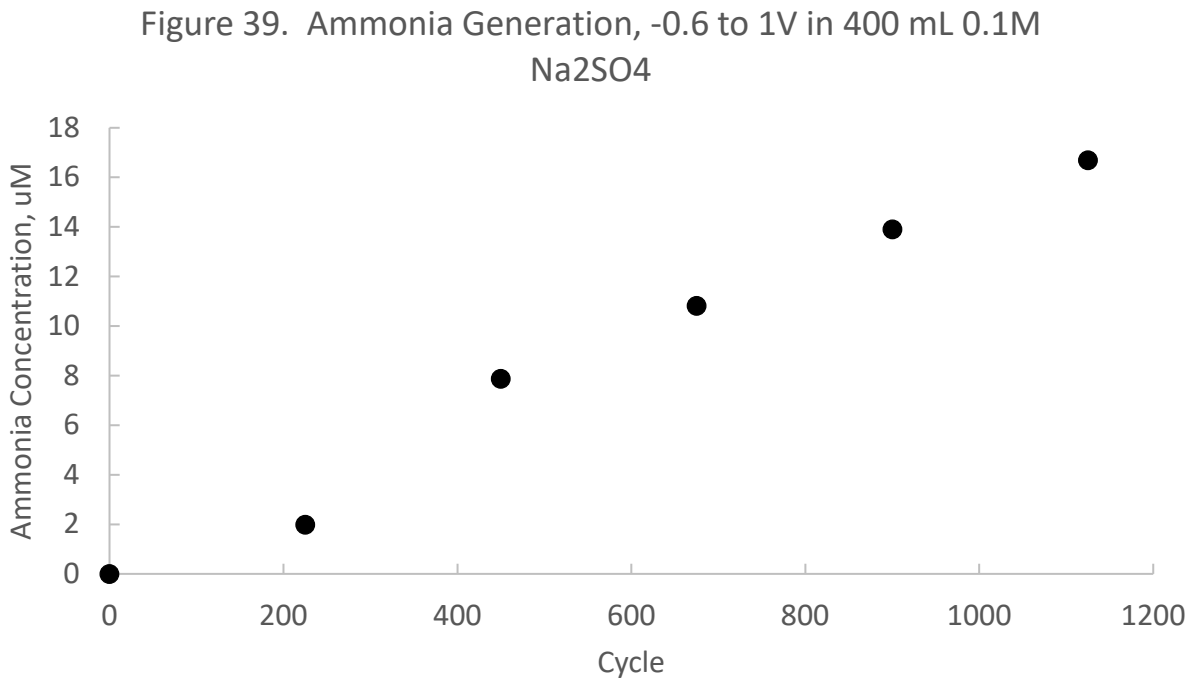

Figure 39. Measured ammonia concentration for 1 biofilm electrode, carbon felt counter and Ag/AgCl reference electrode in 400 mL 0.1 M Na_2SO_4 electrolyte. The biofilm was electrostimulated with square-wave voltammetry, -0.6 to 1 V vs Ag/AgCl, 10 sec steps, 50% duty cycle. Samples were collected every 225 cycles and analyzed with Berthelot assay. Ammonia production was significant and a concentration >16 uM was achieved.

Based on this result further experiments were performed using 0.05 M Na_2SO_4 electrolyte. The lower electrolyte concentration was used based on earlier 0.05 M Na_2SO_4 is the lowest electrolyte concentration without significantly changing the voltammetry. Figure 40 shows ammonia concentration in 400 mL of 0.05 M Na_2SO_4 electrolyte solution. The algae biofilm electrodes were subjected to square-wave voltammetry, -0.6 to 1 V with 10 sec holds. Due to the larger volume, samples were collected every 225 cycles and analyzed for ammonia via Berthelot assay.

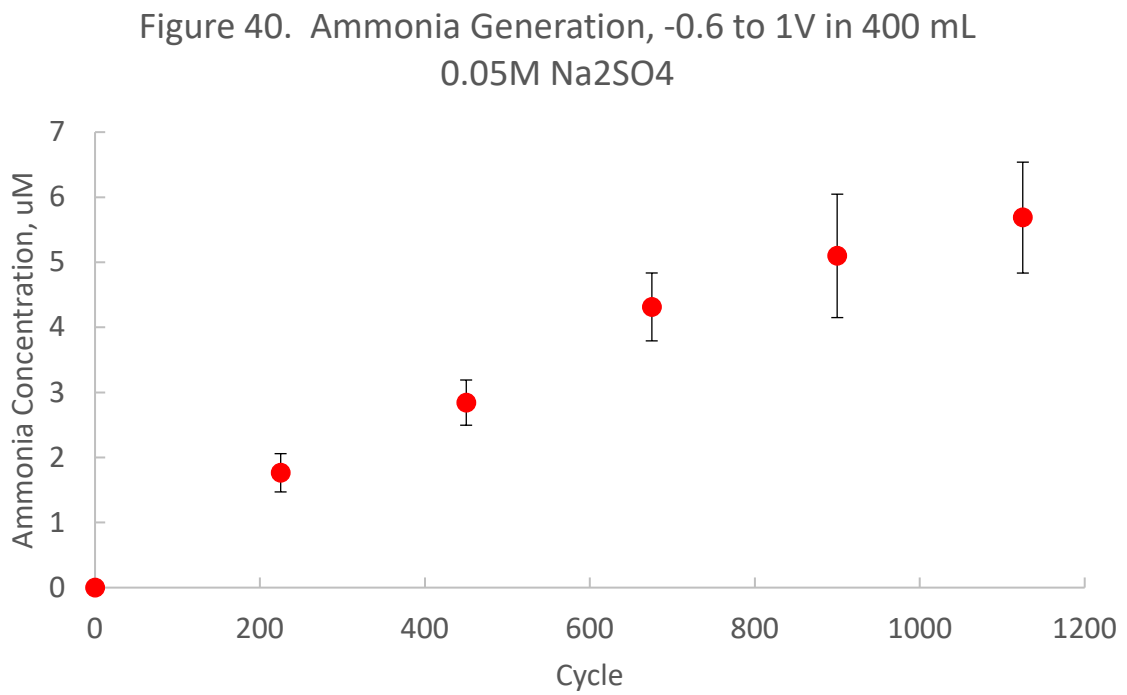

Figure 40. Measured ammonia concentrations for 3 biofilm electrodes using a carbon felt counter electrodes in 400 mL 0.05 M Na_2SO_4 electrolyte solution. The biofilms were electrostimulated with square-wave voltammetry, -0.6 to 1 V, 10 sec steps, 50% duty cycle. Samples were collected every 225 cycles and analyzed with Berthelot assay.

The use of dilute electrolyte solution led to higher ammonia concentrations than with neat media, although lower than when 0.1M electrolyte.

Process Scale-Up

Scaling up the ammonia generation process began by utilizing a larger algae biofilm electrodes, ~100 cm^2, and a larger growth cells, ~350 mL. Two cells with concentric 100 cm^2 carbon felt electrodes were assembled and SA-1 algae were inoculated in both, Figure 41. Biofilm growth and electrical connectivity was electrostimulated using established techniques. Testing has focused on the more mature culture that uses wax coated electrode tabs. Cyclic voltammetry was performed in-situ with a Ag/AgCl reference electrode and electrolyte solution added to bring total salt concentration to ~0.05 M Na_2SO_4. The larger concentric carbon felt electrode was used as the counter. After testing, the electrolyte solution was pumped out and replaced with fresh media.

Figure 41. New SA-1 cultures with 100 cm^2 carbon felt electrodes using a waxed carbon felt tab.

Based on the isolated enzyme voltammetry which suggested nitrogenase reduction at more negative potentials, the potential window was expanded to 0.8 to -1 V vs Ag/AgCl. A representative cyclic voltammogram, 20 mV/s, is shown in Figure 42. There are 2 electrochemical reactions evident voltammogram. On the first scan, a reduction peak at 0.3 V and a corresponding oxidation peak at 0.5 V and a larger reduction peak at -0.7 and less distinct oxidation peak at -0.1 V. After the first scan, the smaller voltammetric peaks in the positive region disappear, while the reaction in the negative region are still present. It is suspected that the voltammetry in the negative region are due to the nitrogenase reactions.

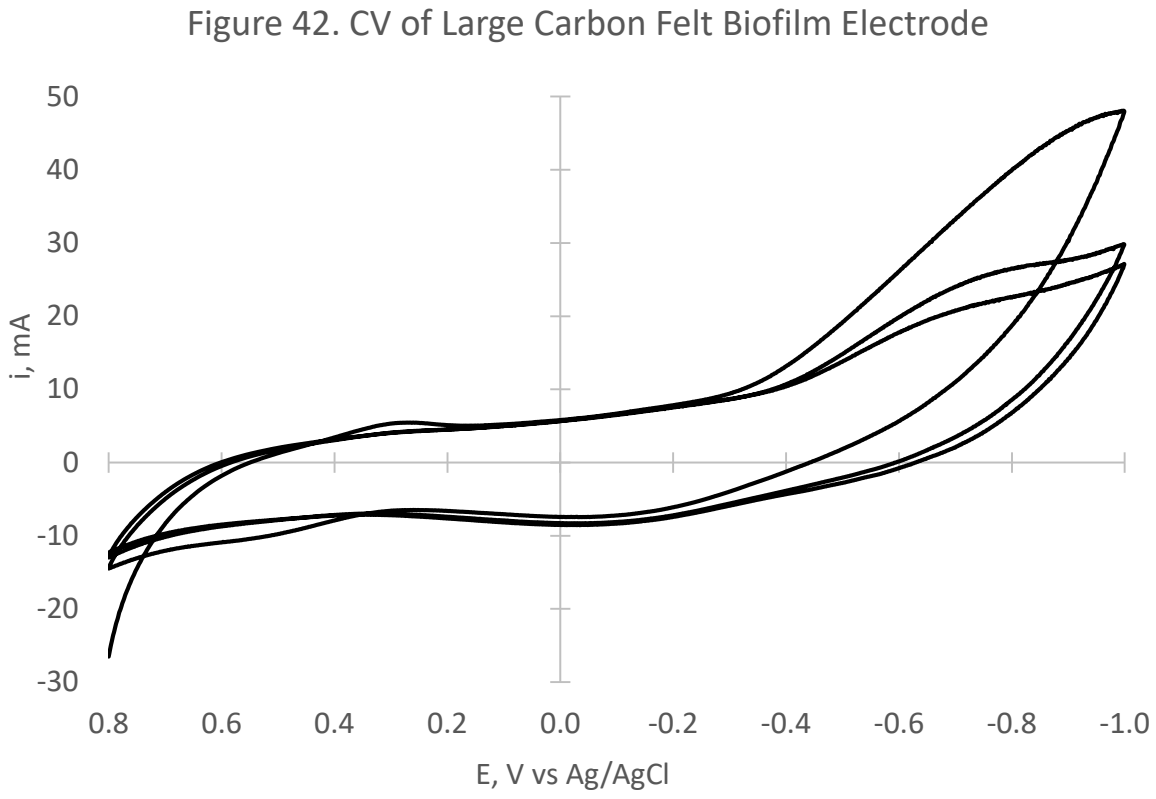

Figure 42. Cyclic voltammogram of the large area, 100 cm^2, carbon felt biofilm electrode in 0.0-5 M Na_2SO_4 with a carbon felt counter electrode. An oxidation and reduction peak are present on the first scan at 0.5 and 0.3 V, respectively and -0.1 and -0.7 V vs Ag/AgCl. It is suspected that the larger, more negative voltammetry corresponds to the nitrogenase reaction.

Square-wave chronoamperometry was repeatedly attempted by applying 0.8 to -1 V vs Ag/AgCl in 0.05 M Na_2SO_4 with 10 sec holds. Samples were collected every 75 cycles and analyzed via Berthelot assay. The ammonia measured was very inconsistent. Some experiments resulted in significant ammonia being measured, > 40 µM, while other runs results in no appreciable change. Of particular note, weekly monitoring of the culture has recorded very high ammonia levels, >200 µM. This may be due to delayed response to the voltammetric perturbation or from the algae making ammonia on its own. If true, this could increase the commercial viability by generating appreciable ammonia without increased electricity costs. Figure 43 shows 2 experimental runs where the initial ammonia in the cell was much higher than previous experiments and increased during the experiment

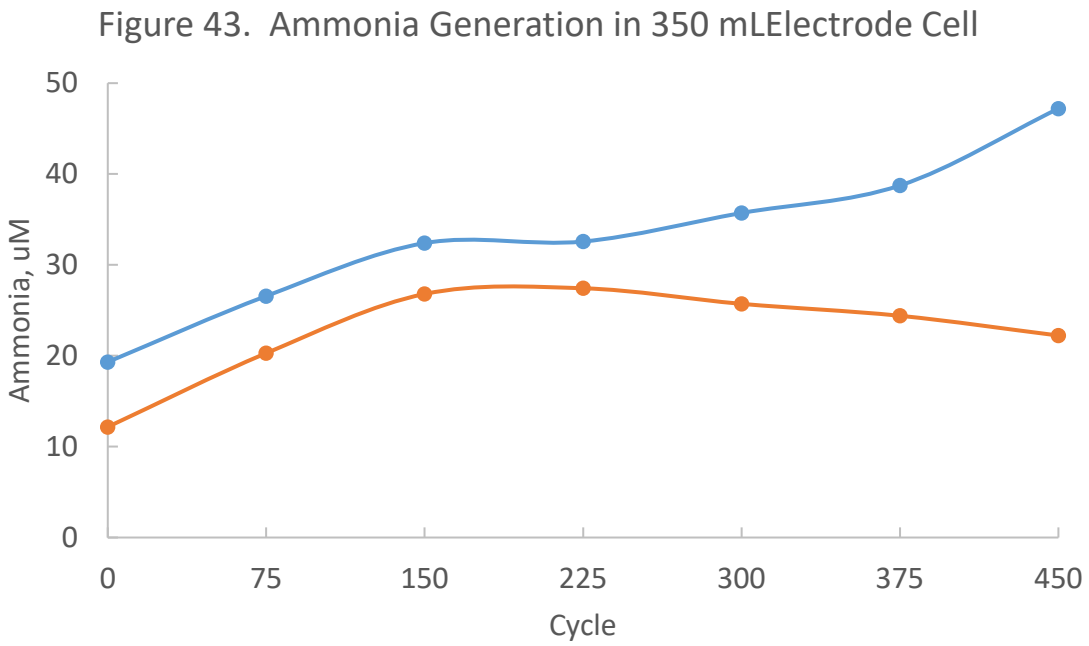

Figure 43. Ammonia concentration for the large electrode cell during chronoamperometry. The high initial ammonia concentration may be due to delayed response or from latent production by the algae without electrochemical perturbation.

A larger ammonia cell, ~3 l, was fabricated and inoculated with SA-1 algae. Two carbon felt electrodes, ~200 cm^2, with conductive carbon fiber current collectors were inserted. This cell

Figure 44. New large volume cell, 3l with carbon felt electrodes and carbon fiber current collectors.

has ports for air input, output and solution sampling, Figure 44. Cyclic voltammetry was performed in-situ with a Ag/AgCl reference electrode and electrolyte solution added to bring total salt concentration to ~0.05 M Na_2SO_4. After testing, the electrolyte solution was pumped out and replaced with fresh media. The larger 3 L cell uses 2 parallel 200 cm^2 carbon felt electrodes connected to conductive carbon fiber current collectors. During testing, a reference electrode is inserted through a port in cap and the no electrolyte is added. The electrodes are ~3 cm apart and the media is mixed with a stir bar. Solution samples are pumped out for analysis and replaced with fresh media. The potential window was expanded to 0.8 to -1 V vs Ag/AgCl. Figure 45 shows representative cyclic voltammograms, 20 mV/s, for the 200 cm^2 and one of the 100 cm^2 biofilm electrodes.

Figure 45. CV of 100 and 200 cm^2 Carbon Felt Biofilms

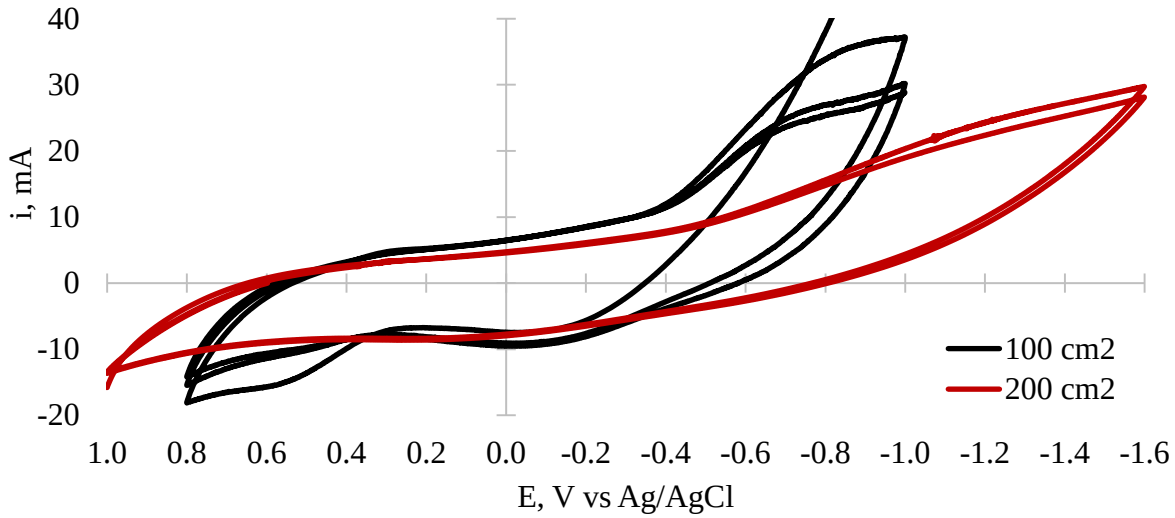

Figure 45. Cyclic voltammogram of the large area, 100 cm2, carbon felt biofilm electrode in 0.0-5 M Na2SO4 with a carbon felt counter electrode. An oxidation and reduction peak are present on the first scan at 0.5 and 0.3 V, respectively and -0.1 and -0.7 V vs AgCl. It is suspected that the larger, more negative voltammetry corresponds to the nitrogenase reaction.

As seen previously, there are 2 electrochemical reactions evident, at 0.4 and -0.5 V. The potential window was increased for the larger cell due to increased ohmic resistance. The reduction reaction is evident but less defined. It is suspected that the voltammetry in the negative region are due to the nitrogenase reactions.

A large SA-1 algae culture ~2 liters was grown with carbon felt working electrodes, Figure 46. These carbon-felt electrodes are the same material used as counter electrodes, Alfa Aesar, 3.18mm, # 43199, and are ~ 20 x 5 cm in size; significantly larger than the vitreous carbon electrodes. While large in dimensions, the actual active area is probably smaller due to the lack of large pores, i.e. the algae biofilm remains on the exterior surface. Biofilm electrostimulation was performed by applying +/- 650 mV for 48 hours in 4 hour intervals in the growth culture. Cyclic voltammetry was performed and exhibited the expected peaks at 650 and 300 mV vs Ag/AgCl. Bioelectrocatalytic nitrogen fixation was attempted several times using a carbon felt counter electrodes and Ag/AgCl reference electrode in 0.1 M $NaSO_4$ using the same square wave voltammetry as described above. Samples were collected at 75 cycle intervals and analyzed via

Berthelot assay. Figure 47 shows the measure ammonia concentrations for the 2 biofilm electrodes.

Figure 47. The experimental setup for algae bioelectrocatalyzed ammonia generation, separation and concentration. The algae biofilm electrode is in the jar on the left and the 3-compartment electrochemical cell is on the right. The white cylinder is a commercial water filter.

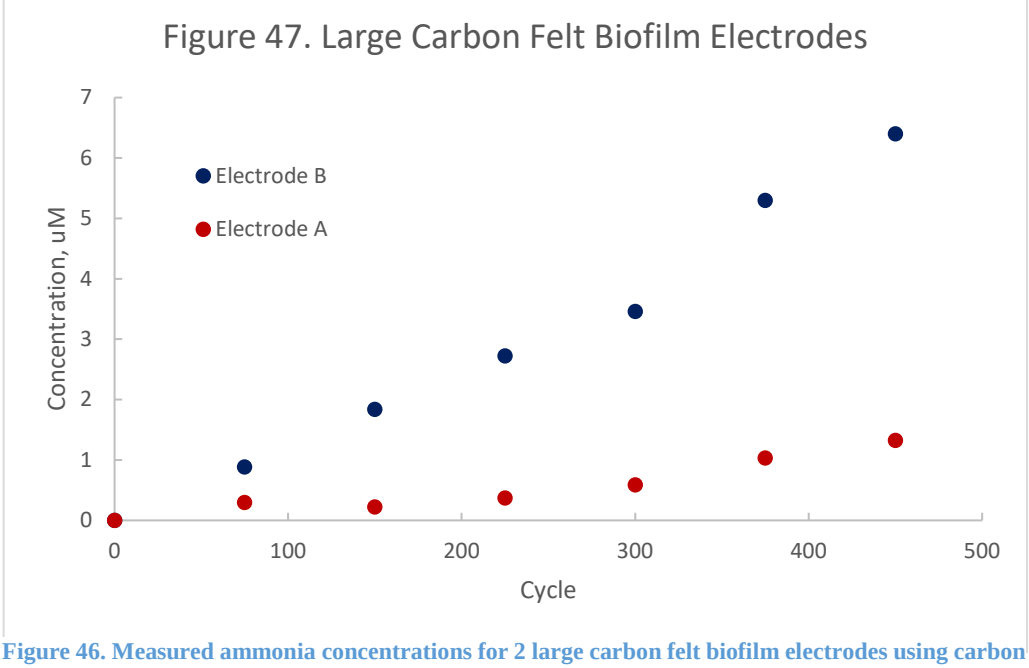

Figure 46. Measured ammonia concentrations for 2 large carbon felt biofilm electrodes using carbon felt counter electrodes and a Ag/AgCl reference electrode. The biofilms were electrostimulated with square-wave voltammetry, 1 to -0.4 V vs Ag/AgCl, 10 sec steps, 50% duty cycle. Samples were collected every 75 cycles and analyzed with Berthelot assay. Ammonia production is lower than the vitreous carbon electrodes, probably due to lower active biofilm area.

Ammonia Separation

A process to separate and isolate ammonia from the cell that does not use added chemicals was assembled. The process used an ElectroCell MicroCell and both cation and anion exchange membrane to protonate the ammonia via local pH change and transport across into a separate storage tank. The pH in the algae stream was moderated by a second electrochemical reaction generating hydroxide. The ultimate output will be an ammonium hydroxide stream and acidic waste. The relevant reactions are:

1)	$H_2O \rightarrow 2H^+ + ½O_2\,(g) + 2e^-$	anode
2)	$NH_3 + H^+ \rightarrow NH_4^+$	Sample solution
3)	$H_2O + e^- \rightarrow OH^- + ½H_2\,(g)$	cathode

Figure 48 shows the preliminary setup. Electrochemical separation of ammonia from solution was investigated using a 3-compartment cell and both anion and cation exchange membranes. Early experiments demonstrated that is possible to remove ~60% of ammonium from the anolyte by electrochemically buffering the sample solution pH. The pH drop is due to water electrolysis and reduces efficiency because of proton conduction across the Nafion membrane. Using an anion exchange membrane can prevent the sample solution pH from dropping and increase the amount of ammonia removed from the sample.

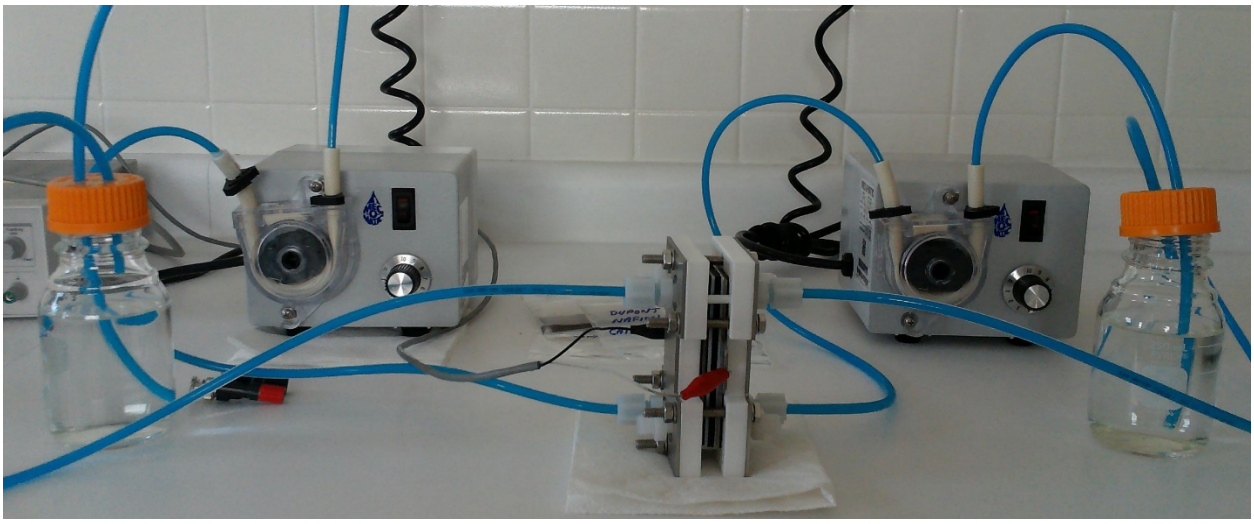

Figure 48. Picture of the preliminary ammonia separation process. A MicroCell with Nafion 424 membrane, DSA and stainless steel cathode are used. A DC power supply applies 3.2 V to split water and change the local pH in the anolyte and transport ammonium across the Nafion membrane to the catholyte solution.

Anion exchange membranes, Membranes International Inc AMI-7001S and Nafion 212 membranes, Alfa Aesar, were assembled in the MicroCell with DSA anode and Nickel cathode. The sample solution was SA-1 growth media with ~40 uM NH_4^+. The anolyte and catholyte was 0.1M $NaSO_4$ in distilled water. The pH of the sample solution was monitored, while the starting and final pH of the anolyte and catholyte were measured. A voltage of 3-4 V DC was applied for 210 minutes. Samples were collected in approximately 30 min. intervals and analyzed via Berthelot assay. Figure 49 shows the results of ammonia separation for 3, 3.5 and 4V and sample pH.

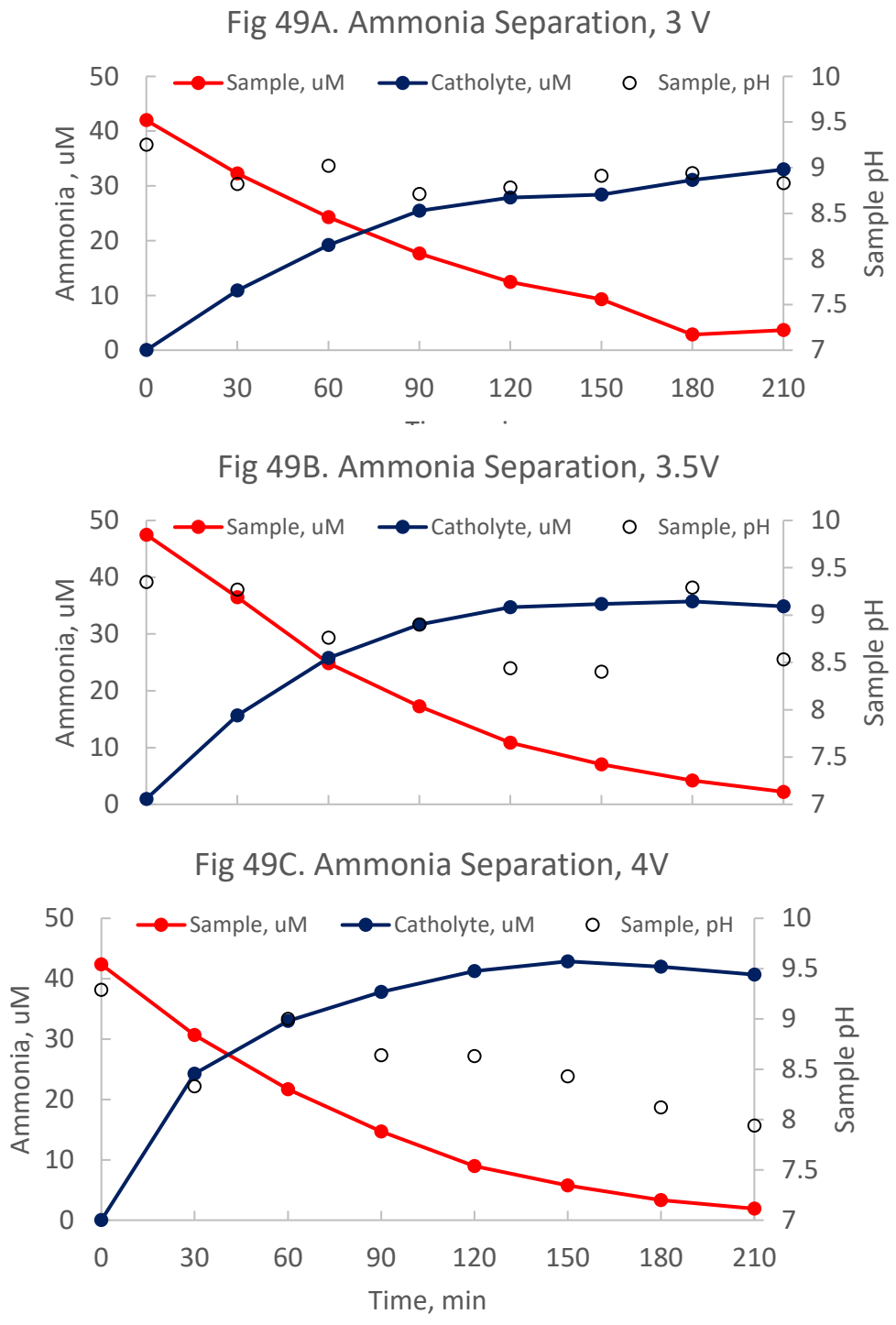

Figure 49. Ammonia concentration of the media sample and catholyte and sample pH during 3-compartment electrochemical separation at 3, 3.5 and 4 V, (4A, B, C). The sample began with ~40 uM ammonium and the anolyte and catholyte 0.1 M NaSO4. Unlike previous experiments, the sample pH was steady and greater than 90% extraction was achieved. No sudden pH change was observed in the growth media sample. A small pH decrease is expected due to removal of ammonia.

When compared to earlier separations, there was no sudden drop in sample pH as the ammonia is removed from solution. As expected that catholyte pH increases from 9 to 11 and the anolyte pH drops from 9 to 4. Interestingly, there was no significant difference in separation rate as a function of applied potential. Greater than 90% separation was achieved without a significant change in the sample solution pH.

Actual growth media with ammonia added was also tested. This sample had algae cultures in it which were filtered using a course filter paper. Experiments were also attempted to

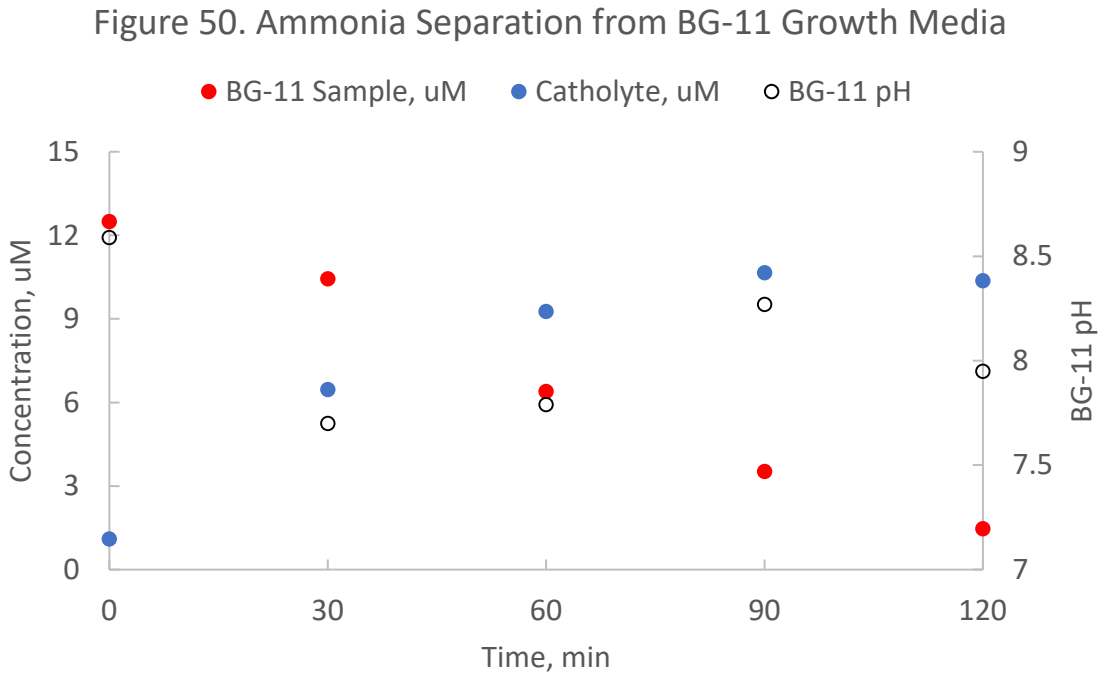

Figure 50. Ammonia concentration of BG-11 growth media sample and catholyte and sample pH during 3-compartment electrochemical separation at 4 V. The sample began with ~12 uM ammonium and the anolyte and catholyte 0.1 M Na2SO4. The sample pH was steady and greater than 90% extraction was achieved. No sudden pH change was observed in the growth media sample. The BG-11 media was from an actual growth culture with ammonia added.

concentrate the ammonia production solution. The same electrochemical cell setup was used. Anion exchange membranes, Membranes International Inc AMI-7001S and cation exchange Nafion 212 membranes, Alfa Aesar, were assembled in the MicroCell with DSA anode and Nickel cathode. The sample solution was SA-1 growth media with ~12 uM NH_4^+. The anolyte and catholyte was 0.1M $NaSO_4$ in distilled water. The pH of the sample solution was monitored, while the starting and final pH of the anolyte and catholyte were measured. A voltage of 4 V DC was applied for 120 minutes. Samples were collected in approximately 30 min. intervals and analyzed via Berthelot assay. Figure 50 represents the ammonia separation and sample pH. There was no sudden drop in sample pH as the ammonia is removed from solution. As expected that catholyte pH increases from 9 to 11 and the anolyte pH drops from 9 to 4. Table 3 presents extraction percentages for multiple runs.

Table 3. Ammonia Separation Efficiency from BG-11 Growth Media

Sample	Percent Extracted
1	98%
2	49%*
3	80%
4	92%
5	92%

*algae filter failure

While the electrochemical separation method has proven that ammonia can be removed, the output is dilute, µM. It would be more useful to be able to generate a concentrated ammonia solution. A large volume, 500 mL of a dilute ammonia, 30 µM, in BG-11 growth media was used as the sample and a smaller, 50 mL, volume catholyte was used to attempt to concentrate the product. Figure 51 shows the resulting concentrations after 180 minutes at 4V. A final product concentration of 0.1 mM ammonia was achieved, 87% molar separation efficiency.

Figure 51. Ammonia Concentration in the Product Stream

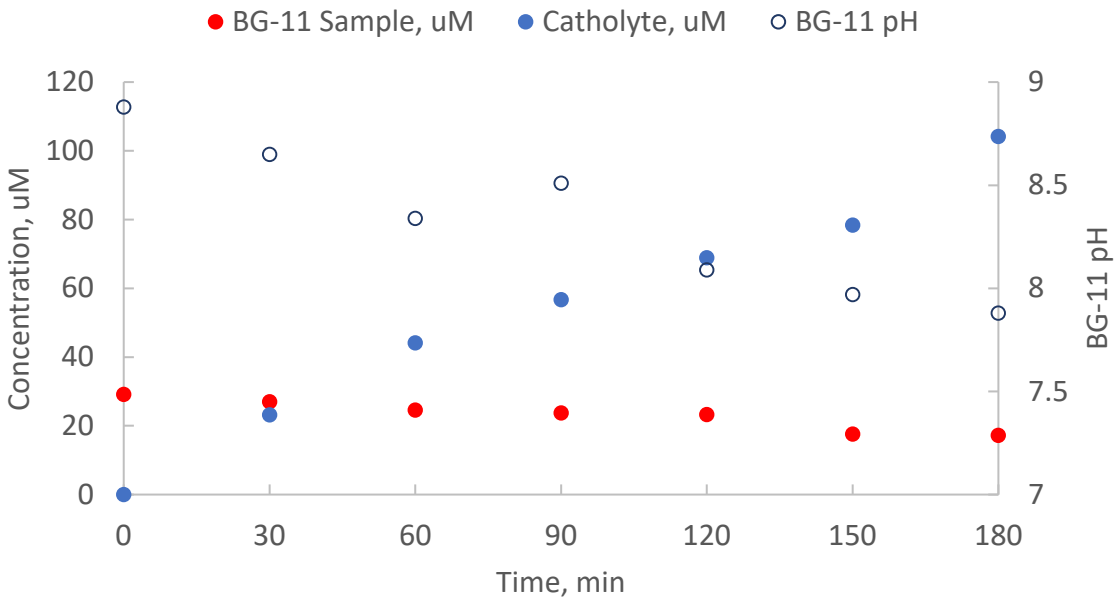

Figure 51. Concentration of dilute ammonia in BG-11 growth media sample. The BG-11 sample, 500 mL, concentration drops from 30 to 17 uM and catholyte ammonia concentration reaches 104 uM in 50 mL. The sample pH during 3-compartment electrochemical separation at 4 V drops slightly. The anolyte and catholyte have 0.1 M Na2SO4.

Algae Nitrogen Fixation Mechanism

Detailed in this report are the results for experiments aimed at determining the mechanism of electron transfer to nitrogenase enzyme in the SA-1 mutant variant of *Anabaena Variabilis*. To ascertain the role of fixed-nitrogen sources on ammonia production, several nitrogen containing species were added to the electrolyte during cyclic voltammetric perturbation. Different voltammetric techniques were employed to understand how the functioning of nitrogenase may be explored. The role of the photosystems were investigated because ATP, which is supplied by the photosystems, is necessary in the biological reduction of dinitrogen to ammonia. Different

electrode materials as well as different methods of whole cell immobilization on an electrode have been investigated to understand the electrode/cell interaction.

Addition of nitrate and nitrite to the electrolyte

To differentiate between ammonia production by nitrate/nitrite reductase and by nitrogenase, nitrate and nitrite were added to the electrolyte solution. Nitrate/nitrite reductase enzyme present in vegetative cells only, uses nitrate and nitrite as substrate for ammonia production. [5-7] Nitrogenase present only in heterocystic cells utilizes only dinitrogen as substrate for ammonia production. [1-4] By employing a vegetative-only cell strain, and adding nitrate and nitrite to the electrolyte, it was hoped that these experiments would yield some information about how to study the two enzymes individually.

Four electrolyte solutions were prepared: 0.02M, 0.05M, and 0.1M and were made in 0.1M Na_2SO_4, not degassed. One solution was left NO_3^-/NO_2^- free. Glassy carbon electrodes, 0.20cm^2, were polished with alumina and soaked in 1M nitric acid then rinsed before use or modification. One was left bare, 6µL of TMOA modified Nafion was cast onto another. Two electrodes received 6µL castings of 2:1 (v/v) ratio of cells:TMOA. After the films were dried, the electrodes with cells received an additional 6µL of TMOA to ensure the cells were not lost to solution during the experiments.

The cell strain used was SA-1 grown with added NO_3^- resulting in a vegetative-only cell culture. The cells were washed of media and cellular debris as described previously. After washing, the cells were suspended in 250µL of electrolyte. 50µL of this cell suspension was mixed with 25µL of TMOA to make the 2:1 (v/v) casting suspension.

The four glassy carbon electrodes were arranged in an array and immersed together in NO_3^-/NO_2^- free electrolyte. The counter electrode was platinum mesh and the reference was a saturated calomel electrode. 100mL of electrolyte was used in every case. In the NO_3^-/NO_2^- free electrolyte, the array was cycled to 10 runs ("warm-up runs") at 100mV/s between -0.5V and 1.1V with 30 seconds between runs. Then the array was set for 10 additional runs in the same fashion. Total perturbation was approximately 20 minutes. The spent electrolyte was collected and analyzed for ammonia content by ammonia selective electrode.

The electrode array was rinsed and immersed in the solution of 0.02M NO_3^-/NO_2^-. The potentiostat was programmed to run 10 consecutive cycles with 30 seconds between runs at 100mV/s. At the end of the 10^{th} run, the electrolyte was collected and analyzed for ammonia content. This was repeated for the 0.05M and 0.1M NO_3^-/NO_2^- solutions successively, and gently rinsing the electrode array between use of each solution. For each of the solutions containing NO_3^-/NO_2^- the total perturbation time was approximately 10 minutes.

Analysis of ammonia content of the spent electrolyte solutions showed an increase in ammonia production with increase in NO_3^-/NO_2^- concentration. The chlorophyll a content was not determined for these experiments. For that reason, the ammonia concentration was normalized to perturbation time. The data for measured ammonia concentration as it relates to the added nitrate/nitrite concentration can be seen in table 4 below.

Table 4. Ammonia production normalized to perturbation time for various concentrations of nitrate/nitrite added to the electrolyte.		
Solution	[NH3]	[NH3] normalized to time
NO_3^-/NO_2^- free	4.79µM	0.24
0.02M NO_3^-/NO_2^-	2.87µM	0.29
0.05M NO_3^-/NO_2^-	5.49µM	0.55
.01M NO_3^-/NO_2^-	10.3µM	1.03

This was the first attempt to establish any correlation between addition of fixed nitrogen species and changes in ammonia production. As more nitrate/nitrite were added, the ammonia concentration increased in a linear fashion as seen in figure 52. This data was for a single biofilm casting, used in several successive solutions and perturbed cyclic voltammetrically. The electrodes were merely rinsed between uses.

In later experiments SA-1 vegetative-only strain used for this series of experiments. To the electrolytes, fixed nitrogen sources were added in 20, 50, and 80 mM concentrations. The fixed nitrogen sources were nitrate, nitrite, and a 1:1 ratio mixture of nitrate and nitrite. The electrolyte/analyte solutions were not degassed prior to use. All concentrations were tested in triplicate.

The addition of fixed sources of nitrogen did not have a universal effect on ammonia production. As seen in figure 53, the addition of nitrate alone had little, if not a deleterious, effect. When nitrite or a mixture of nitrate and nitrite were added, the production of ammonia increased. In the case

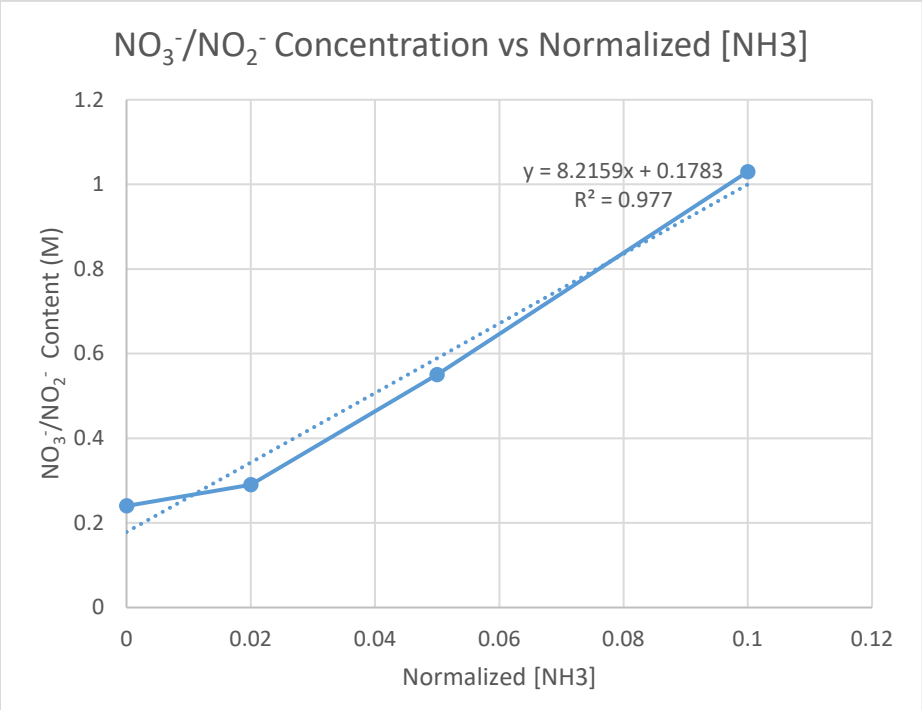

Figure 53. Plot of normalized ammonia production as it relates to the concentration of nitrate/nitrite added to the electrolyte.

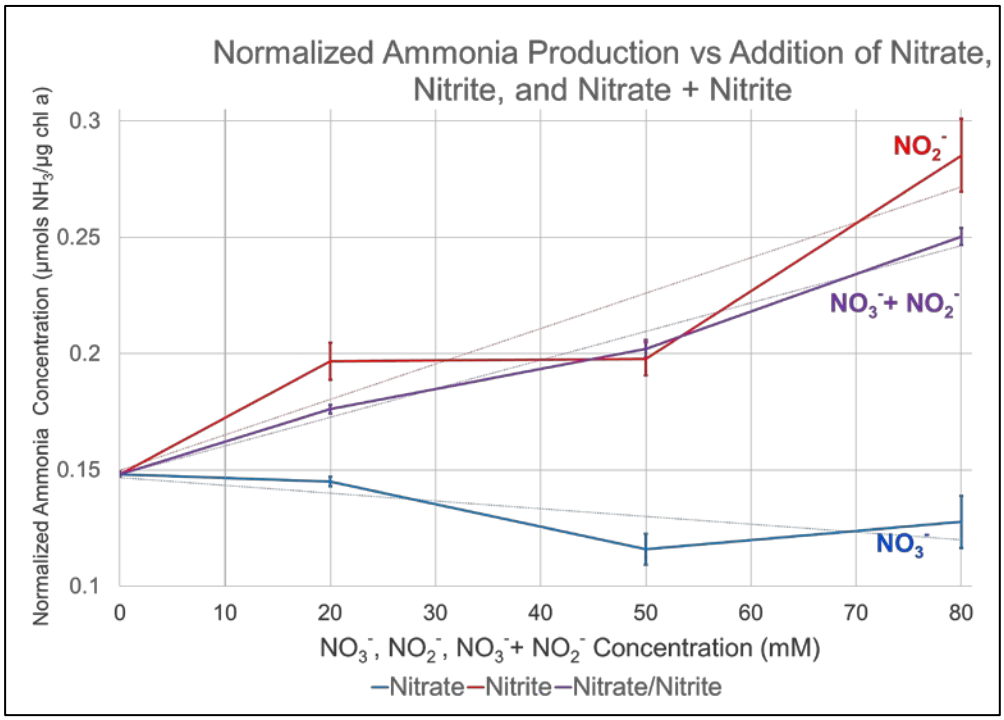

Figure 52. Plot of normalized ammonia production resulting from addition of nitrate and nitrite.

of the mixture of the two species, the relationship is quite linear. The implication of the data is that nitrite is the primary source of nitrogen used by the cyanobacteria. As the strain was grown with a nitrogen source in the media, it was devoid of heterocysts. This means that the ammonia production was done by the vegetative cells alone, and therefore by the nitrate/nitrite reductase complex.

Using the same experimental conditions, higher concentrations of nitrite were also tried:. 20, 50, 80, 100, 120, 150, 180 mM NO_2^-. A minimum of 5 experimental runs were conducted at each nitrite concentration, Table 5.

Table 5. Normalized ammonia production resulting from addition of various concentrations of NO_2^-.

NO_2^- concentration (mM)	Normalized NH_3 production (µmol NH3 / µg Chl a)
0	0.4 ± 0.1
20	0.5 ± 0.1
50	0.54 ± 0.07
80	0.8 ± 0.2
100	0.9 ± 0.3
120	1.2 ± 0.2
150	1.2 ± 0.3
180	0.7 ± 0.2

Based on this data, there seems to be a concentration level at which the nitrite becomes inhibitory. From 0 mM NO_2^- to 120 mM NO_2^- , the increase in ammonia production is mostly linear, as expected from previous work. This behavior is represented in Figure 54. Beyond that concentration, ammonia production drops. If the nitrite were not inhibiting ammonia production at the higher concentrations, the ammonia levels should remain high, suggesting the cells are simply taking what they need and functioning at an increased capacity. Instead, the production drops, indicating an inhibited function. The large error bars are the result fluctuations in the ammonia output. It is likely that even small variations in the electrode film may cause large differences in ammonia output.

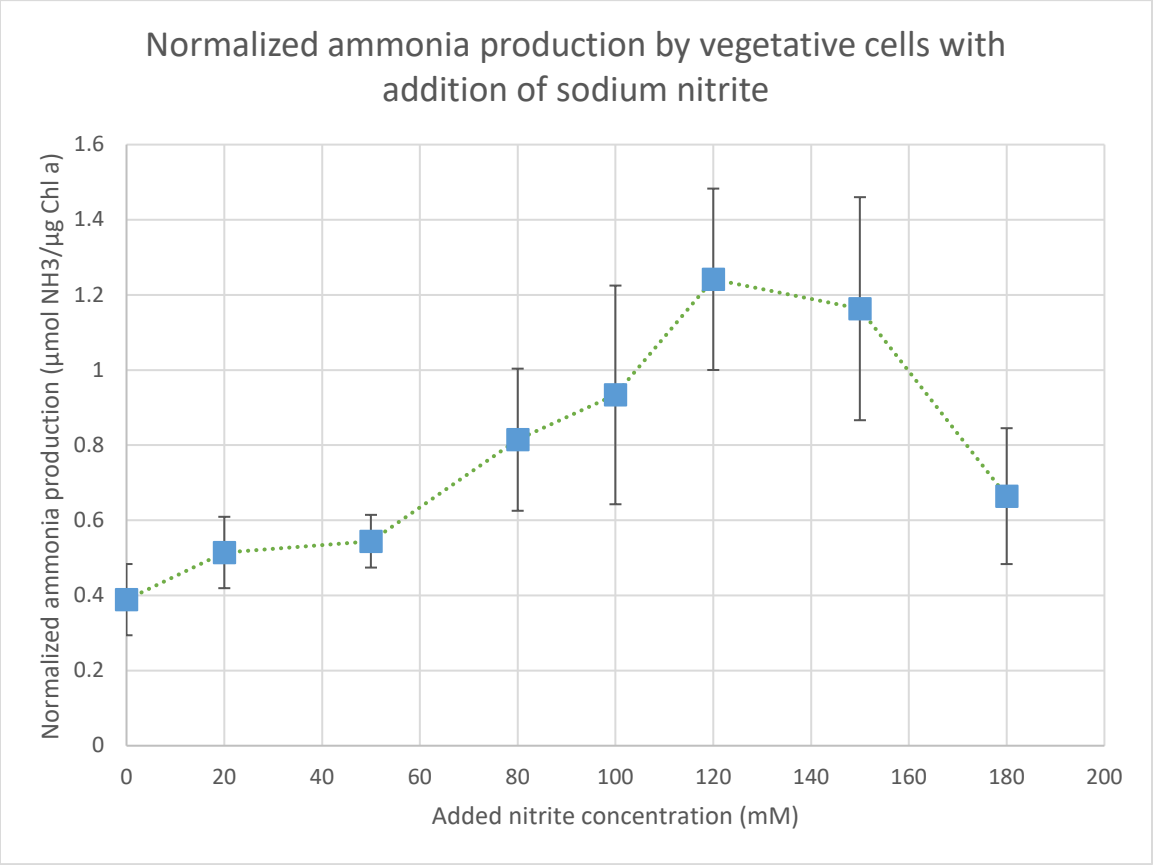

Figure 54. Plot of normalized ammonia production for addition of various concentrations of sodium nitrite to the electrolyte.

Addition of nitrate and nitrite to the electrolyte increases ammonia production by immobilized *A. variabilis*. Early studies were conducted utilizing vegetative-only cell culture (grown with added nitrate in the media), which responded with a linear increase in stimulated ammonia production with addition of a mixture nitrate and nitrite to the electrolyte. The early study only employed nitrate/nitrite concentrations only up to 100 mM. Later studies, also using the vegetative-only cell culture employed different patterns of nitrate and nitrite addition. Electrolyte solutions containing nitrite or a mixture of nitrate and nitrite elicited increased ammonia production. Solutions of nitrate alone did not. This indicates that nitrite is the preferred substrate. When higher concentrations of nitrite were used, it was discovered that ammonia production declined sharply above 150 mM nitrite. These findings are corroborated by work at the University of Utah in their studies of Flavin adenine dinucleotide mediated ammonia production.

Addition of nitrogen sources

There are numerous nitrogen containing species along the path between nitrate and ammonia. Figure 55 shows the various species employed in these experiments, the oxidation states of the nitrogen for each species, and the reduction potentials for each species. Some of these may serve as important intermediates in the path to ammonia formation. To explore the effect of various nitrogen sources on ammonia production, we have added dinitrogen (N_2), nitrous oxide (N_2O), nitric oxide (NO), hydroxyl amine (NH_3OH^+), and hydrazine dihydorchloride ($N_2H_5^+$*2HCl) individually to the electrolyte.

Electrode setup was the same for each experimental run. Glassy carbon electrodes were used (0.2 cm^2). An array of 1 bare, 1 TMODA, and 2 TMODA/cells electrodes with 1:1 ratio of cells:TMODA (v/v) were employed using mixed-cell cultures grown under nitrogen starvation and vegetative-only cell cultures grown with fixed nitrogen.

The electrolyte was the same for each experimental run, with various components added to it. The electrolyte was 100 mL of 0.1 M Na_2SO_4 free of nitrate and nitrite, not degassed. For addition of N_2 and N_2O, the gases were bubbled into a parafilm-covered beaker of electrolyte solution using a disposable pipette connected to the gas line for > 1 hour before use.

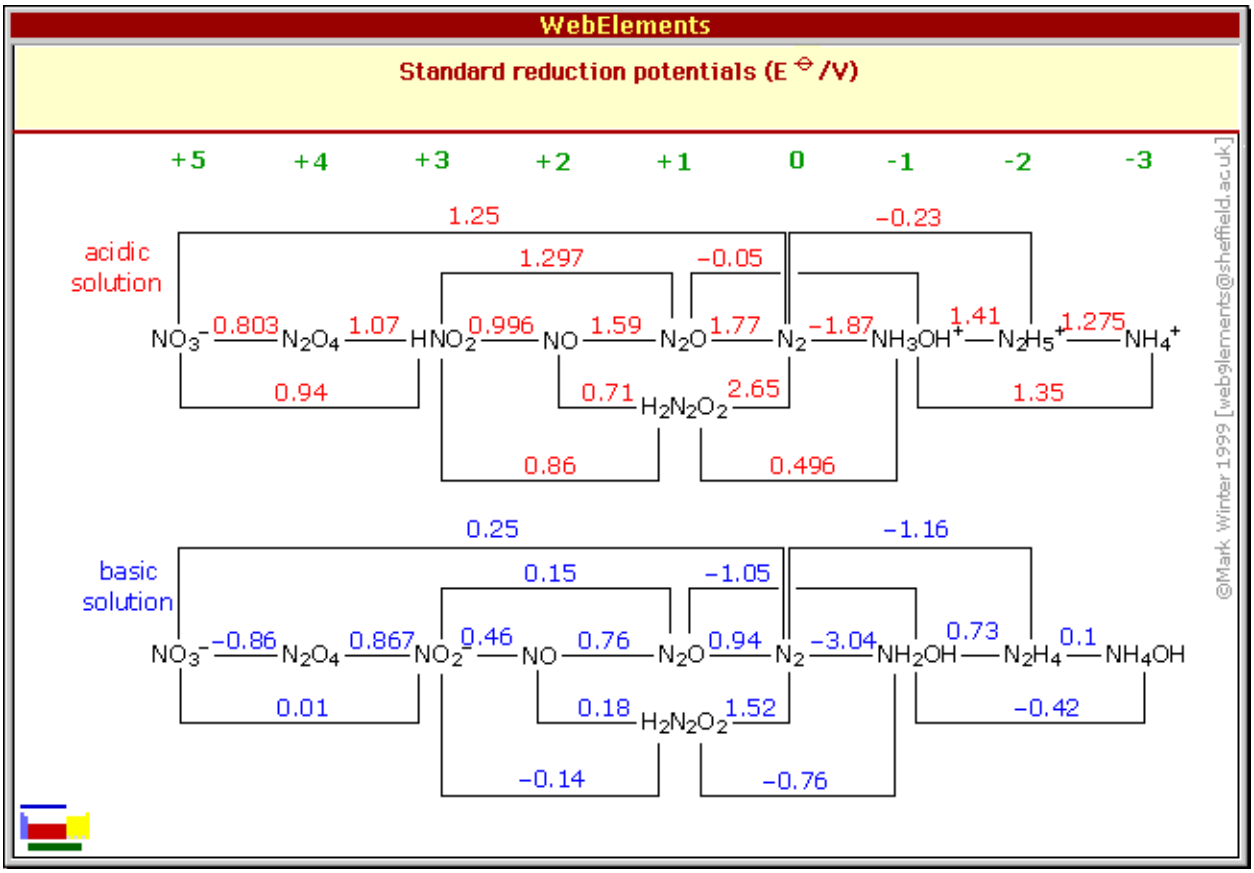

Figure 55. Standard reduction potentials for various nitrogen-containing compounds.

For each experimental run with NO, an approximately 240 mL volume of gas was injected into the electrolyte via luer lock syringes immediately before immersion of the electrodes. Solutions of 1 mM hydrazine dihydrochloride (N_2H_4*2HCl) and hydroxylamine (NH_2OH) were prepared in 100 mL of 0.1 M Na_2SO_4. The electrode array was cycled at 100 mV/s between +1.0 V and -0.5 V. 40 cycles were run resulting in approximately 20 minutes of voltammetric perturbation. Controls were run with four bare electrodes, absent of biofilms, in each of the nitrogen-containing electrolyte solutions. Additionally, controls were run with the same array of electrodes with biofilms, but without addition of nitrogen compounds. Ammonia concentration was measured by spectrophotometric salicylate method. The reported variance results from three replicate runs with each run have an ammonia measurement of three aliquots of sample, as well as three replicate measurements of chlorophyll a. Only one data run was completed for the vegetative-only biofilm control. Figure 56 is plot of the normalized ammonia concentration resulting from

the addition of the different nitrogen species. The ammonia production for each added species is shown for both biofilm types, labeled “veg” for vegetative-only biofilms, or “mixed” for mixed-cell biofilms.

Paschkewitz ran similar experiments with the addition of various gases, including dinitrogen. He noted a slight drop in ammonia output with the addition of N_2. Here, the addition of dinitrogen has suppressed the production of ammonia to nearly zero for both vegetative and mixed-cell biofilms. For mixed-cell biofilms, the addition of nitrous oxide increased ammonia production above that of the control, but remained below the control for vegetative biofilms. The addition of nitric oxide, caused ammonia production to increase above control for mixed cell biofilm, but not for vegetative biofilms.

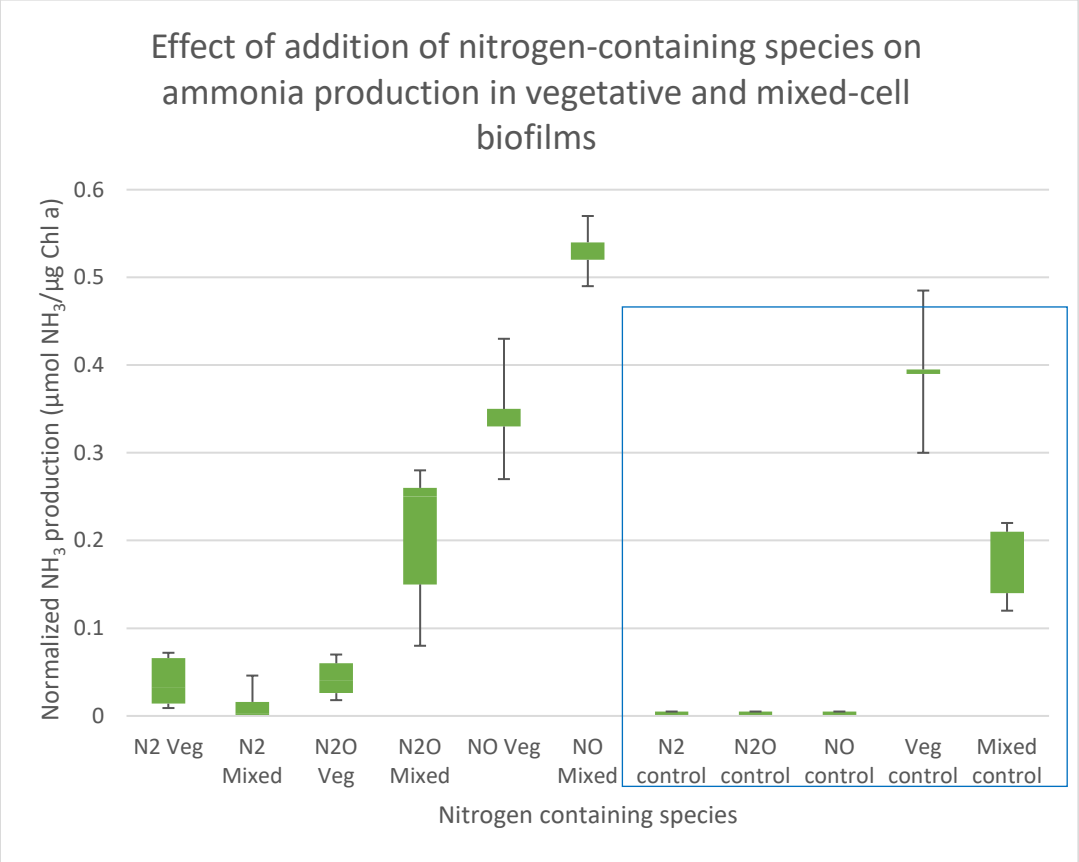

Figure 56. Comparison of the ammonia production in vegetative-only and mixed-cell biofilms with the addition of various nitrogen-containing species.

Additionally, the pH of the resulting electrolyte was more acidic than that of the controls. As seen in table 6, with addition of NO, the pH of the electrolyte averaged to 3.3 for 4 experimental runs. Unaltered sodium sulfate electrolyte typically has a pH of 6.5. The raw values for ammonia production with the additions of hydrazine or hydroxylamine, as seen in table 7, are within experimental error of their respective blanks, indicating that ammonia production was low enough as to be indistinguishable from the background. To verify that the nitrogen-containing species added to the electrolyte were not being electrolyzed to ammonia, solutions sparged with N_2, N_2O,

and NO were run without biofilms. No ammonia was found in these solutions following voltammetry.

Table 6. Electrolyte solution pH after addition of various nitrogen containing species	
Addition to electrolyte	pH
Control	6.5
N_2	5.9
N_2O	6.2
NO	3.3

Table 7. Ammonia concentration after addition of nitrogen compounds.	
Addition to electrolyte	**Measured NH_3-N (µM)**
1 mM hydrazine dihydrochloride w/ biofilm	26.0 ± 4.0
1 mM hydroxylamine w/ biofilm	32.0 ± 7.0
1 mM hydrazine dihydrochloride blank	29.0
1 mM hydroxylamine blank	29.0 ± 7.0

Hydrazine solutions were difficult to measure with the salicylate measurement, so very few aliquots were included for error calculation.

Of the Various nitrogen-containing species, only nitric oxide gas (NO) with mixed-cell biofilms performed above the level of the controls. Nitrous oxide with mixed-cell biofilms performed as well the control with no addition to the electrolyte for mixed-cell film, and nitric oxide with vegetative-only biofilm performed as well as the control for vegetative film without addition. All other species that were added to the electrolyte for either biofilm type suppressed ammonia production.

Chronoamperometry

Explorations were made to discern the role of the applied electrical potential as it relates to the production of ammonia. Work by Paschkewitz indicated that ammonia production varied in a linear fashion with the magnitude of the reduction peak at approximately +350 mV vs SCE. [8] Literature values for the activity of isolated nitrogenase enzyme indicated an optimal range near -220 mV vs SCE. [9,10]. With this information, it was decided to investigate the possibility of enzyme control with applied potential. If isolated nitrogenase enzyme could be at optimal stimulation at negative potentials, it may be possible to target that enzyme while in a whole cell environment using similar potentials. Given the range of reduction potentials for species such as NO_3^- and NO_2^- are more positive than +590 mV vs SCE, it was thought that this range would be most suitable for nitrate/nitrite reductase activity.[11] For these studies, the selected potential was

held for 30 minutes and the ammonia concentration was measured by ammonia selective ISE. Studies were conducted using $BG11_0$ growth media and 0.1 M Na_2SO_4 (both absent of added nitrogen species) separately as electrolyte.

$BG11^o$ as electrolyte:

The working electrodes used were 0.2 cm^2 glassy carbon electrodes. The reference electrode was a saturated calomel, and the counter electrode was platinum mesh. All glassy carbon electrodes were polished with graded alumina powder, soaked in concentrated nitric acid, and rinsed with 18MΩ*cm water prior to film casting. In each experiment a four-electrode array was used. One electrode was bare, one had a film of TMODA with no cells immobilized, and two electrodes had films of TMODA with immobilized cells in a 1:1 ratio (v/v). These were run simultaneously in 100 mL $BG11_0$ nitrate-free growth media pH adjusted to 7.1 (not degassed). Each replicate was run at the target potential for 30 minutes, after which the electrolyte was collected and analyzed for ammonia content by an ammonia selective electrode.

The data are represented in table 8 and figure 57. The ammonia produced at the -300 mV potential indicates the possibility of enhanced nitrogenase activity. The increase in ammonia would seem to point to a similar activity with nitrogenase in whole cells. The unexpectedly high value at +800 mV has no immediate explanation.

Table 8. Ammonia production values for chronoamperometry in $BG11_0$ electrolyte

Potential	**µmol NH3 / µg Chl a / minute** (x 10^{-3})
+800 mV	10.0 ± 1.5
+700 mV	2.9 ± 0.9
+650 mV	3.7 ± 0.8
+500 mV	3.1 ± 0.9
+350 mV	2.2 ± 0.6
+200 mV	1.9 ± 0.7
-100 mV	1.4 ± 0.7
-300 mV	5.0 ± 1.5

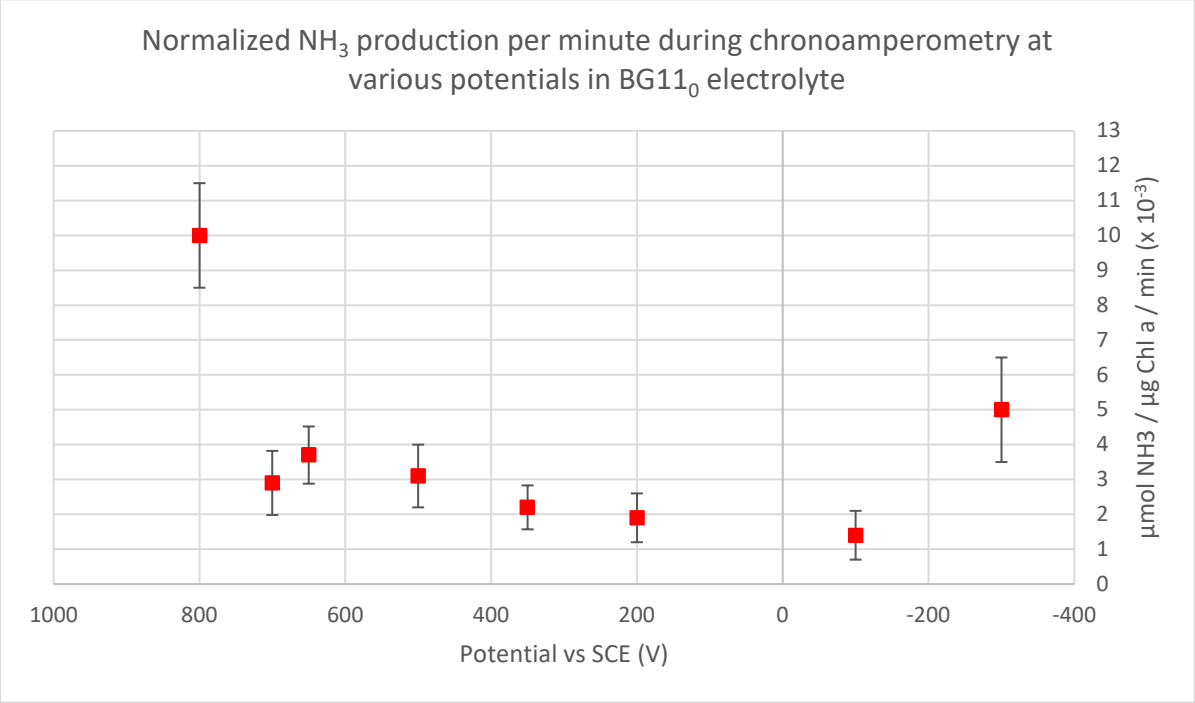

Figure 57. Plot of ammonia production versus applied potential for chronoamperometry in BG11₀ electrolyte

Sodium sulfate electrolyte:

Chronoamperometric experiments were conducted in 0.1 M Na_2SO_4 at pH 6.2. This was done to minimized variation in the components of the electrolyte. To increase the concentration of ammonia to be measured, an array of four algae-immobilized electrodes were used in addition to the bare and TMODA electrodes, for a total of six electrodes per experiment. One electrode was bare, one had a 6 µL casting of TMODA with no cells immobilized, and four electrodes had films of TMODA with immobilized cells in a 1:1 ratio (v/v). These were run simultaneously in 100 mL of 0.1 M Na_2SO_4 at pH 6.2 (not adjusted, buffered, or degassed). Each experiment was run at the target potential for 30 minutes, after which the electrolyte was collected and analyzed for ammonia content by ammonia selective electrode.

The data are represented in table 9 and figure 58. The ammonia produced at the -300 mV potential still indicates the possibility of enhanced nitrogenase activity. The increase in ammonia would seem to point to a similar phenomenon with nitrogenase in whole cells. In general, these data follow the same pattern as that from experiments with growth media as the electrolyte. The highest points of ammonia production occurred at +600 mV and -300 mV. One particularly interesting aspect of this data is that ammonia production was not increased by adding more algae-modified electrodes.

Table 9. Ammonia production for chronoamperometry in 0.1 M Na_2SO_4.

Potential	**µmol NH3 / µg Chl a / minute** (x 10^{-3})
+800 mV	0.5 ± 0.03

+600 mV	1.8 ± 0.4
+500 mV	0.9 ± 0.03
+400 mV	1.0 ± 0.01
+200 mV	0.6 ± 0.08
+100 mV	0.7 ± 0.1
-100 mV	0.9 ± 0.05
-300 mV	1.7 ± 0.6

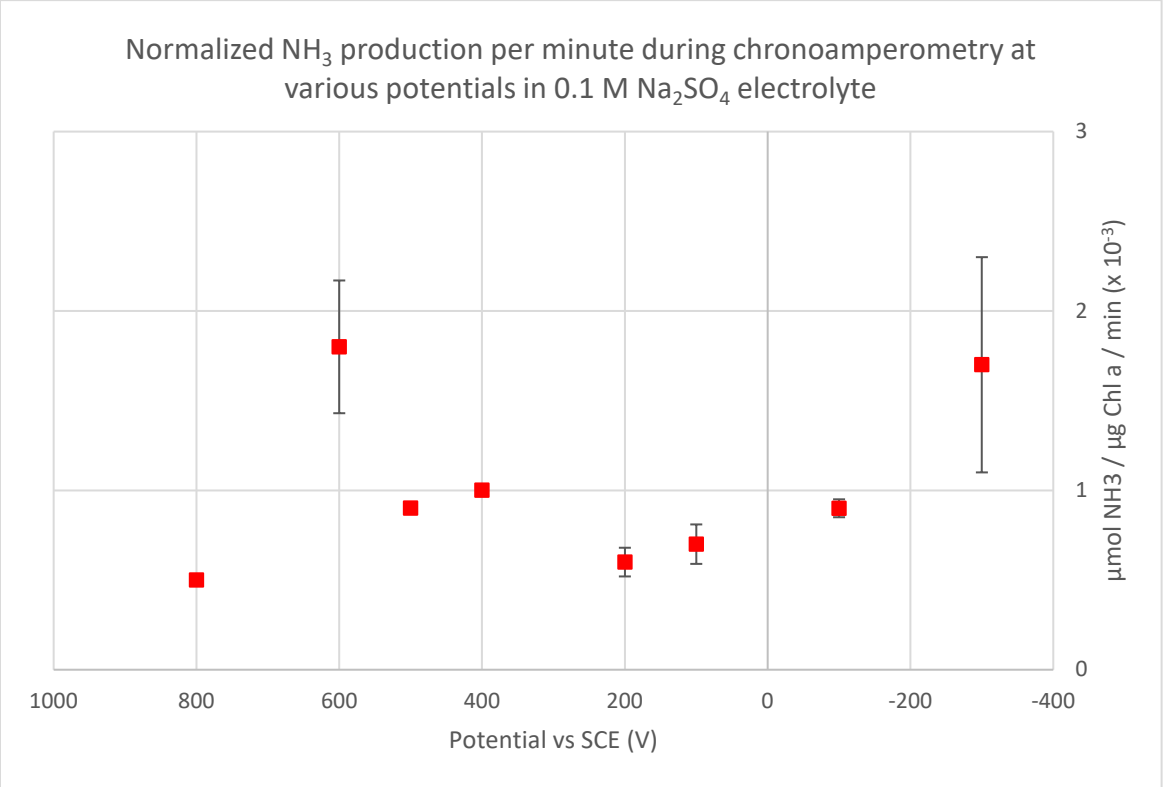

Figure 58. Plot of normalized ammonia production values versus applied potential for chronoamperometric experiments in 0.1 M Na_2SO_4.

Chronoamperometry with addition of nitrite

100 mL of $BG11_0$ was used as the electrolyte with the addition of 50 mM $NaNO_2$. In each experimental run, 4 algae-immobilized electrodes had films of TMODA with immobilized cells in a 1:1 ratio (v/v), as well as one bare electrode and one electrode with a 6 µL casting of TMODA with no cells immobilized. The strain used was grown under nitrogen starvation conditions resulting in the presence of heterocystic cells. A saturated calomel electrode served as reference electrode and a platinum mesh electrode served as counter electrode. The electrodes were run at various potentials for 30 minutes, after which the electrolyte was collected and analyzed for ammonia content by ammonia selective electrode, as well as nitrate/nitrite content. The resulting data for ammonia output can be seen in table 10 and figure 59.

Table 10. Ammonia production for chronoamperometry with 50 mM sodium nitrite to $BG11_0$ electrolyte.

Potential (mV)	**µmol NH3 / µg Chl a / minute** (x 10^{-3})
650	-0.1 ± 0.7
500	-0.1 ± 0.6
350	1.2 ± 0.5

200	0.5 ± 0.4
50	0.43 ± 0.05
-100	0.9 ± 0.2
-250	-0.2 ± 0.1
-400	0.2 ± 0.3

All the samples reported on here were run with $BG11_0$ as the electrolyte, they all have a baseline of ~30 µM ammonia. This value was subtracted from the measured ammonia output of the samples. Some samples were measured to have slightly less ammonia than the blank, resulting in negative values for the output.

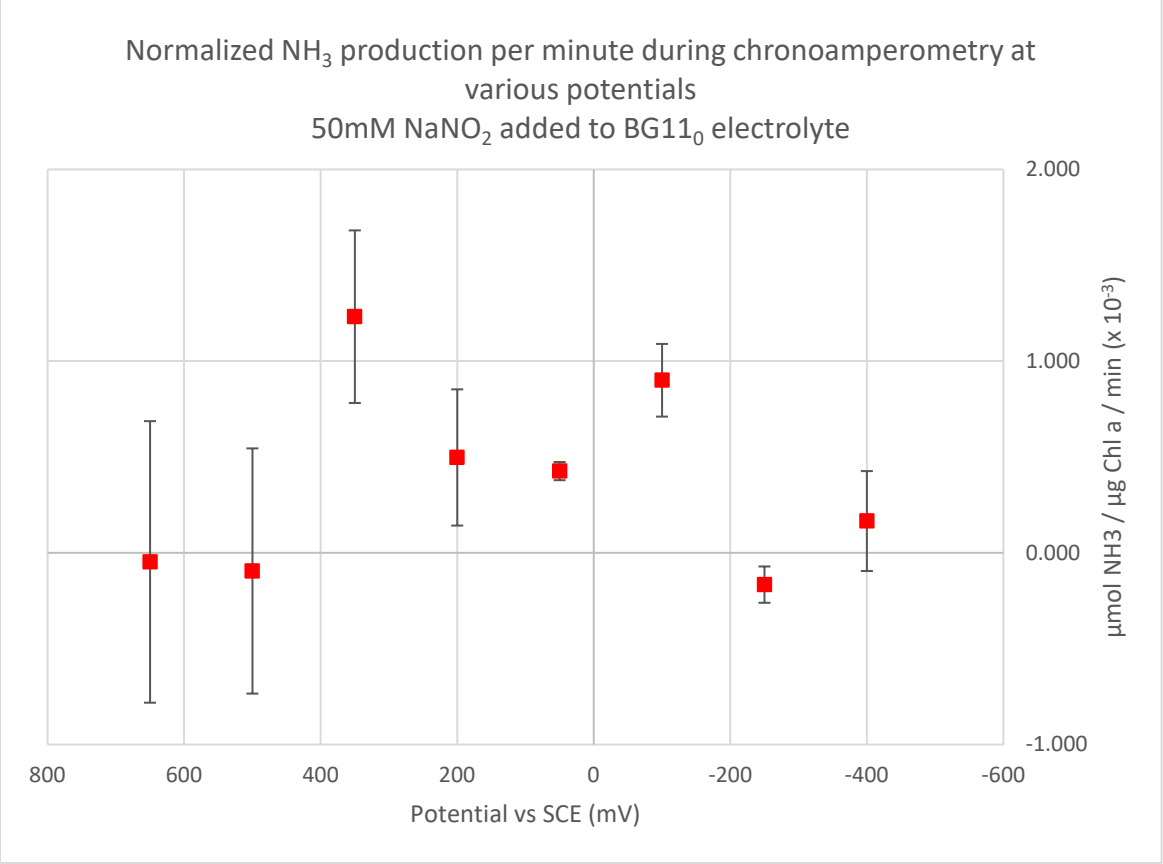

Figure 59. Plot of normalized ammonia production values versus applied potential for chronoamperometric experiments with addition of 50 mM sodium nitrite to $BG11_0$ electrolyte.

Scan rate experiments

Fixed nitrogen in the form of nitrate and nitrite can be store in the cytosols of the vegetative cells for use during periods of nitrogen deprivation. [12] Once those stores are exhausted, the cell culture responds by producing heterocyst cells containing nitrogenase. These experiments were an attempt to determine a point at which the vegetative cells could be exhausted of their fixed nitrogen

sources. That point being reached, ammonia production should then proceed from nitrogenase only, as its substrate is dinitrogen from the air.

In this work, the number of scans per experiments was kept constant while the scan rate was changed. The total number of scans was 60, with a rest time between scans of 5 seconds. The scan rates employed were 50 mV/s and 100 mV/s. This results in total voltammetric perturbation times of 82 minutes and 31 minutes respectively with the same total rest time of 5 minutes.

Both algae strains were used separately. It was expected that after sufficient voltammetric perturbation, the vegetative-only strain will produce less ammonia over time than the strain containing heterocysts as the vegetative cells are exhausted of fixed nitrogen. BG-11_0 growth media was the electrolyte. The nitrate-free media was chosen to encourage ammonia production by the nitrogenase enzyme.

The preparation of algae-immobilized glassy carbon electrodes has also remained the same. The area of the electrode is 0.20 cm^2, and 9 µL of 1:1 ratio (v/v) of algae:TMODA suspension was applied to the surface of the electrode and allowed to dry for 1 hour. In these experimental runs, the electrode array consisted of 1 bare electrode, 1 with a film of TMODA, and 1 with TMODA:cells. The reference electrode was a saturated calomel electrode (SCE), and the counter electrode was platinum mesh. The voltage window was between -0.5 V and +1.1 V, and scans were run at 50 mV/s and 100 mV/s for 60 scans with 5 seconds between scans. Total perturbation time was approximately 82 minutes (at 50 mV/s) or 31 minutes (at 100 mV/s) with total rest time of 5 minutes.

Table 11. Ammonia production per minute for vegetative strain versus heterocystic strain at different scan rates.

Strain	**Voltammetric Time**	**Ammonia Production** (µmol NH_3 / µg Chl a / minute)
Vegetative	31 minutes @ 100 mV/s	4.5 E -2 ± 0.002
Heterocystic	31 minutes @ 100 mV/s	3.9 E -2 ± 0.004
Vegetative	82 minutes @ 50 mV/s	2.7 E -2 ± 0.003
Heterocystic	82 minutes @ 50 mV/s	2.3 E -2 ± 0.006

The data in table 11 indicate that at shorter perturbation times with faster scan rates, ammonia production per minute increases. In general, the vegetative-only biofilms displayed slightly higher ammonia production than mixed-cell biofilms, but these values are within experimental error of each other. **The point at which the vegetative only biofilms cease to produce ammonia has not been found. This is evident by the lack of statistical difference between the two types of biofilms.**

Chronoamperometric studies indicated that potential regions near -300 mV vs SCE are optimal for stimulated ammonia production. Experiments were conduction in both $BG11_0$ growth media and 0.1 M Na_2SO_4. Both electrolytes were tested without addition of nitrite. $BG11_0$ was also tested with the addition of 50 mM NO_2^-. The results with added nitrite showed no pattern. Both electrolytes without nitrite showed increased ammonia output at -300 mV. In sodium sulfate,

there was also an increased production at +600 mV, and in $BG11_0$, there was an increase at +800 mV. The reason for these increases at positive potentials in unclear at this time. The negative potential region where ammonia production was highest corresponds to reduction potential regions for several components in pathway of biological reduction of dinitrogen. Examples in the literature suggest that a reductive environment is necessary for optimal nitrogenase activity.

Effects of photosystems and electrode substrates

The role of the photosystems in stimulated ammonia production has been explored. Experiments were carried out on 0.20 cm^2 glassy carbon electrodes as well as on BA1 (no wet proofing) carbon fabric available from BASF. In all cases, the employed strain is SA-1 grown in nitrate-free media, resulting in a mixed-cell culture consisting of both vegetative and heterocystic cell types. Experiments conducted in the light were done in ambient laboratory conditions on the benchtop. Experiments in the dark were carried out inside a closed Faraday cage in complete darkness. Electrodes feeding into the cage were built in and sealed, preventing any light from entering the compartment.

All experiments were done with 0.1M Na_2SO_4 as the electrolyte. Cyclic voltammetry was employed to scan between +1.1 V and -0.5 V vs SCE, at 150 mV/s with 20 cycles and 30 seconds between runs. With carbon fabric electrodes, two different protocols were used for the immobilization of algae cells on the electrode material. First, algae cells were centrifuged and washed as usual, and the liquid pipetted from the centrifuge tube after the final washing step. The cell slurry was scooped out with a small spatula and smeared onto a small square (~ 2 cm^2) of carbon fabric. On top of this was placed a second piece of carbon fabric to form a kind of sandwich. This was then placed in a Teflon holder with a stainless steel flag as a backing, to which the electrode lead was attached. This whole apparatus was then placed in the electrolyte. The other immobilization protocol was to apply the algae in the same manner and to add a layer of TMODA/Nafion to the top of the algae instead of a second piece of carbon fabric. The volume of polymer applied was 5 µL. All other aspects of use were the same.

Table 12. Normalized ammonia production on glassy carbon electrodes in the light and dark.

Glassy Carbon	**Light**	**Dark**
NH_3 Production (µmol NH_3/µg Chl a)	0.22 ± 0.1	0.15 ± 0.1

Table 13. Normalized ammonia production on carbon fabric electrodes.

Carbon Fabric	NH_3 Production (µmol NH_3/µg Chl a)
Light w/o TMODA	0.06 ± 0.02
Light with TMODA	0.047 ± 0.007
Dark w/o TMODA	0.07 ± 0.01
Dark with TMODA	0.05 ± 0.02

The results indicate a performance difference between light and dark conditions, as well as between electrode substrates. The voltammograms exhibit higher capacitive current in the dark experiments for both glassy carbon and carbon fabric in figures 60 and 61. For glassy carbon, the ammonia production was higher in experiments in the light, as seen in table 12. Table 13 shows that for the carbon fabric, the ammonia production was greater in the dark. The TMODA seemed to have a stabilizing effect on ammonia production and voltammetry between light and dark experiments. However, the ammonia production was generally higher when TMODA was not used, regardless of scenario. This may be due to the sandwich method providing an increased area in which algae cells were in contact with a conductive surface.

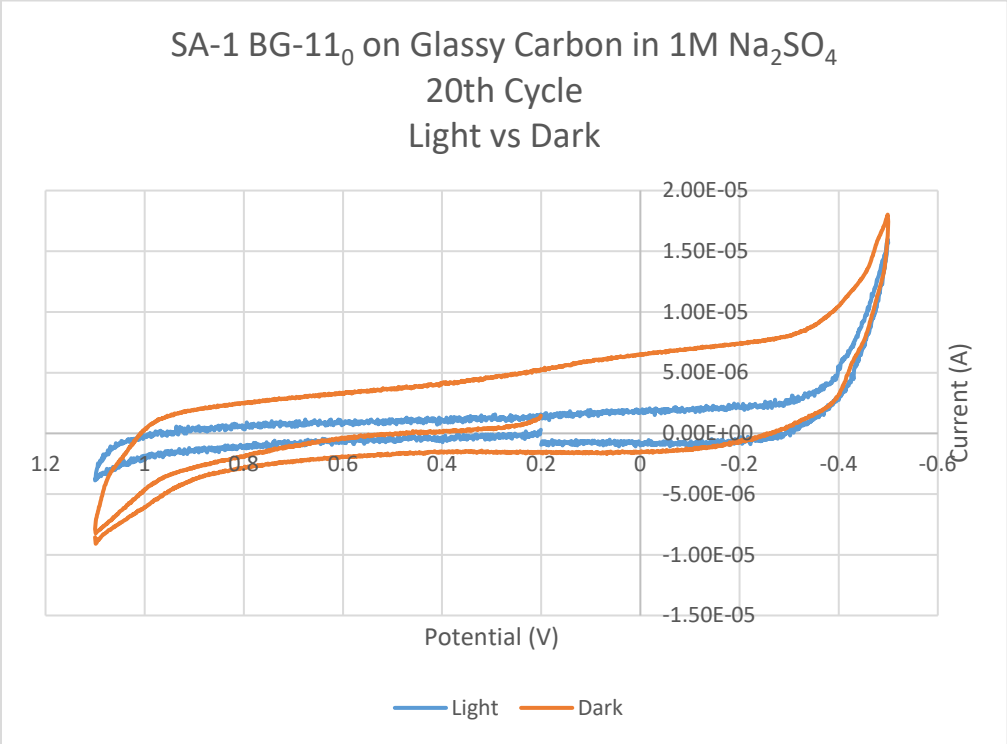

Figure 60. Cyclic voltammograms of algae-immobilized glassy carbon electrodes in light and dark

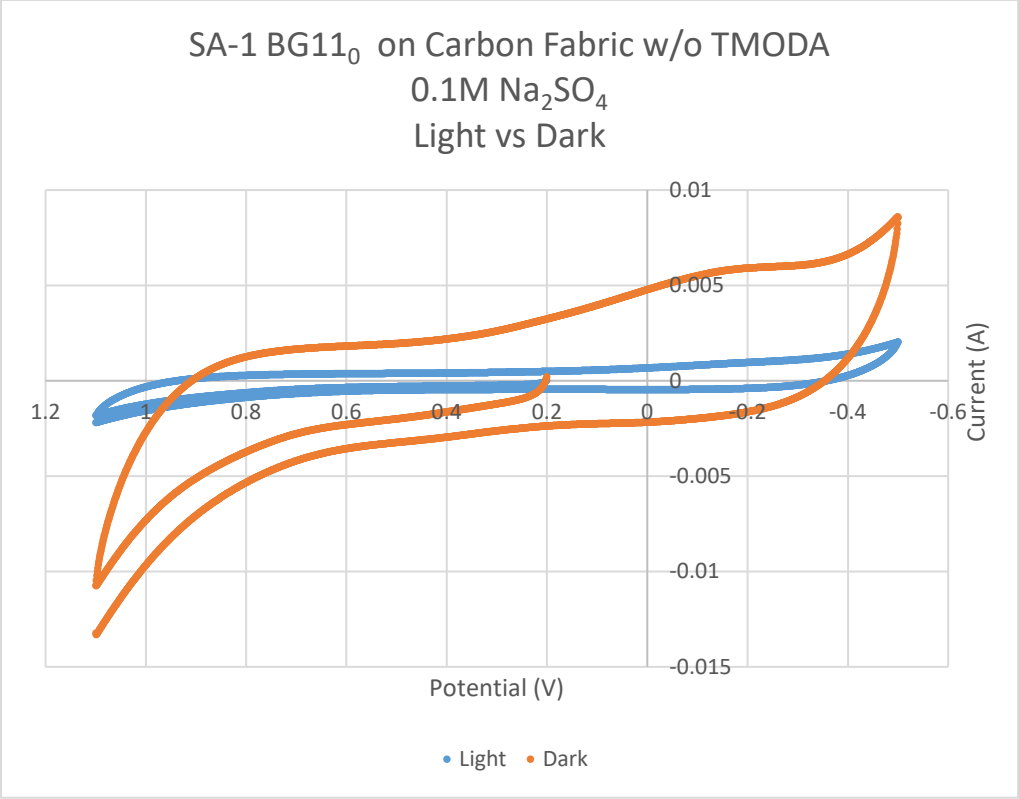

Figure 61. Cyclic voltammograms of algae-immobilized carbon fabric electrodes without TMODA (sandwiched version) in light and dark.

One explanation for the difference between glassy carbon and carbon fabric is that the algae film on the glassy carbon electrode is considerably thinner and therefore more susceptible to changes in light levels. The algae films on the carbon fabric are quite thick, so the cells in contact with the electrode are in the dark already because they are covered by those on the outside. The glassy carbon electrodes performed with much higher efficiency. This is also likely due to more complete and uniform contact between immobilized cells and the electrode surface.

Light is a necessary component for optimal ammonia production. In experiments with biofilms stimulated by cyclic voltammetry in the light and in the dark, ammonia output was higher in the light. These trials were completed on two different electrode substrates. Glassy carbon electrodes and carbon fabric electrodes were employed in these experiments. When normalized ammonia production on each substrate was compared, the glassy carbon electrodes demonstrated greater output. This was compounded when electrode area was taken into consideration. Ammonia production on carbon fabric was only 20% that by the glassy carbon electrodes, yet the area of the glassy carbon electrodes was significantly smaller. On carbon fabric electrodes, it was also demonstrated that cells immobilized without TMODA produced more ammonia than those immobilized with TMODA.

Negative window vegetative biofilms vs heterocyst biofilms

Cyclic voltammetry was used to establish a voltammetric perturbation regime that stimulates nitrogenase activity without activating other ammonia-producing processes. A voltage window, +0.2 to -0.5V at 100 mV/s was used that includes reported reduction potentials of

components in nitrogen fixation pathway [13,14] and reported potentials for optimal nitrogenase activity.[9,10] Heterocyst cells were isolated from cell cultures grown under nitrogen starvation conditions by protocol described by Paschkewitz [8] adapted from protocols used by Lynn and Ownby.[15] The cell concentration in the resulting heterocyst isolate was established by chlorophyll a extraction with methanol. The electrode was cycled continuously for 10 minutes in 0.1 M Na_2SO_4 to establish good contact between the cells and the electrode. The electrolyte was discarded, and replaced with 100 mL of 0.1 M Na_2SO_4. The electrode was then cycled continuously for an additional 30 minutes with no rest time. The electrolyte was analyzed by ammonia-selective ISE. The same protocol was used to examine a film made with vegetative-only cells grown with added nitrate. Data are provided for four experimental runs of heterocyst isolate film and five experimental runs for vegetative-only film, table 14 The variance represents three replicate measurements of chlorophyll a and ammonia measurement of three aliquots of sample.

Table 14. Ammonia concentration for cyclic voltammetry with heterocyst and vegetative cells run in a negative voltage window

Heterocyst isolate		**Vegetative cells**
Voltage window: +0.2V ⇄ -0.5V		Voltage window: +0.2V ⇄ -0.5V
Scan rate: 100 mV/s		Scan rate: 100 mV/s
µmol NH3 / µg Chl a		**µmol NH3 / µg Chl a**
0.164 ± 0.002		0.05 ± 0.02
0.039 ± 0.002		0.030 ± 0.002
0.050 ± 0.001		0.004 ± 0.002
0.098 ± 0.006		0.002 ± 0.001
		0.02 ± 0.01
Average and Standard deviation		**Average and Standard deviation**
0.09 ± 0.06		0.02 ± 0.02

A basic statistical comparison of data for each film type was conducted. A student's *t*-test of the two data sets indicate that they are statistically different for n=7 at 95% confidence. A Grubb's test for outliers determines that all values in both data sets should be included (n=4 and n=5, 95% confidence).

A link between the potential of the cytoplasmic membrane and nitrogenase activity has been suggested in the literature.[16] Reduction potentials for the main species of interest to nitrate/nitrite reductase and nitrogenase enzymes are shown in figure 62. Previous experiments with chronoamperometry suggest that the highest levels of ammonia production are to be found in the regions of +650 mV and -300 mV. These potential regions correspond to the reduction potentials for nitrate and nitrite near +650 mV and components necessary to nitrogenase near -300 mV. At -300 mV the dominant nitrogen containing species is ammonium and thermodynamically, both nitrate and nitrite converted to ammonium.

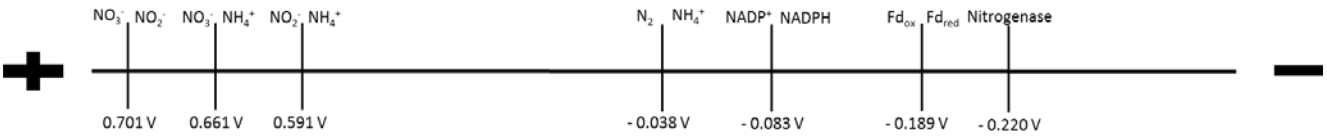

Figure 62. Potential axis showing reduction potentials for various nitrate/nitrite species and components important to nitrogenase function. The reduction potentials are referenced to a saturated calomel electrode.

When isolated heterocyst biofilms were compare to vegetative-only biofilms, the result was that heterocyst isolates performed better than vegetative biofilms when subjected to a predominantly negative voltage profile. When heterocyst-only biofilms were cycled in a negative voltage window, they produced more ammonia than vegetative-only biofilms in the same voltage window.

References

1. Ernst, Anneliese; Kirschenlohr, Heide; Diez, Jesus; Boger, Peter. Glycogen content and nitrogenase activity in Anabaena variabilis. *Arch Microbiol*. **1984**, *140*, 120-125.
2. Giddings, Thomas H. Jr.; Wolk, Peter C. Factors influencing the stability of nitrogenase activity in isolated cyanobacterial heterocysts. *FEMS Microbiology Letters*. **1984**, *10*, 299-302.
3. Kumar, Ashok; Tabita, Robert F.; Van Baalen, Chase. High endogenous nitrogenase activity in isolated heterocysts of Anabaena sp. Strain CA after nitrogen starvation. *Journal of Bacteriology*. Aug **1983**, 493-497.
4. Berman-Frank, Ilana; Lundgren, Pernilla; Falkowski, Paul. Nitrogen fixation and photosynthetic oxygen evolution in cyanobacteria. *Research in Microbiology*. **2003**, *154*, 157-164.
5. Crane, B.; Getzoff, E. The relationship between structure and function for the sulfite reductases. *Cur. Opin. Struct. Biol.* **1996**, *6*, 744-756.
6. Dose, M.; Hirasawa, M.; Kleis-SanFancisco, S.; Lew, E.; Knaff, D. The ferredoxin-binding site of ferredoxin:nitrite oxidoreductase. *Plant Physiol.* **1997**, *114*, 1047-1053.
7. Suzuki, S.; Kataoka, K.; Yamaguchi, K. Metal coordination and mechanism of multicopper nitrite reductase. *Acc. Chem. Res.* **2000**, *33*, 728-735.
8. Paschkewitz, T. Ammonia production at ambient temperature and pressure: An electrochemical and biological approach. Ph.D. thesis. The University of Iowa, 2012.
9. Braaksma, Arnold; Haaker, Huub; Grande, Hans J.; Veeger, Cees. The effect of the redox potential on the activity of the nitrogenase and on the Fe-protein of Azotobacter vinelandii. *Eur. J. Biochem.* **1982**, *121*, 483-491.
10. Pueyo, Jose J.; Gomez-Moreno, Carlos; Mayhew, Stephen G. Oxidation-reduction potentials of ferredoxin-NADP$^+$ reductase and flavodoxin from Anabaena PCC7119 and their electrostatic and covalent complexes. *Eur. J. Biochem.* **1991**, *202*, 1065-1071.
11. Maloy, Joseph T. Nitrogen, Phosphorus, Arsenic, Antimony, and Bismuth. In *Standard Potentials in Aqueous Solution*; Bard, Allen J., Parsons, R., Jordan, J., Eds.; International Union of Pure and Applied Chemistry; Marcel Dekker, Inc.: New York, New York, 1985, pp 129-138.
12. Tsygankov, A. A. Nitrogen-Fixing Cyanobacteria: A Review. *Applied Biochemistry and Microbiology*. **2007**, *43*, 250-259.

13. Smith, Eugene T.; Feinberg, Benjamin A. Redox properties of several bacterial ferredoxins using square wave voltammetry. *J. Biol. Chem.* **1990**, *265* no. 24, 14371-14376.
14. Correll, Carl C.; Ludwig, Martha L.; Bruns, Christopher M.; Karplus, P. Andrew. Structural prototypes for an extended family of flavoprotein reductases: Comparison of phthalate dioxygenase reductase with ferredoxin reductase and ferredoxin. *Protein Science*, **1993,** *2*, 2112-2133.
15. Lynn, M.; Ownby, J. Transcriptional activity of heterocysts isolated from *Anabaena variabilis*. *Arch. Microbiol.* **1987**, 148, 115-120.
16. Haaker, H.; Klugkist, J. The bioenergetics of electron transport in nitrogenase. FEMS Microbiology Reviews. 46 (1987) 57-71.

An equilibrium model for distribution of species at a fixed pH and a range of potentials (E vs NHE) has been developed in an Excel spreadsheet that runs Visual Basic. The model is based on the native distribution of species without any added nitrogen containing species. Results are reported as fraction of species relative to total atomic nitrogen concentration. For example, N_2 is the dominant species between -0.6 and +0.7 V at pH 7 and its fraction is reported as 0.5.

The idea is that the thermodynamic distribution describes the equilibrium situation, which is equivalent to fast kinetics. In the absence of algae, the kinetics slow rates to limit product formation. The products have not yet reached equilibrium and differ from the near equilibrium distribution of species that with facile kinetics will approach the thermodynamically specified, equilibrium distribution. The algae is modeled as an efficient catalyst for all otherwise rate determining reactions.

With the view of algae as an effective catalyst, several views of the cyanobacteria system can developed.

- Native system is a system where no additional nitrogen containing species are added to bias the product distribution. Equilibrium product distributions for the native nitrogen system are mapped as a function of potential E and pH.
- Reactions possibly important in the mechanistic pathways for ammonia|ammonium formation are considered on a potential axis. Reactions and species important to energy generation are considered. Reactions with sufficient energy to break the N N triple bound are noted. that allows cyanobacteria to break N N triple bounds along the nitrogenase pathway are considered. Species identified as present in native distributions as well as tranient intermediates are considered.
- Dominant species in the systems are considered when additional species, such as nitrate are considered and reviewed in light of experimentally determined ammonia production.

  The several spreadsheets may provide semiquantitative assessment of simple molecule, nitrogen containing species in a variety of systems. Possibly significant observations within these models are noted with ★.

1 Native Distribution of Nitrogen Species

In the plots below, $\log f_i$ is plotted against E vs NHE at a given pH. The reactions considered are shown in Appendix A. For species with pK_a values, the concentrations of the individual protonated and deprotonated species are calculated using the fully protonated species and the pK_a values. It was also necessary to include dimers. These details are presented in Appendix B and resulted in the attached spreadsheet with VBA macros, ModelNitrogen08.xslm.

These data are for the native distribution of species, without any species added to the electrolyte. There are no limits placed on concentration. That is, the concentration of N_2 in solution will not reach 1 M but solubility is not a limitation of the model.

Follows are the distribution of species in unit pH changes for pH between 8 and 3. The lower limit of $\log f_i$ of about -21 corresponds to roughly one molecular entity per cm^3.

There are general behaviors to note.

1. The thermodynamic results specify the equilibrium rsults. Thermodynamic results do not account for kinetic limitations (such as perhaps breaking the N N triple bond). There are three general ranges of stability as function of potential. The ranges shift to positive potentials with decrease in pH.
   (a) ★ At the middle potentials, N_2 is the thermodynamically dominant species. There are no other species with thermodynamically allowed concentrations. It will be difficult to generate any other nitrogen species in this range unless the product is trapped in a metastable environment. Such an environment might be engineered within the algae matrix but is not anticipated likely.
   (b) ★ At negative potentials, the dominant species is the desired product(s), ammonium and ammonia. Nitrogen and NH_2OH are minor products tolerated in the negative potential range.

(c) ★ At positive potentials, there are several possible oxidized nitrogen species. Ammonia may be generated if these species participate in diproportionation and similar reactions that dissipate significant energy. (No such reactions were identified and the the nitrogen oxide species may largely serve as a redox buffer.)

(d) ★ In general ammonia and ammonium are generated at negative potentials. Generation of ammonia may be possible if the oxidized (fixed) nitrogen species participate in high energy (high E^0_{cell}) reactions.

i. Ammonia is commonly observed at negative potential polarization of the electrode.

ii. Ammonia is also observed at positive potential polarization of the electrode.

2. As pH decreases, the fraction of ammonia generated is largely ammonium.
3. At negative potentials, the only observed species other than ammonia+ammonium are N_2 and NH_2OH.
4. At positive potentials, a variety of oxidized nitrogen species are available and vary somewhat with pH.
5. Dioxygen may play an additional role in the speciation. The O_2 reduction potential will also shift with pH. Oxygen reduction is not considered in these distribution diagrams. Intact cyanobacteria preotect against oxidation by atmospheric oxygen. In disrupted cells, atmospheric O_2 will likely participate in redox processes if not excluded.

$$E = E^0 - \frac{2.303RT}{4F}\log\frac{1}{[O_2]\,[H^+]^4} = 1.229 - \frac{2.303RT}{4F}\log\frac{1}{[O_2]\,[H^+]^4} \tag{1}$$

6. ★ In general at postitive potentials, the assessible species are $NO_3^- > NO_2^- \approx NO_2 > HNO_2 > NO$. At $pH = 5$ and lower N_2O appears at low concentration. At pH of 4, N_2O_4 appears at very low concentration through the dimerization $2NO_2 \rightleftharpoons N_2O_4$.

1.1 Distribution Diagrams for Native Nitrogen Species

As described above and in Appendix B, distribution diagrams are developed for pH of 8 to 3. In each case, significant species at high and low potentials are noted in the captions. These species are considered on the potential axis in Section 2. Note that when species other than ammonium, N_2, and nitrate are noted in these plots, their equilibrium fraction is very low but these species are thermodynamically stable. Transient species, not thermodynamically stable, may contribute to ammonia formation. This is also considered in Section 2.

For the native distributions, at negative potentials ammonia and hyrdoxylamine are present. At positive potentials, a variety of oxides of nitrogen are present, with a general pattern of $NO_3^- > NO_2^- \approx NO_2 > HNO_2 > NO$ that varies in concentration with pH. At lower pH, N_2O and N_2O_4 are stable at very low concentration.

1.2 Hypothetical Extremophile at $pH = 0$

The model was run for $pH = 0$ to considered whether an extremophile stable under standard conditions would be more facile for ammonia production. The distribution diagram is shown in Figure 7.

► An extremophile at $pH = 0$ could generate significant amounts of ammonia about E near 0. At $pH = 7$, comparable ammonia production requires an additional -600 mV of polarization.

► Alternatively, a domain within the cyanobacteria structures that maintains low pH (and therefore higher ionic strength?) would promote more facile ammonium production.

2 Potential Axis and Stability of Species

A potential axis allows evaluation of reactions such as disproportionation that lead to ammonia and/or intermediates that lead to ammonia. The driving force for a reaction is measured as the difference in potential between two $E^{0'}$ values multiplied by the number of electrons in the reaction, $\Delta G^{0'}_{cell} = -nFE^{0'}_{cell}$ where $E^{0'}_{cell}$ is the difference in the formal potentials $E^{0'}$ for the reactions considered. Formal potential is standard potential corrected for experimental conditions such as pH.. For a reaction to generate species and energy, the reactants must be available in the two half reactions, one as the oxidized species and one as the reduced species. These will appear on the "outsides" of the reactant and products recorded as R|O about E^0 on the potential axis. The potential axis is set up in potentialaxiswithpHAlgae.xlsx, where different sheets (tabs) are described here. There is no VBA code in this program. The pH for the potential axes can be entered in box D1. Generally, when specific potentials are cited, the pH is taken a 7 unless otherwise noted.

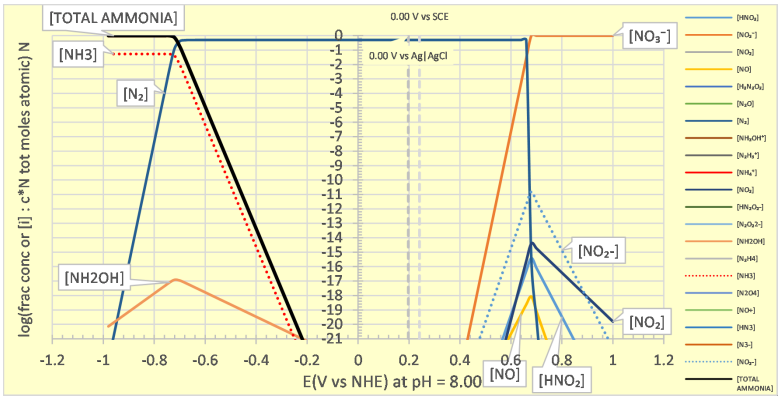

Figure 1: Native Distribution of Species as fraction of molecular entity to total atomic nitrogen at $pH = 8$.
Dominant species at $E \approx -0.7$: $NH_4^+ > NH_3 >> NH_2OH$
Dominant species at $E \approx 0.7$: $NO_3^- >> NO_2^- > NO_2 \gtrsim HNO_2 > NO$

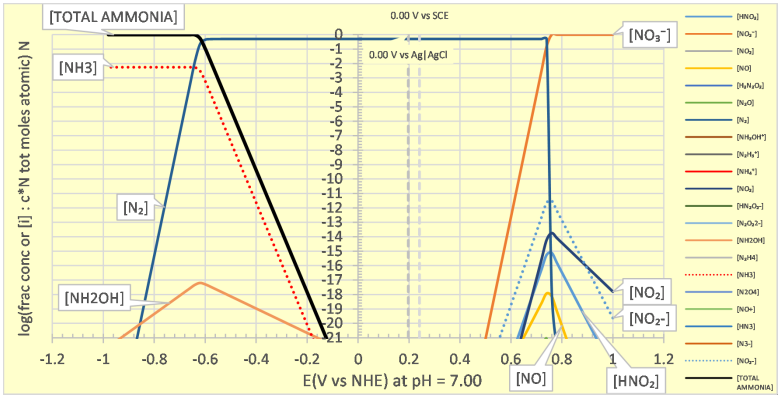

Figure 2: Native Distribution of Species as fraction of molecular entity to total atomic nitrogen at $pH = 7$.
Dominant species at $E \approx -0.6$: $NH_4^+ > NH_3 >> NH_2OH$
Dominant species at $E \approx 0.75$: $NO_3^- >> NO_2 \gtrsim NO_2^- \gtrsim HNO_2 > NO$

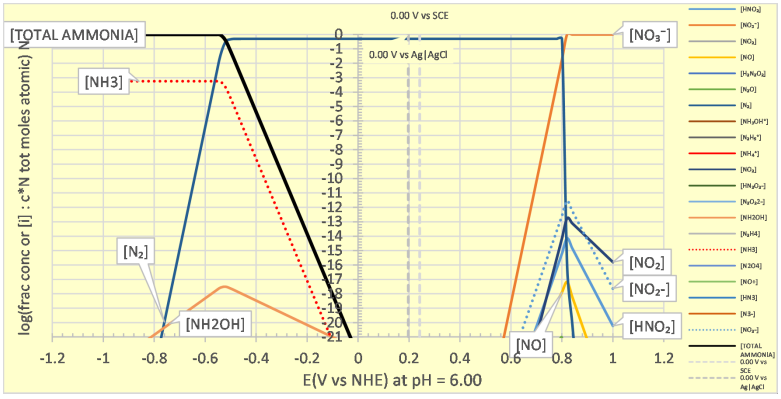

Figure 3: Native Distribution of Species as fraction of molecular entity to total atomic nitrogen at $pH = 6$.
Dominant species at $E \approx -0.4$: $NH_4^+ > NH_3 >> NH_2OH$
Dominant species at $E \approx 0.8$: $NO_3^- >> NO_2 \approx NO_2^- \gtrsim HNO_2 > NO$

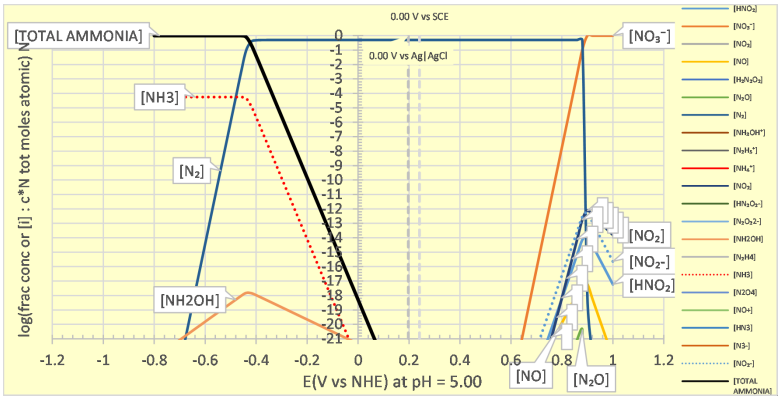

Figure 4: Native Distribution of Species as fraction of molecular entity to total atomic nitrogen at $pH = 5$.
Dominant species at $E \approx -0.4$: $NH_4^+ > NH_3 >> NH_2OH$
Dominant species at $E \approx 0.9$: $NO_3^- >> NO_2 \approx NO_2^- \gtrsim HNO_2 > NO > N_2O$

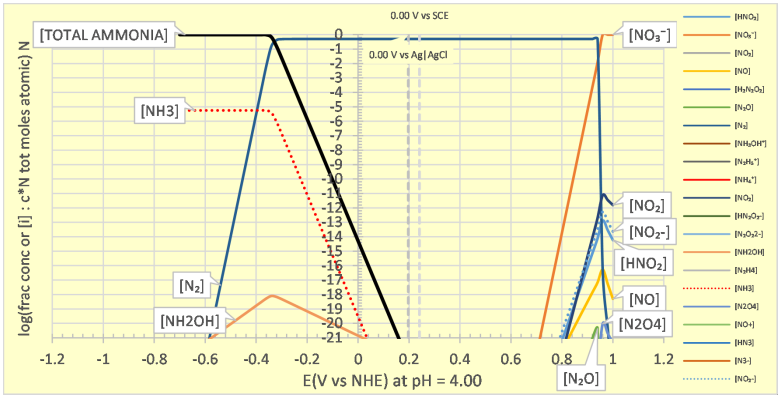

Figure 5: Native Distribution of Species as fraction of molecular entity to total atomic nitrogen at $pH = 4$.
Dominant species at $E \approx -0.3$: $NH_4^+ > NH_3 >> NH_2OH$
Dominant species at $E \approx 0.95$: $NO_3^- >> NO_2 \gtrsim NO_2^- \approx HNO_2 > NO > N_2O_4 \approx N_2O$

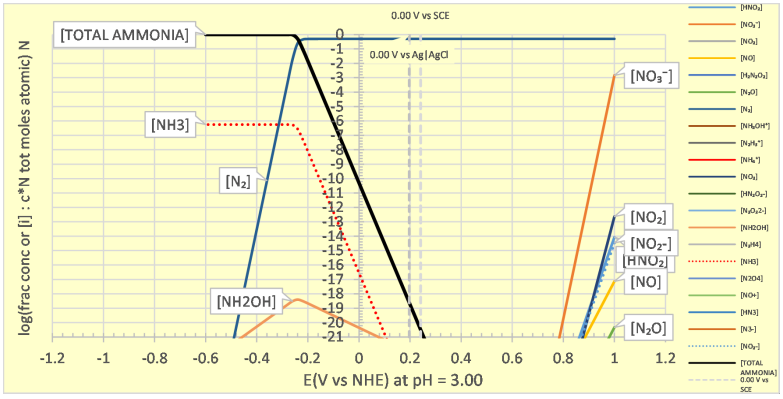

Figure 6: Native Distribution of Species as fraction of molecular entity to total atomic nitrogen at $pH = 3$.
Dominant species at $E \approx -0.2$: $NH_4^+ > NH_3 >> NH_2OH$
Dominant species at $E \approx 1.$: $NO_3^- >> NO_2 \gtrsim NO_2^- \approx HNO_2 > NO > N_2O$

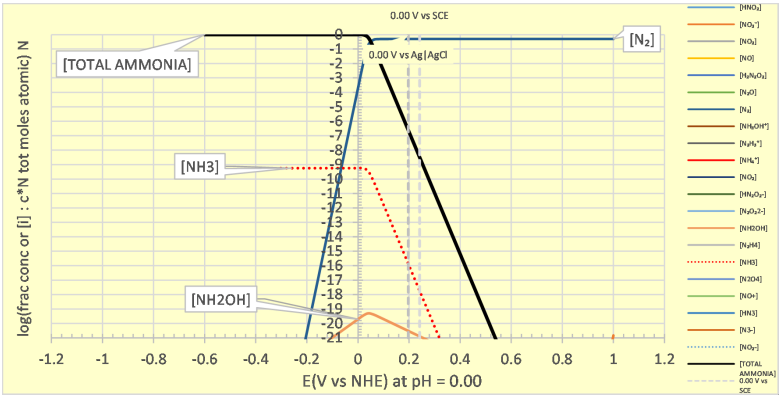

Figure 7: Hypothetical Conditions of $pH = 0$. If the system can be run at $pH = 0$, then significant concentrations of ammonia will exist at $E \gtrsim 0$ V.

Also, here the various states of protonation of a species are all indentified as the fully protonate form (e.g., $N_2H_5^+$ includes N_2H_4 on the potential axis, which differs from the distribution diagrams in Section 1).

Several effects can be evaluated.

1. From the native equilibrium models (Section 1), some species are stable at low concentrations. A potential axis will evaluate whether these species can disproportionate or otherwise react to yield ammonia or other intermediates that lead to ammonia. Two sets of conditions will be evaluated, the negative potential stable species, hydroxylamine|hydroxylammonium and the various NO_x species stable at positive potentials.
2. Are there intermediates available transiently that can yield ammonia and /or energy to break the N N triple bond. The bond energy for $N \equiv N$ is 946 kJ/mol $\approx \Delta G^0_{N_2}$, which is a large energy, almost twice that for $O_2 + 2H_2 \rightleftharpoons 2H_2O$.

2.1 Redox Reactions that Generate Ammonia|Ammonium

In the list of redox reactions in appendix 1, three reactions are listed for generation of ammonium. In each reaction, ammonium is the reduced species. Ammonium cannot undergo disproportionationation. The ammonia will remain stable unless an oxidize species with a formal potential more positive than the ammonia couples is present ($E \gtrsim 1.33$, 0.9, 0.65 for the ammonia reactions).

For each of the pages in the file potentialaxiswithpHAlgae.xlsx the ammonia reactions are marked by red lines. (All plots shown are also available in the attached potentialaxiswithpHAlgae.xlsx where pH and potential range can be further modified.)

2.2 Redox reactions of ammonium with oxygen

Thermodynamically, $E^{0'}$ for $O_2 + 4H^+ + 4e \rightleftharpoons 2H_2O$ is set as $E = E^{0'} - \frac{0.05916}{4} \log \frac{1}{[O_2][H^+]^4} = 1.229 - 0.05916pH - \frac{0.05916}{4} \log \frac{1}{[O_2]}$. At pH of 7, $E^{0'} = 1.229 - 0.05916\,(7) = 0.815$ V. If O_2 is present at unit concentration, O_2 has formal potential sufficient to oxidize ammonium. However, the concentration of dissolved O_2 is typically 0.1 mM in water, so the effective potential is 0.875 V.

★In the presence of O_2 ammonium can be oxidized to NH_2OH^+ and HN_3, at least thermodynamically.

2.2.1 Is there advantage to cyanobacteria to allow reaction of ammonium with O_2?

From the potential axis in Figure 8, oxygen can oxidize ammonium to yield $N_2H_5^+$ based on the potentials shown. Hydrazine can be reduced to yield 2 ammonium.

$$N_2H_5^+ + 3H^+ + 2e \rightleftharpoons 2NH_4^+ \qquad 1.275\ V \text{ at } pH = 7 \tag{2}$$

★ A delicate balance between oxygen and ammonium with near formal potentials and appropriate pH may provide a path to increase ammonia production because each hydrazine yields 2 NH_4^+. without additional interactions in the

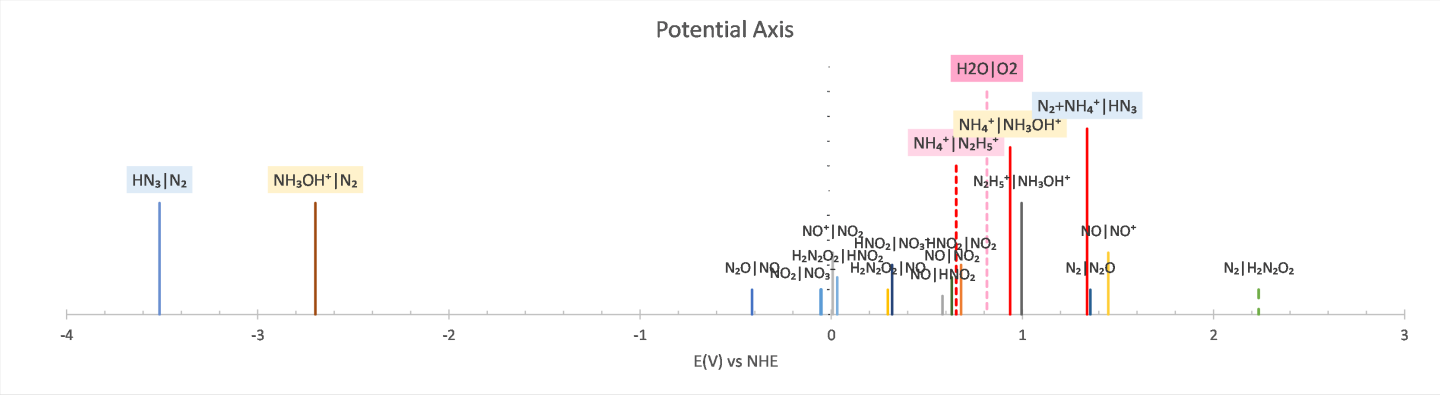

Figure 8: The potential axis at pH = 7 is shown with the reaction $O_2 + 4H^+ + 4e \rightleftharpoons 2H_2O$. Also shown are the three ammonium generating reactions. The potential for oxygen reduction is sufficient that O_2 can oxidize NH_4^+ to HN_3, NH_2OH^+, and $N_2H_5^+$. To determine if there is an advantage to cyanobacteria for ammonium synthesis to allow O_2 to be present, subsequent reactions that allow reduction of HN_3, NH_2OH^+, and $N_2H_5^+$ are also plotted. Note that reduction of $N_2H_5^+$ generates 2 NH_4^+. There is thermodynamic advantage to allow O_2 reduction of hydroylammonium or hydroxylamine to hydrazine as hydrazine yields two ammonium. (Tab AlgaeO2 in potaxiswithpHAlgae.xlsx)

system, the feedback between hydrazine, oxygen, and ammonium will yield no additional ammonium concentration. But, under appropriate conditions where formation of hydrazine is enhanced, increased concentrations of ammonium may be generated. There will be a delicate balance between ammonium generation, oxidation, and removal to enhance ammonium concentration in the electrolyte.

It is of interest to note that for the potential shown, oxygen does not generate hydroxylamine and azide. Conditions may be different at different pHs.

2.3 Minor Species Present under Native Equilibrium

From Section 1, there are species present at negative and positive potentials. The question is whether the presence of these species facilitates formation of ammonia|ammonium.

2.3.1 Dinitrogen N_2 and the Ammonium Reactions.

On the AlgaeN2 tab, the 4 reactions that involve dinitrogen are shown at elevated height. At negative potentials, N_2 is the oxidize species and that positive potentials N_2 is the reduced species. given the formal potentials for these reactions, dinitrogen will tend to be the product for any of these reactions. Dinitrogen is not configured even with change of pH to allow disproportionation.

The three ammonium reactions are described in Subsection 2.1. Note that ammonium is only generated directly from hydrazine, azide, and hydroxylamine. These three species provide the intermediates on the path to ammonium generation.

2.3.2 Species at negative potentials $NH_3OH^+|NH_2OH$

At negative potentials, the species present are ammonia, ammonium, and hydroxyl ammonium|hydroxylamine (NH_3OH^+, NH_2OH). There is dinitrogen N_2 as well,, but as above, N_2 is fairly inert. in addition to the ammonium ammonium reaction, the hydroxyl ammonium|hydroxylamine reactions are plotted on tab AlgaeNH2OH in Figure 10

As described in the caption, hydroxylamine can undergo disproportionation to generate dinitrogen and ammonium. hydroxylamine can react with reduced species with formal potentials negative of about 0.9 V at pH 7. It is noted that hydroxylamine can also form hydrazine on hydroxylamine disproportionation. hydrogen can react with other species including hydroxylamine to subsequently generate ammonium, as shown by the formal potential for $NH_4^+|N_2H_5^+$.

★ The hydroxylamine|hydroxyl ammonium present at positive potentials is likely an important intermediate in

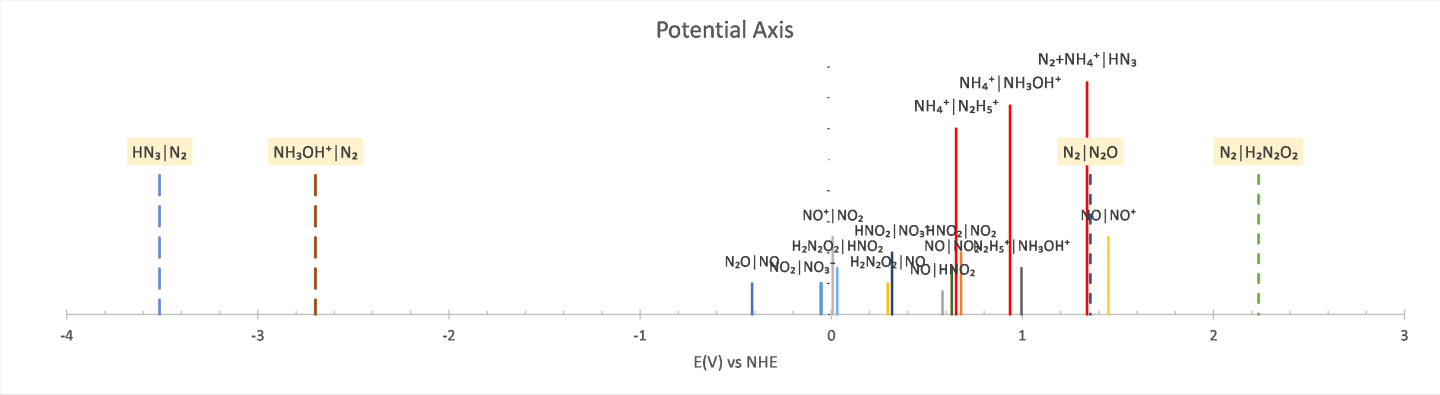

Figure 9: Potential axis for N_2 illustrates that N_2 cannot disproportionate and that given its potentials, N_2 will be the product rather than the reactant in the majority of reactions in which N_2 might participate. Also shown are the three reactions that involve ammonium as marked in red. In each case, NH_4^+ is the reduced part of the redox pair. Unless an oxidized species with formal potential more positive than the ammonia reactions is present in solution, ammonium will be stable. Ammonium cannot undergo disproportionation with ammonium. Thus, N_2 will tend to be unreactive and stable across a wide potential range as in Figures 1 through 6. Ammonium, once formed, will tend to be thermodynamically stable unless a species such as $H_2N_2O_2$ or perhaps NO^+ or N_2O is present. pH can have minor impact on the formal potential of the ammonia reactions. (Tab AlgaeN2 in potaxiswithpHAlgae.xlsx)

the generation of ammonium. There are various routes for ammonia generation from hydroxylamine that include hydroxylamine disproportionation.

2.3.3 Species at positive potentials Oxides of Nitrogen

From the fractional concentration plots, the species stable at positive potentials are various oxides of nitrogen. The rough distribution of species for pHs 8 to 3 are generally $NO_3^- > NO_2^- \approx NO_2 > HNO_2 > NO$ that varies in concentration with pH. At lower pH, N_2O and N_2O_4 are stable at very low concentration. These reactions are highlighted in Figure 11, where the full potential axis and an amplified segment are shown.

★ An examination of potential axis suggest that the oxidized nitrogen species do not provide a direct route to ammonium. Further, given the close proximity of formal potentials for the species, they provide a redox buffer with minimum buffer capacity. The species are likely intermediates along the way as dinitrogen is oxidized to nitrate.

2.4 Intermediates of Interest

An examination of the potential access allows consideration of special intermediates that may be effective in generation of ammonium. Two classes of reactions were considered: disproportionation reactions and transient, high energy intermediates and mediators.

2.4.1 Disproportionations

It is noted that several of the intermediates that can be generated under the reaction conditions can also undergo disproportionation to generate energy within the system. The species under consideration are hydroxylamine, hydrazine, and azide. All three species lead to ammonia generation. Disproportionation is particularly attractive as on generation, the thermodynamics allow generation of the desired ammonium product. Several of the oxides of nitrogen can also undergo disproportionation but no effect on ammonium generation is anticipated for these reactions. The potential access for the disproportionation reactions is shown in Figure 12.

★ Disproportionation of hydroxylamine and azide can contribute directly to ammonia generation.

★ A feedback loop with hydrazine can lead to enhanced ammonium generation as outlined in Section 2.2.1. Oxygen is an example of an oxidant for hydrazine.

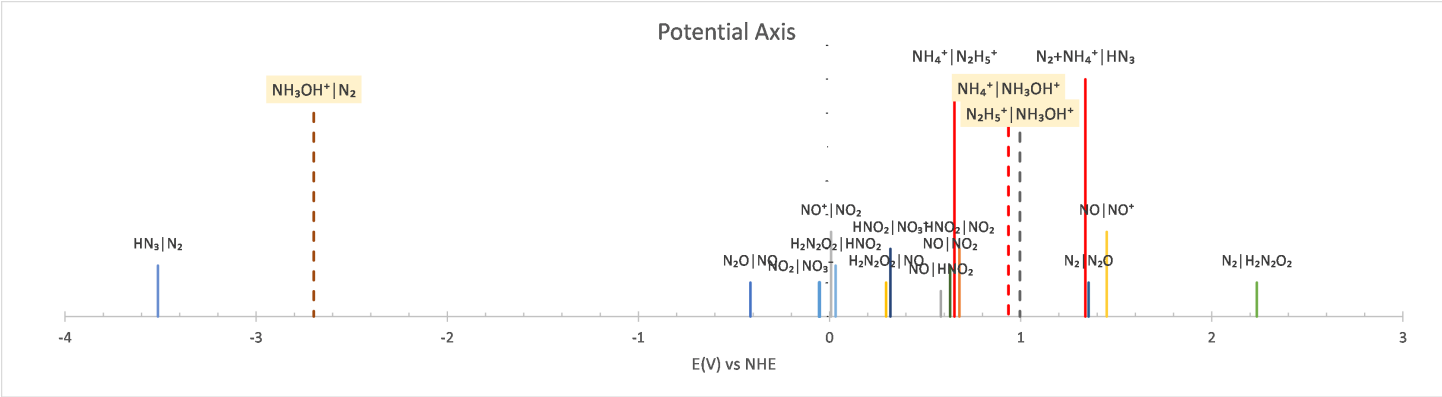

Figure 10: The potential axis is shown with the three ammonia reactions in red and the three hydroxylamine reactions marked as dashed lines. One reaction near0.9 V at pH 7 illustrates generation of ammonium from hydroxylamine. Hydroxylamine is likely a central component in the generation of ammonia. Hydroxylamine can undergo disproportionation to generate N_2 and NH_4^+. At pH 7, the reactions are separated by 3.35 V; for $n = 2$, $\Delta G^{0'} = -nFE^{0'}_{cell} = -2\,(96485)\,(3.352) = -647$ kJ/mol. thermodynamically, disproportionation hydroxylamine is highly favored. (Tab AlgaeNH2OH in potaxiswithpHAlgae.xlsx)

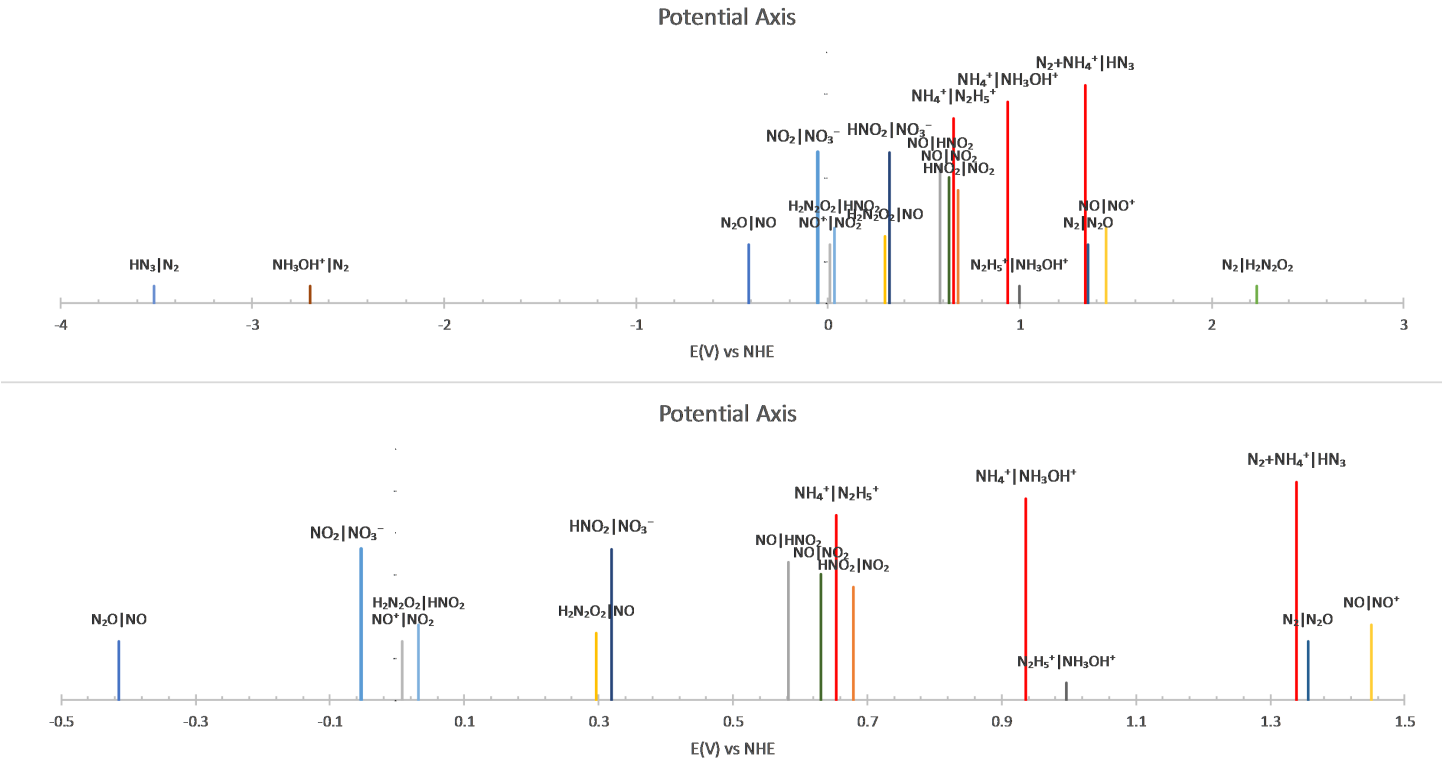

Figure 11: The potential axis at pH 7 is shown for various oxides of nitrogen, stable species identified in the fractional concentration plots for positive potentials. There is no direct route for generation of ammonium based on the oxidized nitrogen species. If oxygen were present, many of these species may be oxidized by O_2. The oxides of nitrogen perhaps provide low capacity redox buffers in the positive potential range. (Tab AlgaeNOxhighE in potaxiswithpHAlgae.xlsx)

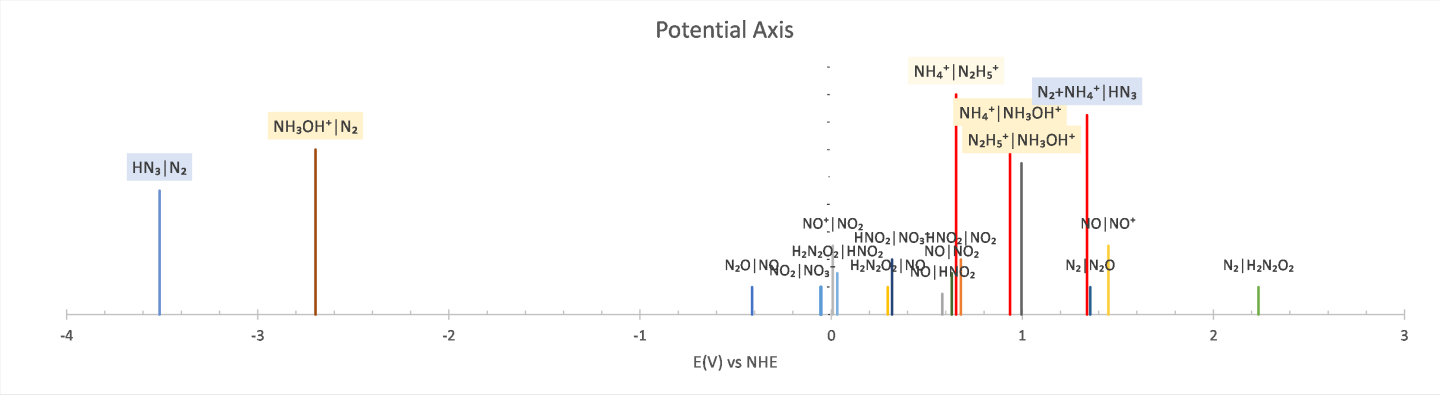

Figure 12: At pH 7, disproportionation reactions that contribute to ammonium generation are highlighted for azide, hydroxylamine, and hydrazine. These three species are the only species that directly generate ammonium. (Tab AlgaeDisp in potaxiswithpHAlgae.xlsx)

2.4.2 Transient high energy mediators

Some unstable species that would not be observed as equilibrium species may provide significant energy to the system that may contribute to breaking the dinitrogen triple bond. Some of these reactions are considered in Figure 13.

The species highlighted include azide (HN_3) and hydrazine ($N_2H_5^+$), which are both used in high energy systems such as explosives. The transient presence of these reduce nitrogen species could provide energy to break the nitrogen nitrogen triple bond.

Hydrazine can participate in a feedback loop to generate ammonia, as described above.

★ Azide can undergo disproportionation to yield 936 kJ/mol, which well matches the energy needed to break the nitrogen triple bond at 946 kJ/mol.

★ Further, Minteer reports that nitrogenase can use azide tto produce ammonia. The concentration of azide must, however, be carefully controlled as azide can damage cyanobacteria.

Several less common oxides of nitrogen are also highlighted: NO^+, $H_2N_2O_2$, N_2O, and.NO.

Disproportionatoin of NO^+ does not materially contribute to the generation of ammonium. However, it can serve as a reducing agent for the hydroxylamine, azide, and hydrazine. The amount of energy generated by these reactions would not be large.

$H_2N_2O_2$ Can undergo disproportionation to yield dinitrogen and NO and nitrous acid. Where $H_2N_2O_2$ is an oxidizing agent, its potential is sufficiently extreme to interact with numerous species in the system. This includes oxidation of ammonium, as well as azide and hydroxylamine to generate ammonium.

Dinitrogen oxide N_2O can undergo disproportionation and serve as an oxidizing agent for azide and hydroxylamine as well as ammonium.

For NO, there is limited opportunity to undergo disproportionation with a range of stability about the hydrazine ammonium reaction.

★ Thus with the exception of azide disproportionation and $H_2N_2O_2$ and perhaps NO^+ as an oxidizing agent, the thermodynamic potentials do not call out any significant reactions that lead to immediate generation of ammonium.

3 Evaluation of Experimental Results under the Thermodynamic Model

Variety of experiment systems were evaluated on cyanobacteria under a variety of experiment conditions. These results are summarized by Jacob Lyon in the attached report, named the Experimental Report. Here, these results are evaluated within the context of the thermodynamic model outlined above.

Where species are added to the electrolyte to view their impact on the rate of ammonia production, the concentration of the added materials will be viewed as invariant on the timescale of the experiment. This is appropriate as the

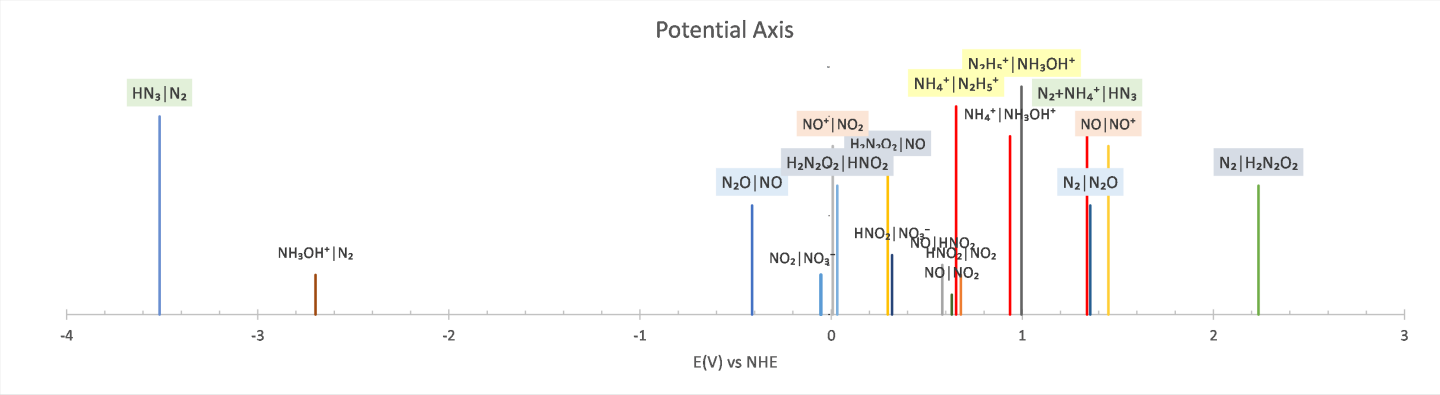

Figure 13: At pH 7, various potentially reactive species are considered on the potential axis. Several of these species would be transient and not mapped under the distribtion diagrams. Most these species would not serve a important mediators for direct converstion to ammonium. The exceptions are $H_2N_2O_2$ and perhaps NO^+ that can serve as oxidizing agents for ammonium and other species including azide and hydroxylamine. The other significant observation is that if azide is present transiently, azide can undergo disproportionation and generate sufficient energy to break the nitrogen nitrogen triple bond. (Tab AlgaeSpecialMediators in potaxiswithpHAlgae.xlsx)

amount of ammonia generated is typically far lower concentration than the concentration of the additives. Where this is not the case, it will be noted. in all cases, the concentration of chlorophyll is determined by assay and the amount of ammonia produced is normalized to the available chlorophyll content.

The various oxidation states of nitrogen are shown sequentially. In azide, the oxidation state of each of the three nitrogens is -1/3.

Ox State N	-3	-2	-1	$-\frac{1}{3}$	0	+1	+2	+3	+4	+5
	NH_4^+	$N_2H_5^+$	NH_3OH^+	HN_3	N_2	N_2O	NO	HNO_2	N_2H_4	HNO_3

3.1 Addition of Nitrate and Nitrite

Several experiments were undertaken for the system where nitrate and nitrite were added to the electrolyte. These experiments arise because the substrate for nitrogenase is dinitrogen whereas the substrate for nitrate reductase and nitrite reductase are respectively nitrate and nitrite. Nitrate and nitrite reductase are sequential enzymes where the nitrate is reduced and nitrite by the nitrate reductase and the nitrite is subsequently reduced by the nitrite reductase.

In Figure 1 of the Experimental Report, the concentration of nitrate plus nitrite was increased as 0, 20, 50, and 100 mM. In this first study the ammonia concentration was not normalized by the available chlorophyll. The amount of ammonia produced increased nearly linearly with the molar concentration of nitrate plus nitrite.

In Figure 2 of the Experiment Report, normalized ammonia concentration per mass of chlorophyll is shown for concentrations of nitrate; nitrite; and a mixture of nitrate plus nitrite for concentrations between 0 and 80 mM. for added nitrite, the normalized ammonia concentration increased. For a mixture of nitrate and nitrite the normalized ammonia concentration also increased but not as steeply as nitrite alone. If the concentration of nitrite alone is considered, the measured normalized ammonia concentration is similar to the values found for nitrite alone. These linearity support a first-order dependence on nitrite concentration. For addition of nitrate along, the normalized ammonia production falls slightly with increasing nitrate concentration. The addition of nitrate partially suppresses ammonia production.

The potential axis for nitrite is shown in Figure 14. Nitrite at pH 7 can undergo disproportionation to yield NO and NO_2, so that NO is more reduced and NO_2 is more oxidized. Because nitrite is present between 0 and 0.7 V and can serve as both an oxidant and reductant, nitrite can promote formation of ammonium through nitrite reductase. One reaction for nitrite is oxidatoin to nitrate. This and the second nitrate reaction is added to Figure 15. In both reactions, nitrate is present as an oxidizing agent as it is the most oxidizd of the nitrogen species. Given the potentials for nitrate, only a few species can reduce nitrate and these can be species that if reduced lead to ammonium directly, hydroxylamine and azide. For both nitrate reactions, where nitrate is an oxidant, increased concentration of nitrate

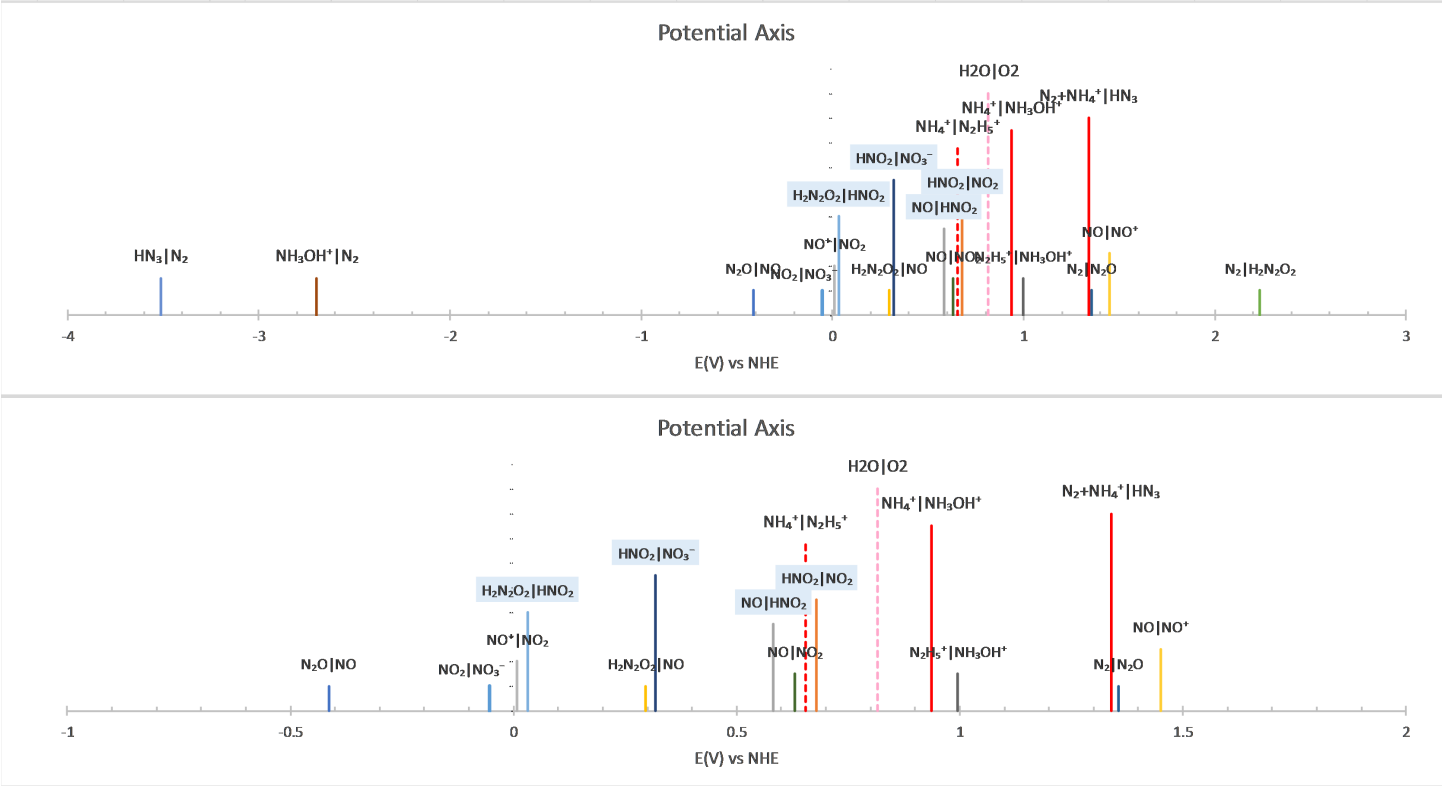

Figure 14: At pH 7, nitrite is highlighted, denoted as HNO_2.

will shift the potentail positive, and at a concommitantly lower ammonium concentration that shifts ammonium reactions to more negative reactions, the reaction of nitrate and ammonium can lead to consumption of the ammonium product. Ammonium nitrate can discharge with substantial driving force (energy). So under appropriate conditions of excess nitrate, genearted ammonia can be consumed to yield lower ammonia production. There is no mechanism for disproportionation of nitrate. Nitrite includes disproportionation reactions that will tend to mitigate oxidation of ammonium by nitrite.

Thus the observed increase in ammonia production in the presence of nitrite and the decreased generation of ammonia in the presence of nitrate are consistent with behaviors drawn from the potential axis. the first order behavior observed for both nitrate and nitrite are consistent with the proposed reactions.

In Figure 3 of the ExperimentalReport, a wide range of nitrite concentrations were evaluated for vegetative cells. The general trend is for an increase in ammonia production with nitrite concentration up to about hundred and 30 mM. At 180 mM there is a significant drop in ammonia production. This may correspond to reactions of nitrite to slow to disproportionate or to a situation where the concentration of ammonium is too low relative to the high concentration of nitrite so that potentials are sufficiently shifted that direct reaction between nitrite and ammonium is possible.

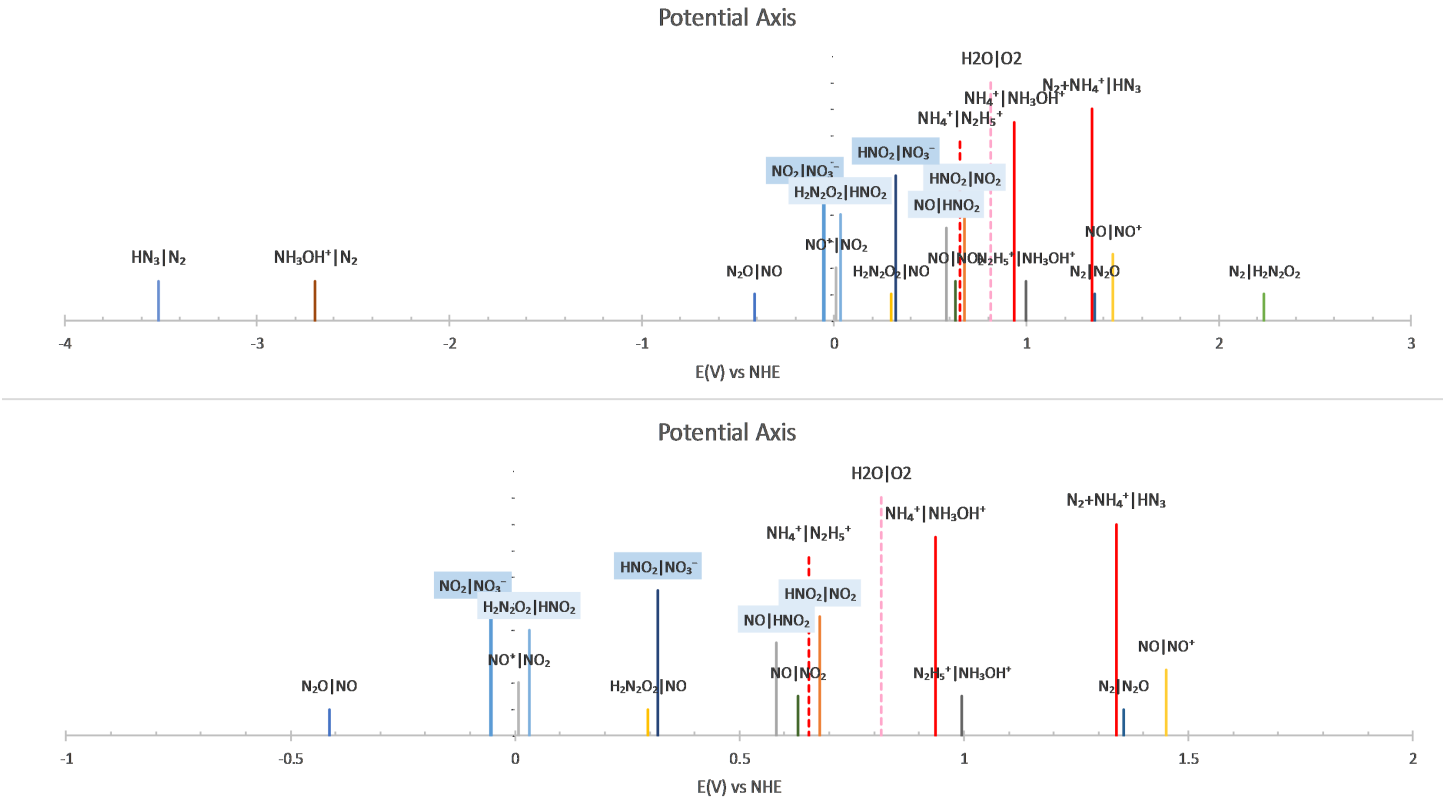

Figure 15: At pH 7, nitrate reactions are added to the potential axis. nitric can only act as an oxidizing agent in the matrix because there is no reduced form of nitrate specified within the system. Therefore, nitrate can under appropriate conditions of concentration react directly with ammonium to deplete the concentration of generated ammonia. Nitrite, conversely, is able to undergo disproportionation reactions that will tend to prevent nitrite serving as an oxidizing agent for ammonium.

3.2 Addition of N_2, N_2O, or NO

In Figure 5 of the Experimental Report, the impact of additions of nitrogen, N_2O, and NO on ammonia production is shown for both vegetative cells and a mixture of vegetative and heterocystic cells.

Addition of dinitrogen has little impact on the amount of ammonia produced and is statistically little different from the controls..This is consistent with tthe discussion in Section 2.3.1 where reactions of dinitrogen are limited.

On addition of N_2O, the mix cells show greater production of ammonia than the vegetative cells. the vegetative cells yield ammonia production only slightly greater then the nitrogen studies. N_2O is able to undergo a disproportionation reaction to yield NO and NO and N_2 with the substantial energy release.

Potentials for NO as a mediator are discussed in Section 2.4.2 and mapped Figure 13. under standard conditions or in cases where the concentration of NO and ammonium are both low, no substantialreactions are anticipated from NO that contribute significantly to the generation of ammonia. in the case where the concentration of NO is much greater than the concentration of ammonium, the potentials can shift. Where NO can serve as an oxidant, its potential will tend to shift positive; where NO serves as a reductive, the potential will tend to shift negative, relative to the potential for the ammonia reactions. uunder these conditions, the reductive and will likely have a larger impact and therefore increase the ammonia production. A larger shift is required for the nitrite oxidation to reduce the amount of ammonia generated

► It is noted that for both N_2O and NO, tthe mixed cells produced more ammonia then the vegetative cells alone. This suggests there may be some feedback between the nitrogenase and nitrite reductase in the effective generation of ammonia.

In Table 3 of the Experimental Report, significant shifts in the pH are noted on addition of these simple nitrogen -containing compounds. Dramatic shifts in the pH can have large impacts on the amount of ammonia produced consistent with large changes in the distribution of species with pH. Most of the reactions here are both electron and proton dependent.. An optimal pH for generation of ammonia is likely.

3.3 Addition of Hydrazine dihydrochloride and Hydroxylamine

In Table 4 of the Experimental Report, impacts of adding hydrazine dihydrochloride and hydroxylamine are reported. For the hydrazine die hydrochloride, there is a possibility of an acidic pH shift. Blanks are also reported for both additives. addition of hydrazine may slightly suppress ammonia production whereas hydroxylamine may slightly elevate ammonia production. However, the statistics for the measurements and controls do not provide a strong case for these roughly qualitative observations.

Because both hydrazine and hydroxylamine are immediate precursors for ammonia generation and both undergo disproportionation reactions to yield ammonia,, it was anticipated that these materials would markedly increase the amount of ammonia generated. For this set of data, no such increase was observed.

3.4 Potential Control

In Figure 6 and Table 5 of Experimental Report, ammonia production is reported as a function of applied electrode potential in a $BG11_0$ electrolyte which contains no nitrate. increased ammonia production is observed at extreme positive and negative potentials of -0.1 and +1.0 V vs NHE.

Similar measurements in sodium sulfate (Figure 7 and Table 6 in Experimental Report), also show enhanced ammonia production at -0.1 and +0.8 V wwith decreased production at +0.1 V vs NHE.

Consistent with the fractional concentration diagram in Figure 2, a rise in ammonia production is anticipated at negative potentials as observed. The speciation diagrams do not however anticipate an increase in ammonia production at positive potentials of 1 V vs NHE. In Figure 16, the impacts of potential control can be considered. For potential at -0.1 V versus NHE, the conversion of intermediate species of azide, hydroxylamine, and hydrazine to ammonia is electrolytically facilitated, as consistent with the fractional concentration plots. At 0.8 to 1 V, the potential may generate ammonia from azide, hydroxylamine, and hydrazine. There are only a few nitrogen species present in the system in this potential range, so that direct direct electrolysis to ammonia is possible. At 1 V, the generation of ammonia should be less efficient then at 0.8 V but the conditions in the two different electrolytes may shift potentials because of pH and other components of the matrix. Consistent with the potential access shown in Figure 16, applied potentials in the range from 0.6 to 0 V will cause conversion of the various oxides of nitrogen which may be in higher concentration than the less stable azide, hydroxylamine, and hydrazine. A low rate of ammonia production is anticipated in this redox buffer range.

In Figure 8 and Table 7 of the Experimental Report, a similar experiment is executed in the presence of 50 mM sodium nitrite in $BG11_0$ electrolyte. In this case, there is no systematic pattern to the amount of ammonia produced and an argument can be made that all of the values are statistically equivalent. Ammonia production in the presence

of excess nitrite is suppressed. This may be because the excess nitrite is generating a redox buffer in the general range between 0.2 and 0.6 vaults where the concentration of nitrite is much higher than the concentration of intermediates available to directly generate ammonia. The nitrite redox buffer is masking any electrode linked electrolysis and likely the intermediates needed to generate ammonia.

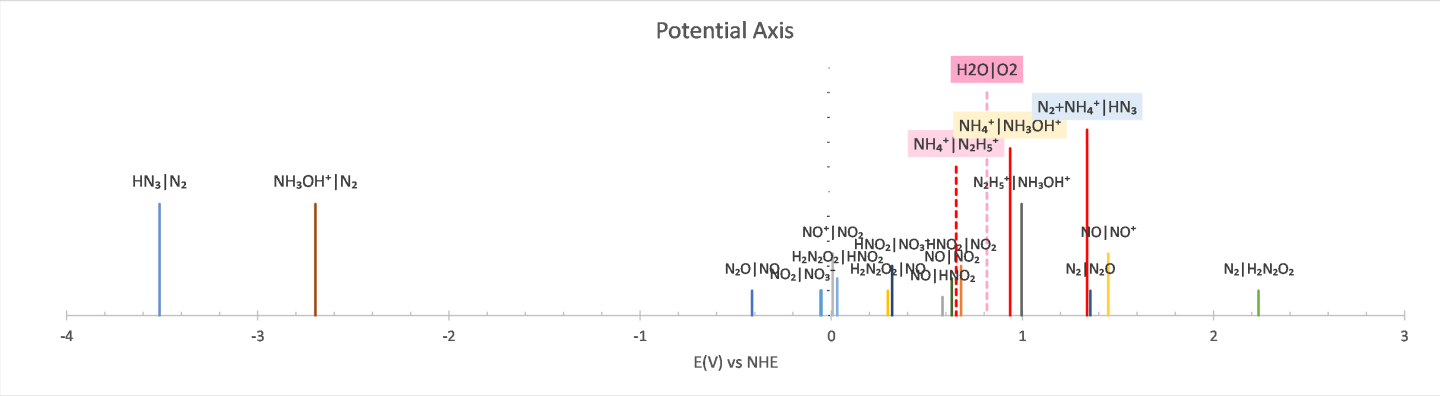

Figure 16: Control of the potential to 0.8 to 1.0 V and -0.1 V vs NHE yields increased ammonia production.

3.4.1 Vegetative and Hetertocystic Cells

Data for vegetative and hetero cystic cells are compared in Table 8 of the Experiment Report. the data are consistent with vegetative cells producing 10 to 20% more ammonia under different experiment conditions of scan rate. the higher skin rate for shorter. Generated more ammonia than a slower scan rate for a longer period. This may correlate with kinetics associated with the ammonia generating process.

In Table 11 and Figure 13 of the Experimental Report, heterocystic cells generate more ammonia then vegetative cells in the negative potential range, although the uncertainties on the reported values are high. The heterocysts contain nitrogenous days and tend to exclude oxygen whereas the vegetative cells contain nitrate and nitrite reductase and are less effective at excluding oxygen. tthe higher production of ammonia by hetero cysts at negative voltages suggests that the nitrogenase is more effective at ammonia generation under these experimental conditions. This result suggests that conversion of dinitrogen to ammonia may be achieved with greater efficiency then allowed by nitrate nitrite reductase, under appropriate experimental conditions.

3.5 Light and Dark

In Tables 9 and 10 and Figures 9 and 10 in the Experimental Report, llight is shown to facilitate ammonia production consistent with photosystem an important energy source for generation of ammonia. Components that drive the photosystem may be important to generation of ammonia, but this was not explored extensively. In Figures 11 and 12 of the Experimental Report, data suggest that ammonia will be generated even in the dark given a sufficient induction period. this suggest that the cells may be able to generate energy, perhaps from generated ammonia to drive further ammonia generation. This may be related to the different enzyme paths in cyanobacteria.

4 Summary

A model based on dynamic potentials has been developed for the various nitrogen species associated with ammonia production. the model generates a distribution diagram is a function of pH and potential for native nitrogen compositions. A potential access is exploited to predict various behaviors under various experimental conditions for different nitrogen containing components along the pathway to ammonia generation. Finally, experimental results recorded for cyanobacteria under a range of experimental conditions and nitrogen additives is evaluated through the model. The model is generally effective in predicting or explaining the observed experimental outcomes.

In discussion of the models, several notions are raised as to the mechanism by which ammonia is generated.

- Feedback between hydrazine and ammonia under appropriate conditions may lead to enhanced ammonia production.
- Disproportionation of azide and hydroxylamine provide significant energy and allows direct generation of ammonium.
- Under some conditions, trace oxygen may enhance the production of ammonia.
- Potential control to generate ammonia can be anticipated based on the potential access and concentrations of intermediates relative to the ammonia concentration.
- In the range where there are numerous oxides of nitrogen, redox buffering will tend to dominate the electrochemical processes and thereby suppress ammonia production.
- At low concentrations, azide may serve to enhance ammonia production.
- An extremophile tolerant of very acidic conditions may allow generation of ammonia at less extreme potentials..

5 Appendix A: Reactions Included in Native Distribution

These reactions were included in the native equilibria calculations. Reactions with more than 2 electrons are captured as combinations of these reactions. No other species were noted as generated by reactions with $n > 2$.

5.1 Species Names and Notations

The species considered are:

NO_3^-	A	nitrate	N_2	G	dinitrogen
NO_2	B		NH_3OH^+	H	hydroxylammonium
HNO_2	C	nitrous acid	$N_2H_5^+$	J	
NO	D		NH_4^+	K	ammonium
$H_2N_2O_2$	E	hyponitrous	N_2O_4	B2	
N_2O	F		HN_3	Z	
NO^+	L				
NO_2^-	CC	nitrite	N_3^-	ZZ	azide
$HN_2O_2^-$	EE		NH_2OH	HH	hydroxylamine
$N_2O_2^{2-}$	EEE		N_2H_4	JJ	hydrazine
			NH_3	KK	ammonia

5.2 Redox Reactions Considered

The redox reactions considered are:

Table A1a

			mH^+	ne^- $\rightleftharpoons$			H_2O	E^0
1}	1	NO_3^-	2	1	1	NO_2	1	0.775
2}	1	NO_2	1	1	1	HNO_2		1.093
3}	1	HNO_2	1	1	1	NO	1	0.996
4}	2	NO	2	2	1	$H_2N_2O_2$		0.71
5}	2	NO	2	2	1	N_2O	1	1.59
6}	1	$H_2N_2O_2$	2	2	1	N_2	2	2.65
7}	1	N_2O	2	2	1	N_2	1	1.77
8}	1	N_2	4	2	2	NH_3OH^+	-2	-1.87
9}	2	NH_3OH^+	1	1	1	$N_2H_5^+$	2	1.41
10}	1	$N_2H_5^+$	3	2	2	NH_4^+		1.275

Table A1b

			mH^+	ne^- $\rightleftharpoons$			H_2O	E^0
11}	1	NO_3^-	3	2	1	HNO_2	1	0.94
12}	1	NO_2	2	2	1	NO	1	1.045
13}	2	HNO_2	4	2	1	$H_2N_2O_2$	2	0.86
14}	1	NH_3OH^+	2	2	1	NH_4^+	1	1.35
15}	1	NO_2	2	1	1	NO^+	1	0.836
16}	1	NO^+		1	1	NO		1.45
17}	3	N_2	2	2	2	HN_3		-3.10
18}	1	HN_3	3	2	1	$N_2 + NH_4^+$		1.96

5.3 Reactions Not Redox

5.3.1 Acidity Equilibria

For assorted deprotonated species,	$CC = C \times 10^{pH} 10^{-3.398}$	$\alpha_C = 10^{pH} 10^{-3.398}$	nitrous acid / nitrite
	$EE = E \times 10^{pH} 10^{-7.21}$	$\alpha_E = 10^{pH} 10^{-7.21}$	hyponitrous acid /
	$EEE = E \times 10^{2pH} 10^{-18.75}$	$\alpha_{2E} = 10^{2pH} 10^{-18.75}$	
	$HH = H \times 10^{pH} 10^{-5.95}$	$\alpha_H = 10^{pH} 10^{-5.95}$	hydroxylammonium/hydroxylamine
	$JJ = J \times 10^{pH} 10^{-8.10}$	$\alpha_J = 10^{pH} 10^{-8.10}$	/hydrazine
	$KK = K \times 10^{pH} 10^{-9.25}$	$\alpha_K = 10^{pH} 10^{-9.25}$	ammonium/ ammonia

5.3.2 Dimer

There is only one dimer pair in the table.

$$N_2O_4 \rightleftharpoons 2NO_2 \qquad K_d = 5.9 \times 10^{-3} \text{ at 298 K} \tag{3}$$

$$pK_d = 2.23 \tag{4}$$

Reactions of NO_2 (B) are already included above. By analogy to the weak acids, given $[NO_2]$, $[N_2O_4]$ is calculated from the equilibrium constant as

$$K_d = \frac{[NO_2]^2}{[N_2O_4]} \tag{5}$$

$$[N_2O_4] = \frac{[NO_2]^2}{K_d} \tag{6}$$

$$[B2] = \frac{[B]^2}{K_d} \tag{7}$$

6 Appendix B: Derivation of the Distribution Equations

7 Introduction

Significant amounts of data have been collected for algae modified electrodes. This is an attempt to model / identify the important thermodynamic processes perhaps made possible by enzymes of the algae, nitrogenase in the heterocysts and nitrate/nitrite reductase in the vegetative cells.

The data indicate that the largest NH_3 increases are on addiction of $HNO_2 > N_2O > NO >> N_2 \approx N_2H_5^+$

Here is a run at developing a model for the thermodynamics of what might be there in the end and what species are part of the mechanism.

7.1 Approaches to Use of the Thermodynamic Model

Some questoins to be addressed by the model are:

1. Assume the algae is 100 % efficient at achieving the thermodynamic values.
   (a) What species are available for disproportionation to provide the energy to break N_2 bond. Will a disproportionation work?

7.2 Notes

1. Many of the nitrogen compounds are explosive and propellants and very unstable. If one is made there should be energy to break NN triple bound. If I have the idea of bond energy (NN triple of 226 kcal/mol) correctly, or 54. kJ/mol, for $n = 1$ $\Delta G/ - nF = E = \frac{54000\ J/mol}{96485 C/mol} = 0.56V$

7.3 Notes on this version

Version05, have eliminated fractional concentrations as individual cases assume only two species in the system and getting steady f_{N_2} is 0.5 instead of 1.0.

8 Development of the Thermodynamic Model Equations

8.1 Acids

Develop the thermodynamic equations for various cases, here laid out in increasing complexity.

Case $\mathcal{AA}$: Simple Electron Transfer Consider

$$A + ne \rightleftharpoons B \tag{8}$$

Nernst is

$$E = E^0 - \frac{2.303RT}{nF} \log \frac{[B]}{[A]} \tag{9}$$

$$= E^0 - \frac{1}{n\gamma} \log \frac{[B]}{[A]} \tag{10}$$

where $\gamma = F/2.303RT$, a constant for given temperature. Rearrange

$$-n\gamma \left(E - E^0\right) = \log \frac{[B]}{[A]} \tag{11}$$

$$\theta = 10^{-n\gamma\left(E-E^0\right)} = \frac{[B]}{[A]} \tag{12}$$

$$\mathbf{A + ne \rightleftharpoons B} \tag{13}$$

Let $\theta = 10^{-n\gamma\left(E-E^0\right)}$.

Case $\mathcal{BB}$: Add m H^+ For m protons needed to balance the redox reaction in acid,

$$A + mH^+ + ne \rightleftharpoons B \tag{14}$$

Nernst is

$$\begin{aligned} E &= E^0 - \frac{2.303RT}{nF}\log\frac{[B]}{[A]\left[H^+\right]^m} && (15)\\ &= E^0 - \frac{1}{n\gamma}\log\frac{[B]}{[A]\left[H^+\right]^m} && (16)\\ &= E^0 - \frac{m}{n\gamma}\log\frac{1}{\left[H^+\right]} - \frac{1}{n\gamma}\log\frac{[B]}{[A]} && (17)\\ &= E^0 - \frac{m}{n\gamma}pH - \frac{1}{n\gamma}\log\frac{[B]}{[A]} && (18) \end{aligned}$$

Rearrange where $\theta = 10^{-n\gamma\left(E-E^0\right)}$

$$\begin{aligned} E &= E^0 - \frac{m}{n\gamma}pH - \frac{1}{n\gamma}\log\frac{[B]}{[A]} && (19)\\ -n\gamma\left(E-E^0\right) &= mpH + \log\frac{[B]}{[A]} && (20)\\ -n\gamma\left(E-E^0\right) - mpH &= \log\frac{[B]}{[A]} && (21)\\ 10^{-n\gamma\left(E-E^0\right)}10^{-mpH} &= \frac{[B]}{[A]} && (22)\\ \theta 10^{-mpH} &= \frac{[B]}{[A]} && (23)\\ \mathbf{A + mH^+ + ne \rightleftharpoons B} && && (24) \end{aligned}$$

8.1.1 Generic Nernst Expression

Case $\mathcal{GN}$: Generic Nernst For

$$\begin{aligned} \mathbf{rR + mH^+ + ne} &\rightleftharpoons \mathbf{qP} && (25)\\ E &= E^0 - \frac{1}{n\gamma}\log\frac{[P]^q}{[R]^r\left[H^+\right]^m} && (26)\\ -n\gamma\left(E-E^0\right) &= m\log\frac{1}{\left[H^+\right]} + \log\frac{[P]^q}{[R]^r} && (27)\\ &= mpH + \log\frac{[P]^q}{[R]^r} && (28)\\ 10^{-n\gamma\left(E-E^0\right)}10^{-mpH} &= \frac{[P]^q}{[R]^r} && (29) \end{aligned}$$

Where P and/or R is a weak acid, the concentrations of the deprotonated species are calculated from K_A. For

$$R + H_2O \rightleftharpoons aH_3O^+ + \bar{R} \quad \beta_{A,R_i} = \frac{\left[H_3O^+\right]^a\left[\bar{R}\right]}{[R]} \text{ where } \beta_{A,R_i} = \Pi_{i=1}^a K_{A,R_i} \tag{30}$$

$$P + H_2O \rightleftharpoons bH_3O^+ + \bar{P} \quad \beta_{A,P_i} = \frac{\left[H_3O^+\right]^b\left[\bar{P}\right]}{[P]} \text{ where } \beta_{A,P_i} = \Pi_{i=1}^a K_{A,P_i} \tag{31}$$

For monoprotics, a and/or b are 1. For polyprotics, a and/or b are set by the particular proton lost. For the first proton, a and/or b are 1; for the second, a and/or b are 2; for the third, a and/or b are 3..... The reactions lead to the following, where the fully protonated species is H_zA.

$$H_zA + xH_2O \rightleftharpoons xH_3O^+ + H_{z-x}A^{z-x} \tag{32}$$

$$\beta = \frac{\left[H_3O^+\right]^x \left[H_{z-x}A^{z-x}\right]}{\left[H_zA\right]} \tag{33}$$

$$\left[H_{z-x}A^{z-x}\right] = \beta \left[H_zA\right] \left[H_3O^+\right]^{-x} = \underbrace{\beta 10^{xpH}}_{\alpha} \left[H_zA\right] \tag{34}$$

8.1.2 Review of JTM's data for simplify to acid forms and monomer of all dimers

JTM's data were sorted for the fully protonated species and less than 2 electrons (with one exception). This captures all the 11 species and 10 reactions in the latimer diagram in pairs that are directly adjacent. (Directly adjacnet means n of 1 or 2. higher n is found by combining other reactions.) May need to add some of the other pathways subsequently. No dimers are yet included.

Started with fully protonated species (where $a = 0$ and $b = 0$) and then added acid reactions as above

$\gamma = 38.92/2.303 = 16.900$

$\theta = 10^{-n\gamma\left(E-E^0\right)}$

8.1.3 Solve system equations

Let $f_i = I$, fractional concentration of I

NO_3^-	A	nitrate	N_2	G	dinitrogen
NO_2	B		NH_3OH^+	H	Hydroxylammonium weak base
HNO_2	C	nitrous acid	$N_2H_5^+$	J	
NO	D		NH_4^+	K	ammonium
$H_2N_2O_2$	E	hyponitrous	N_2O_4	B2	
N_2O	F				
NO_2^-	CC	nitrite	NH_2OH	HH	Hydroxylamine
$HN_2O_2^-$	EE		N_2H_4	JJ	
$N_2O_2^{2-}$	EEE		NH_3	KK	ammonia

Note that none of the above solution work for all pH and E. Will chack again if the introduction of dimers does not give better solution steps.□

Solve to G $\mathbf{N}_2$

$$\begin{array}{ll}
\frac{B}{A} = a & A = \frac{B}{a} = \sqrt{\frac{G}{dfa^2b^2c^2}} = \sqrt{\frac{G}{gea^2b^2c^2}} \\
\frac{C}{B} = b & B = \frac{C}{b} = \sqrt{\frac{G}{dfb^2c^2}} = \sqrt{\frac{G}{geb^2c^2}} \\
\frac{D}{C} = c & C = \frac{D}{c} = \sqrt{\frac{G}{dfc^2}} = \sqrt{\frac{G}{gec^2}} \\
\frac{E}{D^2} = d & D = \sqrt{\frac{E}{d}} = \sqrt{\frac{G}{df}} \\
\frac{F}{D^2} = e & D = \sqrt{\frac{F}{e}} = \sqrt{\frac{G}{ge}} \qquad ge = df \checkmark \\
\frac{G}{E} = f & E = \frac{G}{f} \\
\frac{G}{F} = g & F = \frac{G}{g} \\
\frac{H^2}{G} = h & H = \sqrt{Gh} \\
\frac{J}{H^2} = j & J = jH^2 = jhG \\
\frac{K^2}{J} = k & K = \sqrt{kJ} = \sqrt{kjhG}
\end{array}$$

Table 1

			mH^+	$ne \rightleftharpoons$			H_2O	E^0						
1}	1	NO_3^-	1 2	1	1	NO_2	1	0.775	$\frac{[NO_2]}{[NO_3^-]}$	$\frac{[B]}{[A]}$	a	θ	10^{-2pH}	$\frac{[B]}{[A]}$	
2}	1	NO_2	1	1	1	HNO_2		1.093	$\frac{[HNO_2]}{[NO_2]}$	$\frac{[C]}{[B]}$	b	θ_{RP}	10^{-pH}	$\frac{[C]}{[B]}$	$p\beta_{C,P1} = 3.398, b = 1$ for $NO_2^- = CC$ $CC = C \times 10^{pH} 10^{-3.398}$
3}	1	HNO_2	1	1	1	NO	1	0.996	$\frac{[NO]}{[HNO_2]}$	$\frac{[D]}{[C]}$	c	θ_{RP}	10^{-pH}	$\frac{[D]}{[C]}$	
4}	2	NO	2	2	1	$H_2N_2O_2$		0.71	$\frac{[H_2N_2O_2]}{[NO]^2}$	$\frac{[E]}{[D]^2}$	d	θ_{RP}	10^{-2pH}	$\frac{[E]}{[D]^2}$	$p\beta_{E,P1} = 7.21, b = 1$ for $HN_2O_2^- = EE$ $p\beta_{E,P2} = 11.54 + 7.21, b = 2$ for $N_2O_2^{-2} = EEE$ $EE = E \times 10^{pH} 10^{-7.21}$ $EEE = E \times 10^{2pH} 10^{-18.75}$
5}	2	NO	2	2	1	N_2O	1	1.59	$\frac{[N_2O]}{[NO]^2}$	$\frac{[F]}{[D]^2}$	e	θ	10^{-2pH}	$\frac{[F]}{[D]^2}$	
6}	1	$H_2N_2O_2$	2	2	1	N_2	2	2.65	$\frac{[N_2]}{[H_2N_2O_2]}$	$\frac{[G]}{[E]}$	f	θ_{RP}	10^{-2pH}	$\frac{[G]}{[E]}$	
7}	1	N_2O	2	2	1	N_2	1	1.77	$\frac{[N_2]}{[N_2O]}$	$\frac{[G]}{[F]}$	g	θ	10^{-2pH}	$\frac{[G]}{[F]}$	
8}	1	N_2	4	4 2	2	NH_3OH^+	-2	-1.87	$\frac{[NH_3OH^+]^2}{[N_2]}$	$\frac{[H]^2}{[G]}$	h	θ_{RP}	10^{-4pH}	$\frac{[H]^2}{[G]}$	$p\beta_{H,P1} = 5.95, b = 1$ for $NH_2OH = HH$ $HH = H \times 10^{pH} 10^{-5.95}$
9}	2	NH_3OH^+	1	1	1	$N_2H_5^+$	2	1.41	$\frac{[N_2H_5^+]}{[NH_3OH^+]^2}$	$\frac{[J]}{[H]^2}$	j	θ_{RP}	10^{-pH}	$\frac{[J]}{[H]^2}$	$p\beta_{J,P_1} = 8.10, b = 1$ for $N_2H_4 = JJ$ $JJ = J \times 10^{pH} 10^{-8.10}$
10}	1	$N_2H_5^+$	3	2	2	NH_4^+	-2	1.275	$\frac{[NH_4^+]^2}{[N_2H_5^+]}$	$\frac{[K]^2}{[J]}$	k	θ_{RP}	10^{-3pH}	$\frac{[K]^2}{[J]}$	$p\beta_{K,P_1} = 9.25, b = 1$ for $NH_3 = KK$ $KK = K \times 10^{pH} 10^{-9.25}$

For assorted deprotonated species, $CC = C \times 10^{pH} 10^{-3.398}$ $\alpha_C = 10^{pH} 10^{-3.398}$
$EE = E \times 10^{pH} 10^{-7.21}$ $\alpha_E = 10^{pH} 10^{-7.21}$
$EEE = E \times 10^{2pH} 10^{-18.75}$ $\alpha_{2E} = 10^{2pH} 10^{-18.75}$
$HH = H \times 10^{pH} 10^{-5.95}$ $\alpha_H = 10^{pH} 10^{-5.95}$
$JJ = J \times 10^{pH} 10^{-8.10}$ $\alpha_J = 10^{pH} 10^{-8.10}$
$KK = K \times 10^{pH} 10^{-9.25}$ $\alpha_K = 10^{pH} 10^{-9.25}$

Converted all to α where $[A^{x-}] = \beta [H_x A] [H^+]^{-x} = \beta [H_x A] 10^{xpH} = [H_x A] \alpha$, which now yields sum concentrations (fractionals?) at 1□

Mass balance $c^* = [A] + [B] + [C] + [CC] + [D] + 2\{[E] + [EE] + [EEE]\} + 2[F] + 2[G] + [H] + [HH] + 2[J] + 2[JJ] + [K] + [KK]$

moles total atomic N per volume

$c^* = [A] + [B] + [C](1 + \alpha_C) + [D] + 2\{[E](1 + \alpha_E + \alpha_{E2})\} + 2[F] + 2[G] + [H](1 + \alpha_H) + 2[J](1 + \alpha_J) + [K](1 + \alpha_K)$

$1 = A + B + C(1 + \alpha_C) + D + 2E(1 + \alpha_E + \alpha_{E2}) + 2F + 2G + H(1 + \alpha_H) + 2J(1 + \alpha_J) + K(1 + \alpha_K)$

$1 = A + B + C(1 + \alpha_C) + D + H(1 + \alpha_H) + K(1 + \alpha_K) + 2\{E(1 + \alpha_E + \alpha_{E2}) + F + G + J(1 + \alpha_J)\}$

Solve to G, dinitrogen:

$1 = \sqrt{\frac{G}{gea^2b^2c^2}} + \sqrt{\frac{G}{geb^2c^2}} + \sqrt{\frac{G}{gec^2}} + \sqrt{\frac{G}{ge}} + \sqrt{Gh}(1 + \alpha_H) + \sqrt{kjhG}(1 + \alpha_K) + 2\left\{\frac{G}{f}(1 + \alpha_E + \alpha_{E2}) + \frac{G}{g} + G + jhG(1 + \alpha_J)\right.$

$1 = \sqrt{\frac{G}{ge}}\left\{\sqrt{\frac{1}{a^2b^2c^2}} + \sqrt{\frac{1}{b^2c^2}} + \sqrt{\frac{1}{c^2}} + 1 + \sqrt{geh}(1 + \alpha_H) + \sqrt{kjhge}(1 + \alpha_K)\right\} + G2\left\{\frac{1}{f}(1 + \alpha_E + \alpha_{E2}) + \frac{1}{g} + 1 + jh(1 +\right.$

Let $\sqrt{G} = x$

$1 = x\underbrace{\frac{1}{\sqrt{ge}}\left\{\sqrt{\frac{1}{a^2b^2c^2}} + \sqrt{\frac{1}{b^2c^2}} + \sqrt{\frac{1}{c^2}} + 1 + \sqrt{geh}(1 + \alpha_H) + \sqrt{kjhge}(1 + \alpha_K)\right\}}_{v} + x^2\underbrace{2\left\{\frac{1}{f}(1 + \alpha_E + \alpha_{E2}) + \frac{1}{g} + 1 + j\right.}_{w}$

$wx^2 + vx - 1 = 0$

quadratic equation (negative x is ok as yeilds $x = \sqrt{G}$)

$x = \frac{-b \pm \sqrt{b^2 - 4ac}}{2a} = \frac{-v \pm \sqrt{v^2 + 4w}}{2w} \xrightarrow{?} \frac{-v + \sqrt{v^2 + 4w}}{2w} = \sqrt{G}$

So what do we see? thermo make lots ammonia negative potentials;potentials shift in at acid. highest concentration ammonia produced when no nitrogen in system?

Works except when nitrate dominant and $N_2 \longrightarrow 0$

Solve to D NO NO is not anticipated in high concentrations but its equation are simple.

$\frac{B}{A} = a$ $A = \frac{B}{a} = \frac{D}{abc}$
$\frac{C}{B} = b$ $B = \frac{C}{b} = \frac{D}{bc}$
$\frac{D}{C} = c$ $C = \frac{D}{c}$
$\frac{E}{D^2} = d$ $E = dD^2$
$\frac{F}{D^2} = e$ $F = eD^2$
$\frac{G}{E} = f$ $G = fE = fdD^2$ $ge = df$✓
$\frac{G}{F} = g$ $G = gF = geD^2$
$\frac{H^2}{G} = h$ $H = \sqrt{hG} = \sqrt{hge}D$
$\frac{J}{H^2} = j$ $J = jH^2 = j(hge)^2 D^2$
$\frac{K^2}{J} = k$ $K = \sqrt{kJ} = hge\sqrt{kj}D$

$c^* = [A] + [B] + [C](1 + \alpha_C) + [D] + 2\{[E](1 + \alpha_E + \alpha_{E2})\} + 2[F] + 2[G] + [H](1 + \alpha_H) + 2[J](1 + \alpha_J) + [K](1 + \alpha_K)$

$1 = A + B + C(1 + \alpha_C) + D + 2E(1 + \alpha_E + \alpha_{E2}) + 2F + 2G + H(1 + \alpha_H) + 2J(1 + \alpha_J) + K(1 + \alpha_K)$

$1 = A + B + C(1 + \alpha_C) + D + H(1 + \alpha_H) + K(1 + \alpha_K) + 2\{E(1 + \alpha_E + \alpha_{E2}) + F + G + J(1 + \alpha_J)\}$

Solve to D, NO

$1 = \frac{D}{abc} + \frac{D}{bc} + \frac{D}{c}(1 + \alpha_C) + D + \sqrt{hge}D(1 + \alpha_H) + hge\sqrt{kj}D(1 + \alpha_K) + 2\left\{dD^2(1 + \alpha_E + \alpha_{E2}) + eD^2 + fdD^2 + j(hge)^2 D^2\right.$

$1 = D\left\{\frac{1}{abc} + \frac{1}{bc} + \frac{1}{c}(1 + \alpha_C) + 1 + \sqrt{hge}(1 + \alpha_H) + hge\sqrt{kj}(1 + \alpha_K)\right\} + 2D^2\left\{d(1 + \alpha_E + \alpha_{E2}) + e + fd + j(hge)^2(1 +\right.$

$$D^2 2\underbrace{\left\{d\left(1+\alpha_E+\alpha_{E2}\right)+e+fd+j\left(hge\right)^2\left(1+\alpha_J\right)\right\}}_{w}+D\underbrace{\left\{\frac{1}{abc}+\frac{1}{bc}+\frac{1}{c}\left(1+\alpha_C\right)+1+\sqrt{hge}\left(1+\alpha_H\right)+hge\sqrt{kj}\left(1+\alpha\right.\right.}_{v}$$

$1=0$

$wx^2+vx-1=0$

quadratic equation (negative x is ok as yeilds $x=D$)

$x=\frac{-b\pm\sqrt{b^2-4ac}}{2a}=\frac{-v\pm\sqrt{v^2+4w}}{2w}\xrightarrow{?}\frac{-v+\sqrt{v^2+4w}}{2w}=D$

Solve to E $\mathbf{H_2N_2O_2}$ $H_2N_2O_2$ is not anticipated in high concentrations but provides the largest i

$\frac{B}{A}=a \qquad A=\frac{B}{a}=\frac{1}{abc}\sqrt{\frac{E}{d}}$

$\frac{C}{B}=b \qquad B=\frac{C}{b}=\frac{1}{bc}\sqrt{\frac{E}{d}}$

$\frac{D}{C}=c \qquad C=\frac{D}{c}=\frac{1}{c}\sqrt{\frac{E}{d}}$

$\frac{E}{D^2}=d \qquad D=\sqrt{\frac{E}{d}}$

$\frac{F}{D^2}=e \qquad F=eD^2=\frac{e}{d}E$

$\frac{G}{E}=f \qquad G=fE \qquad fd=ge\checkmark$

$\frac{G}{F}=g \qquad G=gF=\frac{ge}{d}E$

$\frac{H^2}{G}=h \quad H=\sqrt{hG}=\sqrt{\frac{hge}{d}E}$

$\frac{J}{H^2}=j \qquad J=jH^2=\frac{jhge}{d}E$

$\frac{K^2}{J}=k \quad K=\sqrt{kJ}=\sqrt{\frac{jkhge}{d}E}$

$c^*=[A]+[B]+[C]\left(1+\alpha_C\right)+[D]+2\left\{[E]\left(1+\alpha_E+\alpha_{E2}\right)\right\}+2\left[F\right]+2\left[G\right]+[H]\left(1+\alpha_H\right)+2\left[J\right]\left(1+\alpha_J\right)+$
$[K]\left(1+\alpha_K\right)$

$1=A+B+C\left(1+\alpha_C\right)+D+2E\left(1+\alpha_E+\alpha_{E2}\right)+2F+2G+H\left(1+\alpha_H\right)+2J\left(1+\alpha_J\right)+K\left(1+\alpha_K\right)$

$1=A+B+C\left(1+\alpha_C\right)+D+H\left(1+\alpha_H\right)+K\left(1+\alpha_K\right)+2\left\{E\left(1+\alpha_E+\alpha_{E2}\right)+F+G+J\left(1+\alpha_J\right)\right\}$

Solve to E, NO

$1=A+B+C\left(1+\alpha_C\right)+D+H\left(1+\alpha_H\right)+K\left(1+\alpha_K\right)+2\left\{E\left(1+\alpha_E+\alpha_{E2}\right)+F+G+J\left(1+\alpha_J\right)\right\}$

$1=\frac{1}{abc}\sqrt{\frac{E}{d}}+\frac{1}{bc}\sqrt{\frac{E}{d}}+\frac{1}{c}\sqrt{\frac{E}{d}}\left(1+\alpha_C\right)+\sqrt{\frac{E}{d}}+\sqrt{\frac{hge}{d}E}\left(1+\alpha_H\right)+\sqrt{\frac{jkhge}{d}E}\left(1+\alpha_K\right)+2\left\{E\left(1+\alpha_E+\alpha_{E2}\right)+\frac{e}{d}E+\frac{ge}{d}E+\right.$

$1=\sqrt{\frac{E}{d}}\left\{\frac{1}{abc}\sqrt{\frac{E}{d}}+\frac{1}{bc}\sqrt{\frac{E}{d}}+\frac{1}{c}\sqrt{\frac{E}{d}}\left(1+\alpha_C\right)+\sqrt{\frac{E}{d}}+\sqrt{\frac{hge}{d}E}\left(1+\alpha_H\right)+\sqrt{\frac{jkhge}{d}E}\left(1+\alpha_K\right)\right\}+2\frac{E}{d}\left\{d\left(1+\alpha_E+\alpha_{E2}\right)+\right.$

$\frac{E}{d}2\left\{d\left(1+\alpha_E+\alpha_{E2}\right)+e+ge+jhge\left(1+\alpha_J\right)\right\}+\sqrt{\frac{E}{d}}\left\{\frac{1}{abc}\sqrt{\frac{E}{d}}+\frac{1}{bc}\sqrt{\frac{E}{d}}+\frac{1}{c}\sqrt{\frac{E}{d}}\left(1+\alpha_C\right)+\sqrt{\frac{E}{d}}+\sqrt{\frac{hge}{d}E}\left(1+\alpha_H\right)+\sqrt{\right.$
$1=0$

Let $x=\sqrt{\frac{E}{d}}$

$$x^2\underbrace{2\left\{d\left(1+\alpha_E+\alpha_{E2}\right)+e+ge+jhge\left(1+\alpha_J\right)\right\}}_{w}+x\underbrace{\left\{\frac{1}{abc}+\frac{1}{bc}+\frac{1}{c}\left(1+\alpha_C\right)+1+\sqrt{hge}\left(1+\alpha_H\right)+\sqrt{jkhge}\left(1+\alpha_K\right)\right\}}_{v}-$$

$1=0$

$wx^2+vx-1=0$

quadratic equation (negative x is ok as yeilds $x=D$)

$x=\frac{-b\pm\sqrt{b^2-4ac}}{2a}=\frac{-v\pm\sqrt{v^2+4w}}{2w}\xrightarrow{?}\frac{-v+\sqrt{v^2+4w}}{2w}=D$

8.2 Dimers

There is only one dimer pair in the table.

$$N_2O_4 \rightleftharpoons 2NO_2 \qquad K_d=5.9\times10^{-3} \text{ at 298 K} \tag{35}$$

$$pK_d = 2.23 \tag{36}$$

Reactions of NO_2 (B) are already included above. By analogy to the weak acids, given $[NO_2]$, $[N_2O_4]$ is calculated from the equilibrium constant as

$$K_d = \frac{[NO_2]^2}{[N_2O_4]} \tag{37}$$

$$[N_2O_4] = \frac{[NO_2]^2}{K_d} \tag{38}$$

$$[B2] = \frac{[B]^2}{K_d} \tag{39}$$

where $B2$ is N_2O_4.

NO_3^-	A	nitrate	N_2	G	dinitrogen
NO_2	B		NH_3OH^+	H	Hydroxylammonium weak base
HNO_2	C	nitrous acid	$N_2H_5^+$	J	
NO	D		NH_4^+	K	ammonium
$H_2N_2O_2$	E	hyponitrous	N_2O_4	B2	
N_2O	F				
NO_2^-	CC	nitrite	NH_2OH	HH	Hydroxylamine
$HN_2O_2^-$	EE		N_2H_4	JJ	
$N_2O_2^{2-}$	EEE		NH_3	KK	ammonia

where $[B2] = [B]^2/K_d$

$c^* = [A] + [B] + 2[B2] + [C](1+\alpha_C) + [D] + 2\{[E](1+\alpha_E+\alpha_{E2})\} + 2[F] + 2[G] + [H](1+\alpha_H) + 2[J](1+\alpha_J) + [K](1+\alpha_K)$

$1 = A+B+2B2+C(1+\alpha_C)+D+2E(1+\alpha_E+\alpha_{E2})+2F+2G+H(1+\alpha_H)+2J(1+\alpha_J)+K(1+\alpha_K)$

$1 = A+B+C(1+\alpha_C)+D+H(1+\alpha_H)+K(1+\alpha_K)+2\{E(1+\alpha_E+\alpha_{E2})+F+G+J(1+\alpha_J)+B2\}$

Solve toward B

$\frac{B}{A} = a \qquad A = \frac{B}{a}$

$\frac{C}{B} = b \qquad C = bB$

$\frac{D}{C} = c \qquad D = cC = cbB$

$\frac{E}{D^2} = d \qquad E = dD^2 = d(cbB)^2$

$\frac{F}{D^2} = e \qquad F = eD^2 = e(cbB)^2$

$\frac{G}{E} = f \qquad G = fE = fd(cbB)^2 \qquad fd = ge\checkmark$

$\frac{G}{F} = g \qquad G = gF = ge(cbB)^2$

$\frac{H^2}{G} = h \qquad H = \sqrt{hG} = cbB\sqrt{hge}$

$\frac{J}{H^2} = j \qquad J = jH^2 = jhge(cbB)^2$

$\frac{K^2}{J} = k \qquad K = \sqrt{kJ} = \sqrt{kjhge}cbB$

$B2 = B^2/K_d \qquad B2 = B^2/K_d$

$1 = A+B+C(1+\alpha_C)+D+H(1+\alpha_H)+K(1+\alpha_K)+2\{E(1+\alpha_E+\alpha_{E2})+F+G+J(1+\alpha_J)+B2\}$

$1 = \frac{B}{a}+B+bB(1+\alpha_C)+cbB+cbB\sqrt{hge}(1+\alpha_H)+\sqrt{kjhge}cbB(1+\alpha_K)+2\left\{d(cbB)^2(1+\alpha_E+\alpha_{E2})+e(cbB)^2+fd(cb\right.$

$2\left\{d(cbB)^2(1+\alpha_E+\alpha_{E2})+e(cbB)^2+fd(cbB)^2+jhge(cbB)^2(1+\alpha_J)+B^2/K_d\right\}+\frac{B}{a}+B+bB(1+\alpha_C)+$
$cbB+cbB\sqrt{hge}(1+\alpha_H)+\sqrt{kjhge}cbB(1+\alpha_K)-1=0$

$(cbB)^2\,2\left\{d(1+\alpha_E+\alpha_{E2})+e+fd+jhge(1+\alpha_J)+\frac{1}{(cb)^2K_d}\right\}+cbB\left\{\frac{1}{abc}+\frac{1}{bc}+\frac{(1+\alpha_C)}{c}+1+\sqrt{hge}(1+\alpha_H)+\sqrt{kjhge}\right.$
$1=0$

Let $cbB = x$

$$\underbrace{x^2 2\left\{d(1+\alpha_E+\alpha_{E2})+e+fd+jhge(1+\alpha_J)+1/(cb)^2K_d\right\}}_{w}+\underbrace{x\left\{\frac{1}{abc}+\frac{1}{bc}+\frac{(1+\alpha_C)}{c}+1+\sqrt{hge}(1+\alpha_H)+\sqrt{kjhg}\right.}_{v}$$

$1=0$

$x = \frac{-b\pm\sqrt{b^2-4ac}}{2a} = \frac{-v\pm\sqrt{v^2+4w}}{2w} \xrightarrow{?} \frac{-v+\sqrt{v^2+4w}}{2w} = cbB$

8.3 Some remaining reactions with unusual reactant/products

The original 10 reacitons were the species in the latimer diagram. The dimer N_2O_4 has been added. There are several reactions that involve unusual species. Here we itemize the species provided that there are at least two redox reactions and the species can be both a product and reactant. Added the species in small groups in case some particular species has a large impact. First group is 11} to 14} where there are no new species. So, actually redundant reactions at least from an algbraic perspective. Will wait on adding these to the spreadsheet as they are redundant.

The new species ones are added and are for reactions 15} to 18}?.

Given

$$N_2O_4 + 4H^+ + 2e \rightleftharpoons 2NO^+ + 2H_2O \qquad 0.77\,V \tag{40}$$

$$E = E^0 - \frac{2.303RT}{nF}\log\frac{[NO^+]^2}{[N_2O_4]\,[H^+]^4} \tag{41}$$

Given

$$K_d = \frac{[NO_2]^2}{[N_2O_4]} \tag{42}$$

$$[N_2O_4] = \frac{[NO_2]^2}{K_d} \tag{43}$$

$$E = E^0 - \frac{2.303RT}{2F}\log\frac{[NO^+]^2}{[N_2O_4]\,[H^+]^4} \tag{44}$$

$$= E^0 - \frac{2.303RT}{2F}\log\frac{[NO^+]^2}{\frac{[NO_2]^2}{K_d}\,[H^+]^4} \tag{45}$$

$$= E^0 - \frac{1}{2\gamma}\log\frac{K_d\,[NO^+]^2}{[NO_2]^2\,[H^+]^4} \tag{46}$$

$$= E^0 - \frac{1}{2\gamma}\log K_d - \frac{1}{2\gamma}\log\frac{[NO^+]^2}{[NO_2]^2} - \frac{1}{2\gamma}\log\frac{1}{[H^+]^4} \tag{47}$$

$$= E^0 + \frac{1}{2\gamma}pK_d - \frac{1}{\gamma}\log\frac{[NO^+]}{[NO_2]} - \frac{4}{2\gamma}pH \tag{48}$$

$$E = E^0 + \frac{1}{2\gamma}pK_d - \frac{2}{\gamma}pH - \frac{1}{\gamma}\log\frac{[NO^+]}{[NO_2]} \tag{49}$$

$$= 0.77 + \frac{1}{2\,(16.9)}\,(2.23) - \frac{2}{\gamma}pH - \frac{1}{\gamma}\log\frac{[NO^+]}{[NO_2]} \tag{50}$$

$$= 0.836 - \frac{2}{\gamma}pH - \frac{1}{\gamma}\log\frac{[NO^+]}{[NO_2]} \tag{51}$$

$$-\gamma\,(E - 0.836) - 2pH = \log\frac{[NO^+]}{[NO_2]} \tag{52}$$

$$10^{-\gamma(E-0.836)}10^{-2pH} = \frac{[NO^+]}{[NO_2]} \tag{53}$$

This characterizes $E = E^0 - \frac{1}{\gamma}\log\frac{[NO^+]}{[NO_2][H^+]^2}$ for

$$NO_2 + 2H^+ + 1e \rightleftharpoons NO^+ + H_2O \qquad E^0 = 0.836\,V$$

This checks and is reaction 15}. NO^+ appears in 16}.

New species HN_3 appears in equations 17} and 18}. Note that HN_3 is a weak acid with pK_A =4.6 and K_A of 2.5×10^{-5}.

Table 1

			mH^+	ne^- ⇌			H_2O	E^0						
11}	1	NO_3^-	3	2	1	HNO_2	1	0.94	$\frac{[HNO_2]}{\left[NO_3^-\right]}$	$\frac{[C]}{[A]}$	l	θ	10^{-3pH}	$\frac{[C]}{[A]}$
12}	1	NO_2	2	2	1	NO	1	1.045	$\frac{[NO]}{[NO_2]}$	$\frac{[D]}{[B]}$	m	θ	10^{-2pH}	$\frac{[D]}{[B]}$
13}	2	HNO_2	4	2	1	$H_2N_2O_2$	2	0.86	$\frac{[H_2N_2O_2]}{[HNO_2]^2}$	$\frac{[E]}{[C]^2}$	n	θ	10^{-4pH}	$\frac{[E]}{[C]^2}$
14}	1	NH_3OH^+	2	2	1	NH_4^+	1	1.35	$\frac{\left[NH_4^+\right]}{[NH_3OH^+]}$	$\frac{[K]}{[H]}$	p	θ	10^{-2pH}	$\frac{[K]}{[H]}$
15}	1	NO_2	2	1	1	NO^+	1	0.836	$\frac{\left[NO^+\right]}{[NO_2]}$	$\frac{[L]}{[B]}$	q	θ	10^{-2pH}	
16}	1	NO^+		1	1	NO		1.45	$\frac{[NO]}{[NO^+]}$	$\frac{[D]}{[L]}$	r	θ		
17}	3	N_2	2	2	2	HN_3		-3.10	$\frac{[HN_3]^2}{[N_2]^3}$	$\frac{[Z]^2}{[G]^3}$	s	θ	10^{-2pH}	
18}	1	HN_3	3	2	1	$N_2 + NH_4^+$		1.96	$\frac{[N_2]\left[NH_4^+\right]}{[HN_3]}$	$\frac{[G][K]}{[Z]}$	t	θ	10^{-3pH}	$\alpha_z, K_A = 2.5 \times 10^{-5}$
19}														
20}														

NO_3^-	A	nitrate	N_2	G	dinitrogen
NO_2	B		NH_3OH^+	H	Hydroxylammonium weak base
HNO_2	C	nitrous acid	$N_2H_5^+$	J	
NO	D		NH_4^+	K	ammonium
$H_2N_2O_2$	E	hyponitrous	N_2O_4	B2	
N_2O	F		HN_3	Z	
NO^+	L				
NO_2^-	CC	nitrite	N_3^-	ZZ	
$HN_2O_2^-$	EE		NH_2OH	HH	Hydroxylamine
$N_2O_2^{2-}$	EEE		N_2H_4	JJ	
			NH_3	KK	ammonia

8.3.1 Add NO^+

Add NO^+ separately from HN_3, with NO^+ first.

Solve toward G

$\frac{B}{A} = a \qquad A = \frac{B}{a} = \frac{1}{abc}\sqrt{\frac{G}{eg}}$.

$\frac{C}{B} = b \qquad B = \frac{C}{b} = \frac{1}{bc}\sqrt{\frac{G}{eg}}$.

$\frac{D}{C} = c \qquad C = \frac{D}{c} = \frac{1}{c}\sqrt{\frac{G}{eg}}$.

$\frac{E}{D^2} = d \qquad D = \sqrt{\frac{E}{d}} = \sqrt{\frac{G}{df}}$

$\frac{F}{D^2} = e \qquad D = \sqrt{\frac{F}{e}} = \sqrt{\frac{G}{eg}}$.

$\frac{G}{E} = f \qquad E = \frac{G}{f} \qquad fd = ge$✓

$\frac{G}{F} = g \qquad F = \frac{G}{g}$

$\frac{H^2}{G} = h \qquad H = \sqrt{hG}$

$\frac{J}{H^2} = j \qquad J = jhG$

$\frac{K^2}{J} = k \qquad K = \sqrt{kJ} = \sqrt{kjhG}$

$B2 = B^2/K_d \qquad B2 = \frac{B^2}{K_d} = \frac{1}{(bc)^2}\frac{G}{egK_d}$.

$\frac{L}{B} = q \qquad L = qB = \frac{q}{bc}\sqrt{\frac{G}{eg}}$.

$\frac{D}{L} = r \qquad L = \frac{D}{r} = \frac{1}{r}\sqrt{\frac{G}{eg}} \qquad .bc = qr?$

$1 = A{+}B{+}C\left(1+\alpha_C\right){+}D{+}H\left(1+\alpha_H\right){+}K\left(1+\alpha_K\right){+}L{+}2\left\{E\left(1+\alpha_E+\alpha_{E2}\right)+F+G+J\left(1+\alpha_J\right)+B2\right\}$

$1 = \frac{1}{abc}\sqrt{\frac{G}{eg}}{+}\frac{1}{bc}\sqrt{\frac{G}{eg}}{+}\frac{1}{c}\sqrt{\frac{G}{eg}}\left(1+\alpha_C\right){+}\sqrt{\frac{G}{eg}}{+}\sqrt{hG}\left(1+\alpha_H\right){+}\sqrt{kjhG}\left(1+\alpha_K\right){+}\frac{1}{r}\sqrt{\frac{G}{eg}}{+}2\left\{\frac{G}{f}\left(1+\alpha_E+\alpha_{E2}\right)+\frac{G}{g}+G+\right.$

$0 = 2\left\{\frac{G}{f}\left(1+\alpha_E+\alpha_{E2}\right)+\frac{G}{g}+G+jhG\left(1+\alpha_J\right)+\frac{1}{(bc)^2}\frac{G}{egK_d}\right\}+\frac{1}{abc}\sqrt{\frac{G}{eg}}+\frac{1}{bc}\sqrt{\frac{G}{eg}}+\frac{1}{c}\sqrt{\frac{G}{eg}}\left(1+\alpha_C\right)+$

$\sqrt{\frac{G}{eg}}+\sqrt{hG}\left(1+\alpha_H\right)+\sqrt{kjhG}\left(1+\alpha_K\right)+\frac{1}{r}\sqrt{\frac{G}{eg}}-1$

$0 = G2\left\{\frac{1}{f}\left(1+\alpha_E+\alpha_{E2}\right)+\frac{1}{g}+1+jh\left(1+\alpha_J\right)+\frac{1}{(bc)^2egK_d}\right\}+\sqrt{G}\left\{\frac{1}{abc}\sqrt{\frac{1}{eg}}+\frac{1}{bc}\sqrt{\frac{1}{eg}}+\frac{1}{c}\sqrt{\frac{1}{eg}}\left(1+\alpha_C\right)+\sqrt{\frac{1}{eg}}+\sqrt{h}\left(1\right.\right.$

1

Let $\sqrt{G} = x$

$$1 = x\underbrace{\left\{\frac{1}{abc\sqrt{eg}}+\frac{1}{bc\sqrt{eg}}+\frac{1}{c\sqrt{eg}}\left(1+\alpha_C\right)+\frac{1}{\sqrt{eg}}+\sqrt{h}\left(1+\alpha_H\right)+\sqrt{kjh}\left(1+\alpha_K\right)+\frac{1}{r\sqrt{eg}}\right\}}_{v}+x^2\underbrace{2\left\{\frac{1}{f}\left(1+\alpha_E+\alpha_{E2}\right)+\right.}$$

$wx^2 + vx - 1 = 0$

quadratic equation (negative x is ok as yeilds $x = \sqrt{G}$)

$x = \frac{-b\pm\sqrt{b^2-4ac}}{2a} = \frac{-v\pm\sqrt{v^2+4w}}{2w} \xrightarrow{?} \frac{-v+\sqrt{v^2+4w}}{2w} = \sqrt{G}$

8.3.2 Add HN_3

Now add HN_3, reactions 17} and 18}. note HN_3 has 3 N. and will need weak acid HN_3

Because hydrazine leads to a third order polynomial, used solver in excel VBA to solve. Alternative is roots of cubuc eqn. [1]

Solve toward G

$$\frac{B}{A}=a \qquad A=\frac{B}{a}=\frac{1}{abc}\sqrt{\frac{G}{eg}}$$
$$\frac{C}{B}=b \qquad B=\frac{C}{b}=\frac{1}{bc}\sqrt{\frac{G}{eg}}$$
$$\frac{D}{C}=c \qquad C=\frac{D}{c}=\frac{1}{c}\sqrt{\frac{G}{eg}}$$
$$\frac{E}{D^2}=d \qquad D=\sqrt{\frac{E}{d}}=\sqrt{\frac{G}{df}}$$
$$\frac{F}{D^2}=e \qquad D=\sqrt{\frac{F}{e}}=\sqrt{\frac{G}{eg}}$$
$$\frac{G}{E}=f \qquad E=\frac{G}{f} \qquad fd=ge\checkmark$$
$$\frac{G}{F}=g \qquad F=\frac{G}{g}$$
$$\frac{H^2}{G}=h \qquad H=\sqrt{hG}$$
$$\frac{J}{H^2}=j \qquad J=jhG$$
$$\frac{K^2}{J}=k \qquad K=\sqrt{kJ}=\sqrt{kjhG}$$
$$B2=B^2/K_d \qquad B2=\frac{B^2}{K_d}=\frac{1}{(bc)^2}\frac{G}{egK_d}$$
$$\frac{L}{B}=q \qquad L=qB=\frac{q}{bc}\sqrt{\frac{G}{eg}}$$
$$\frac{D}{L}=r \qquad L=\frac{D}{r}=\frac{1}{r}\sqrt{\frac{G}{eg}} \qquad bc=qr?$$
$$\frac{Z^2}{G^3}=s \qquad Z=\sqrt{sG^3}$$
$$\frac{GK}{Z}=t \qquad Z=\frac{GK}{t}=\frac{\sqrt{kjhG^3}}{t} \qquad s=\frac{kjh}{t^2}?$$

$$1=A+B+C\left(1+\alpha_C\right)+D+H\left(1+\alpha_H\right)+K\left(1+\alpha_K\right)+L+2\left\{E\left(1+\alpha_E+\alpha_{E2}\right)+F+G+J\left(1+\alpha_J\right)+B2\right\}+3Z$$

$$3Z+2\left\{E\left(1+\alpha_E+\alpha_{E2}\right)+F+G+J\left(1+\alpha_J\right)+B2\right\}+A+B+C\left(1+\alpha_C\right)+D+H\left(1+\alpha_H\right)+K\left(1+\alpha_K\right)+L-1=0$$

$$3\sqrt{sG^3}+2\left\{\frac{G}{f}\left(1+\alpha_E+\alpha_{E2}\right)+\frac{G}{g}+G+jhG\left(1+\alpha_J\right)+\frac{G}{egK_d(bc)^2}\right\}+\frac{1}{abc}\sqrt{\frac{G}{eg}}+\frac{1}{bc}\sqrt{\frac{G}{eg}}+\frac{1}{c}\sqrt{\frac{G}{eg}}\left(1+\alpha_C\right)+\sqrt{\frac{G}{eg}}+\sqrt{hG}\left(1+\alpha_H\right)+\sqrt{kjhG}\left(1+\alpha_K\right)+\frac{1}{r}\sqrt{\frac{G}{eg}}-1=0$$

$$G^{3/2}3\sqrt{s}+2G\left\{\frac{1}{f}\left(1+\alpha_E+\alpha_{E2}\right)+\frac{1}{g}+1+jh\left(1+\alpha_J\right)+\frac{1}{egK_d(bc)^2}\right\}+\sqrt{G}\left\{\frac{1}{abc}\sqrt{\frac{1}{eg}}+\frac{1}{bc}\sqrt{\frac{1}{eg}}+\frac{1}{c}\sqrt{\frac{1}{eg}}\left(1+\alpha_C\right)+\sqrt{\frac{1}{eg}}+1=0\right.$$

Let $x=\sqrt{G}$

$$x^3 3\sqrt{s}+x^2 2\left\{\frac{1}{f}\left(1+\alpha_E+\alpha_{E2}\right)+\frac{1}{g}+1+jh\left(1+\alpha_J\right)+\frac{1}{egK_d(bc)^2}\right\}+x\left\{\frac{1}{abc}\sqrt{\frac{1}{eg}}+\frac{1}{bc}\sqrt{\frac{1}{eg}}+\frac{1}{c}\sqrt{\frac{1}{eg}}\left(1+\alpha_C\right)+\sqrt{\frac{1}{eg}}+\sqrt{h}1=0\right.$$

$$ax^3+bx^2+cx-1=0$$

where

$$a=3\sqrt{s}$$
$$b=2\left\{\frac{1}{f}\left(1+\alpha_E+\alpha_{E2}\right)+\frac{1}{g}+1+jh\left(1+\alpha_J\right)+\frac{1}{egK_d(bc)^2}\right\}$$
$$c=\left\{\frac{1}{abc}\sqrt{\frac{1}{eg}}+\frac{1}{bc}\sqrt{\frac{1}{eg}}+\frac{1}{c}\sqrt{\frac{1}{eg}}\left(1+\alpha_C\right)+\sqrt{\frac{1}{eg}}+\sqrt{h}\left(1+\alpha_H\right)+\sqrt{kjh}\left(1+\alpha_K\right)+\frac{1}{r}\sqrt{\frac{1}{eg}}\right\}$$
$$d=-1$$

[1] From the Cubic Formula, www.math.vanderbilt.edu/~schectex/courses/cubic

$$p=-\frac{b}{3a}$$
$$q=p^3+\frac{bc-3ad}{6a^2}$$
$$r=\frac{c}{3a}$$
$$x=\left[q+\left[q^2+\left(r-p^2\right)^3\right]^{1/2}\right]^{1/3}+\left[q-\left[q^2+\left(r-p^2\right)^3\right]^{1/2}\right]^{1/3}+p$$

8.3.3 Add HN_3 and N_3^-

Now add HN_3, reactions 17} and 18}. note HN_3 has 3 N. and here add weak acid $HN_3 \rightleftharpoons H_3O^+ + N_3^-$

Because hydrazine leads to a third order polynomial, used solver in excel VBA to solve. Alternative is roots of cubic eqn. [2]

Solve toward G

$$\begin{array}{ll}
\frac{B}{A} = a & A = \frac{B}{a} = \frac{1}{abc}\sqrt{\frac{G}{eg}} \\
\frac{C}{B} = b & B = \frac{C}{b} = \frac{1}{bc}\sqrt{\frac{G}{eg}} \\
\frac{D}{C} = c & C = \frac{D}{c} = \frac{1}{c}\sqrt{\frac{G}{eg}} \\
\frac{E}{D^2} = d & D = \sqrt{\frac{E}{d}} = \sqrt{\frac{G}{df}} \\
\frac{F}{D^2} = e & D = \sqrt{\frac{F}{e}} = \sqrt{\frac{G}{eg}} \\
\frac{G}{E} = f & E = \frac{G}{f} \qquad fd = ge\checkmark \\
\frac{G}{F} = g & F = \frac{G}{g} \\
\frac{H^2}{G} = h & H = \sqrt{hG} \\
\frac{J}{H^2} = j & J = jhG \\
\frac{K^2}{J} = k & K = \sqrt{kJ} = \sqrt{kjhG} \\
B2 = B^2/K_d & B2 = \frac{B^2}{K_d} = \frac{1}{(bc)^2}\frac{G}{egK_d} \\
\frac{L}{B} = q & L = qB = \frac{q}{bc}\sqrt{\frac{G}{eg}} \\
\frac{D}{L} = r & L = \frac{D}{r} = \frac{1}{r}\sqrt{\frac{G}{eg}} \qquad .bc = qr? \\
\frac{Z^2}{G^3} = s & Z = \sqrt{sG^3} \\
\frac{GK}{Z} = t & Z = \frac{GK}{t} = \frac{\sqrt{kjhG^3}}{t} \qquad .s = \frac{kjh}{t^2}?
\end{array}$$

$1 = A{+}B{+}C\left(1+\alpha_C\right){+}D{+}H\left(1+\alpha_H\right){+}K\left(1+\alpha_K\right){+}L{+}2\left\{E\left(1+\alpha_E+\alpha_{E2}\right)+F+G+J\left(1+\alpha_J\right)+B2\right\}+3Z\left(1+\alpha_Z\right)$

$3Z\left(1+\alpha_Z\right){+}2\left\{E\left(1+\alpha_E+\alpha_{E2}\right)+F+G+J\left(1+\alpha_J\right)+B2\right\}{+}A{+}B{+}C\left(1+\alpha_C\right){+}D{+}H\left(1+\alpha_H\right){+}K\left(1+\alpha_K\right)+L-1=0$

$3\sqrt{sG^3}\left(1+\alpha_Z\right){+}2\left\{\frac{G}{f}\left(1+\alpha_E+\alpha_{E2}\right)+\frac{G}{g}+G+jhG\left(1+\alpha_J\right)+\frac{G}{egK_d(bc)^2}\right\}{+}\frac{1}{abc}\sqrt{\frac{G}{eg}}{+}\frac{1}{bc}\sqrt{\frac{G}{eg}}{+}\frac{1}{c}\sqrt{\frac{G}{eg}}\left(1+\alpha_C\right){+}\sqrt{\frac{G}{eg}}+\sqrt{hG}\left(1+\alpha_H\right)+\sqrt{kjhG}\left(1+\alpha_K\right)+\frac{1}{r}\sqrt{\frac{G}{eg}}-1=0$

$G^{3/2}3\sqrt{s}\left(1+\alpha_Z\right){+}2G\left\{\frac{1}{f}\left(1+\alpha_E+\alpha_{E2}\right)+\frac{1}{g}+1+jh\left(1+\alpha_J\right)+\frac{1}{egK_d(bc)^2}\right\}{+}\sqrt{G}\left\{\frac{1}{abc}\sqrt{\frac{1}{eg}}+\frac{1}{bc}\sqrt{\frac{1}{eg}}+\frac{1}{c}\sqrt{\frac{1}{eg}}\left(1+\alpha_C\right)1=0$

Let $x=\sqrt{G}$

$x^3 3\sqrt{s}\left(1+\alpha_Z\right){+}x^2 2\left\{\frac{1}{f}\left(1+\alpha_E+\alpha_{E2}\right)+\frac{1}{g}+1+jh\left(1+\alpha_J\right)+\frac{1}{egK_d(bc)^2}\right\}{+}x\left\{\frac{1}{abc}\sqrt{\frac{1}{eg}}+\frac{1}{bc}\sqrt{\frac{1}{eg}}+\frac{1}{c}\sqrt{\frac{1}{eg}}\left(1+\alpha_C\right)+\sqrt{1=0}$

$ax^3+bx^2+cx-1=0$

where

$a=3\sqrt{s}\left(1+\alpha_Z\right)$

$b=2\left\{\frac{1}{f}\left(1+\alpha_E+\alpha_{E2}\right)+\frac{1}{g}+1+jh\left(1+\alpha_J\right)+\frac{1}{egK_d(bc)^2}\right\}$

$c=\left\{\frac{1}{abc}\sqrt{\frac{1}{eg}}+\frac{1}{bc}\sqrt{\frac{1}{eg}}+\frac{1}{c}\sqrt{\frac{1}{eg}}\left(1+\alpha_C\right)+\sqrt{\frac{1}{eg}}+\sqrt{h}\left(1+\alpha_H\right)+\sqrt{kjh}\left(1+\alpha_K\right)+\frac{1}{r}\sqrt{\frac{1}{eg}}\right\}$

$d=-1$

---

[2] From the Cubic Formula, www.math.vanderbilt.edu/~schectex/courses/cubic

$p=-\frac{b}{3a}$

$q=p^3+\frac{bc-3ad}{6a^2}$

$r=\frac{c}{3a}$

$x=\left[q+\left[q^2+\left(r-p^2\right)^3\right]^{1/2}\right]^{1/3}+\left[q-\left[q^2+\left(r-p^2\right)^3\right]^{1/2}\right]^{1/3}+p$

Solve toward A

$$\begin{array}{rcll}
\frac{B}{A}=a & B=aA & & \\
\frac{C}{B}=b & C=bB=abA & & \\
\frac{D}{C}=c & D=cC=abcA & & \\
\frac{E}{D^2}=d & E=dD^2=d(abcA)^2 & & \\
\frac{F}{D^2}=e & F=eD^2=ed(abcA)^2 & & \\
\frac{G}{E}=f & G=fE=df(abcA)^2 & & \\
\frac{G}{F}=g & G=gF=ged(abcA)^2 & f=ge? & \\
\frac{H^2}{G}=h & H=\sqrt{hG}=\sqrt{hdf(abcA)^2}=(abcA)\sqrt{hdf} & & \\
\frac{J}{H^2}=j & J=jH^2=(abcA)^2jhdf & & \\
\frac{K^2}{J}=k & K=\sqrt{kJ}=\sqrt{(abcA)^2jkhdf}=(abcA)\sqrt{jkhdf} & & \\
B2=B^2/K_d & B2=B^2/K_d=(aA)^2/K_d & & \\
\frac{L}{B}=q & L=qB=qaA & & \\
\frac{D}{L}=r & L=\frac{D}{r}=\frac{abc}{r}A & qr=bc? & \\
\frac{Z^2}{G^3}=s & Z=\sqrt{sG^3}=\sqrt{(df(abcA)^2)^3\,s}=(abcA)^3\sqrt{dfs} & & \\
\frac{GK}{Z}=t & Z=\frac{GK}{t}=\frac{df(abcA)^2(abcA)\sqrt{jkhdf}}{t}=\frac{(abcA)^3df\sqrt{jkhdf}}{t} & \frac{df\sqrt{jkhdf}}{t}=\sqrt{dfs} & \\
 & & \sqrt{jkhdfdf}=\sqrt{s}t? &
\end{array}$$

where
$$\begin{array}{ll}
CC=C\times10^{pH}10^{-3.398} & \alpha_C=10^{pH}10^{-3.398}\\
EE=E\times10^{pH}10^{-7.21} & \alpha_E=10^{pH}10^{-7.21}\\
EEE=E\times10^{2pH}10^{-18.75} & \alpha_{2E}=10^{2pH}10^{-18.75}\\
HH=H\times10^{pH}10^{-5.95} & \alpha_H=10^{pH}10^{-5.95}\\
JJ=J\times10^{pH}10^{-8.10} & \alpha_J=10^{pH}10^{-8.10}\\
KK=K\times10^{pH}10^{-9.25} & \alpha_K=10^{pH}10^{-9.25}
\end{array}$$

$1=A+B+C\left(1+\alpha_C\right)+D+H\left(1+\alpha_H\right)+K\left(1+\alpha_K\right)+L+2\left\{E\left(1+\alpha_E+\alpha_{E2}\right)+F+G+J\left(1+\alpha_J\right)+B2\right\}+3Z\left(1+\alpha_Z\right)$

$1=A+aA+abA\left(1+\alpha_C\right)+abcA+(abcA)\sqrt{hdf}\left(1+\alpha_H\right)+(abcA)\sqrt{jkhdf}\left(1+\alpha_K\right)+qaA+2\left\{d(abcA)^2\left(1+\alpha_E+\alpha_{E2}\right)+ed\right.$

$3\frac{(abcA)^3df\sqrt{jkhdf}}{t}\left(1+\alpha_Z\right)$

$(abcA)^3 3\frac{df\sqrt{jkhdf}}{t}\left(1+\alpha_Z\right)+(abcA)^2 2\left\{d\left(1+\alpha_E+\alpha_{E2}\right)+ed+df+jhdf\left(1+\alpha_J\right)+\frac{1}{(bc)^2K_d}\right\}+abcA\left\{\frac{1}{abc}+\frac{1}{bc}+\frac{(1+\alpha_C)}{c}+\right.$

$1=0$

Let $x=A$ where $aaAx^3+bbAx^2+ccAx-1=0$

$aaA=3\frac{df\sqrt{jkhdf}}{t}\left(1+\alpha_Z\right)(abc)^3$

$bbA=2\left\{d\left(1+\alpha_E+\alpha_{E2}\right)+ed+df+jhdf\left(1+\alpha_J\right)+\frac{1}{(bc)^2K_d}\right\}(abc)^2$

$ccA=\left\{\frac{1}{abc}+\frac{1}{bc}+\frac{(1+\alpha_C)}{c}+1+\sqrt{hdf}\left(1+\alpha_H\right)+\sqrt{jkhdf}\frac{(1+\alpha_K)}{abc}+\frac{q}{bc}\right\}(abc)$

$ccA=\left\{\frac{1}{abc}+\frac{q+1}{bc}+\frac{(1+\alpha_C)}{c}+1+\sqrt{hdf}\left(1+\alpha_H\right)+\sqrt{jkhdf}\frac{(1+\alpha_K)}{abc}\right\}(abc)$

$ddA=-1$